

University of Windsor

Scholarship at UWindor

Electronic Theses and Dissertations

Theses, Dissertations, and Major Papers

1984

Basement heat loss a parametric study.

Suneel Kumar. Bhardwaj
University of Windsor

Follow this and additional works at: <https://scholar.uwindsor.ca/etd>

Recommended Citation

Bhardwaj, Suneel Kumar., "Basement heat loss a parametric study." (1984). *Electronic Theses and Dissertations*. 1270.
<https://scholar.uwindsor.ca/etd/1270>

This online database contains the full-text of PhD dissertations and Masters' theses of University of Windsor students from 1954 forward. These documents are made available for personal study and research purposes only, in accordance with the Canadian Copyright Act and the Creative Commons license—CC BY-NC-ND (Attribution, Non-Commercial, No Derivative Works). Under this license, works must always be attributed to the copyright holder (original author), cannot be used for any commercial purposes, and may not be altered. Any other use would require the permission of the copyright holder. Students may inquire about withdrawing their dissertation and/or thesis from this database. For additional inquiries, please contact the repository administrator via email (scholarship@uwindsor.ca) or by telephone at 519-253-3000ext. 3208.



National Library
of Canada

Bibliothèque nationale
du Canada

Canadian Theses Service

Services des thèses canadiennes

Ottawa, Canada
K1A 0N4

CANADIAN THESES

THÈSES CANADIENNES

NOTICE

The quality of this microfiche is heavily dependent upon the quality of the original thesis submitted for microfilming. Every effort has been made to ensure the highest quality of reproduction possible.

If pages are missing, contact the university which granted the degree.

Some pages may have indistinct print especially if the original pages were typed with a poor typewriter ribbon or if the university sent us an inferior photocopy.

Previously copyrighted materials (journal articles, published tests, etc.) are not filmed.

Reproduction in full or in part of this film is governed by the Canadian Copyright Act, R.S.C. 1970, c. C-30. Please read the authorization forms which accompany this thesis.

THIS DISSERTATION
HAS BEEN MICROFILMED
EXACTLY AS RECEIVED

AVIS

La qualité de cette microfiche dépend grandement de la qualité de la thèse soumise au microfilmage. Nous avons tout fait pour assurer une qualité supérieure de reproduction.

S'il manque des pages, veuillez communiquer avec l'université qui a conféré le grade.

La qualité d'impression de certaines pages peut laisser à désirer, surtout si les pages originales ont été dactylographiées à l'aide d'un ruban usé ou si l'université nous a fait parvenir une photocopie de qualité inférieure.

Les documents qui font déjà l'objet d'un droit d'auteur (articles de revue, examens publiés, etc.) ne sont pas microfilmés.

La reproduction, même partielle, de ce microfilm est soumise à la Loi canadienne sur le droit d'auteur, SRC 1970, c. C-30. Veuillez prendre connaissance des formules d'autorisation qui accompagnent cette thèse.

LA THÈSE A ÉTÉ
MICROFILMÉE TELLE QUE
NOUS L'AVONS REÇUE

BASEMENT HEAT LOSS - A PARAMETRIC STUDY

by

Suneel Kumar Bhardwaj

A thesis
presented to the University of Windsor
in partial fulfillment of the
requirements for the degree of
Master of Applied Science
in
Department of Mechanical Engineering

Windsor , Ontario, 1984

(c) Suneel Kumar Bhardwaj, 1984

I hereby declare that I am the sole author of this thesis.

I authorize the University of Windsor to lend this thesis to other institutions or individuals for the purpose of scholarly research.

Suneel Kumar Bhardwaj

I further authorize the University of Windsor to reproduce this thesis by photocopying or by other means, in total or in part, at the request of other institutions or individuals for the purpose of scholarly research.

Suneel Kumar Bhardwaj

The University of Windsor requires the signatures of all persons using or photocopying this thesis. Please sign below, and give address and date.

ABSTRACT

A finite difference computer program (HEATING 5) has been acquired and is utilized to predict the thermal performance of basements. This program has been validated by comparing results with data acquired from an actual instrumented residential basement in Columbus, Ohio. The model considers a two-dimensional cross-section and incorporates time-varying soil thermal properties. All soil/air interface boundary heat transfer is characterized by associated uniform convective coefficients. In all calculations, except one, radiation and evapo-transpiration effects are neglected.

A parametric study is done on the Ohio basement to investigate the effects of the following parameters on the basement heat loss :-

1. Soil thermal conductivity
2. Proximity to adjacent structures
3. Ground water level
4. Ground surface conditions
 - a) Snow cover
 - b) Asphalt cover
5. Insulation placement

a) Placement on the full length of the exterior wall

b) Placement on the top half of the exterior wall

6. Basement temperature

It is found that the soil thermal conductivity can exert a significant influence on the basement heat loss. It is essential that values close to the actual soil thermal conductivities be used for heat loss calculations.

Similar structures (not closer than 3m from the basement wall) do not significantly affect the wall heat losses (only up to 8%), but can reduce the maximum floor heat loss by as much as 50%.

The ground water level plays an important role in the determination of the floor heat loss, but its effect on the wall heat loss is almost negligible.

The ground cover can have a significant influence on the wall and floor heat loss (especially the wall heat loss). Snow cover is very effective in reducing the wall heat loss. A 5.7 inch snow cover can reduce the wall and floor heat loss by as much as 33% and 8% respectively. An asphalt cover minimizes the heat loss due to evaporation from the ground. A 4 inch asphalt cover can reduce the wall and floor heat loss by 19% and 9.4% respectively during the heating season.

It has also been found that full length insulation placement is more effective than half length insulation

placement. But the beneficial cooling season heat losses are also reduced by the added insulation.

ACKNOWLEDGEMENTS

I am deeply grateful to Dr. H.J. Tucker, for his constant supervision, advice and encouragement.

I am also very grateful to the faculty members of the Building Energy Group for their constructive comments and encouragement.

I must also acknowledge many fruitful discussions with my colleagues at the Department of Mechanical Engineering which have helped in numerous ways.

Finally, I am deeply grateful to my parents for all their support, encouragement and patience.

The financial support which made this project possible was provided by NSERC grant No.9081 and is gratefully acknowledged.

TABLE OF CONTENTS

ABSTRACT -----	iv
ACKNOWLEDGEMENTS -----	vii
TABLE OF CONTENTS -----	viii
LIST OF FIGURES -----	x
LIST OF TABLES -----	xiv
NOMENCLATURE -----	xv

Chapter	Page
I. INTRODUCTION -----	1
1.1 LITERATURE SURVEY -----	2
1.1.1 SOIL TEMPERATURES -----	3
1.1.2 SOIL THERMAL PROPERTIES -----	7
1.1.3 BASEMENT HEAT LOSS STUDIES -----	11
1.2 OBJECTIVES -----	17
II. HEATING 5 COMPUTER PROGRAM -----	20
2.1 SIMULATION PROCEDURE -----	22
2.1.1 REGIONS -----	22
2.1.2 LATTICE ARRANGEMENT -----	25
2.1.3 ANALYTICAL AND TABULAR FUNCTIONS --	25
2.1.4 BOUNDARY CONDITIONS -----	26
III. MODEL ASSUMPTIONS -----	29
3.1 MODEL VALIDATION -----	30
3.1.1 RESULTS -----	38

IV.	RESULTS AND DISCUSSIONS OF THE PARAMETRIC STUDY	57
4.1	SOIL THERMAL CONDUCTIVITY	57
4.1.1	SEASONAL VARIATION COMPARED TO FIXED SOIL CONDUCTIVITIES	58
4.1.2	COMPARISON OF FIXED SOIL CONDUCTIVITIES	62
4.2	PROXIMITY OF ADJACENT STRUCTURES	64
4.3	GROUND WATER LEVEL	68
4.4	GROUND SURFACE CONDITIONS	71
4.4.1	SNOW COVER	72
4.4.2	ASPHALT COVER	73
4.5	INSULATION PLACEMENT	90
4.6	BASEMENT TEMPERATURE	103
V.	ANALYSIS OF THE DBR/NRC BASEMENT IN OTTAWA	105
5.1	MODEL ASSUMPTIONS	106
5.2	MODEL ANALYSIS	109
5.3	RESULTS	118
VI.	CONCLUSIONS AND RECOMMENDATIONS	120
6.1	CONCLUSIONS	120
6.2	RECOMMENDATIONS	122
	REFERENCES	125

Appendix	Page
A. NUMERICAL TECHNIQUE	129
B. CARD INPUT FOR HEATING 5	143
C. JCL REQUIRED TO RUN HEATING 5	174
D. CARD INPUT AND JCL REQUIRED TO RUN HEATPLOT	181

LIST OF FIGURES

Figure		Page
1	Heat flow from Basement to ground surface -----	13
2.a	Region division according to rule 1 and 2 -----	24
2.b	Region division according to boundary conditions	24
3	Ground temperature probe locations for the Ohio House -----	32
4	Basement model showing boundary conditions -----	34
5	Dry bulb air temperatures -----	36
6	Basement air temperatures -----	37
7	Average outside basement wall temperatures -----	39
8	Soil temperature at 0.91m from the basement wall and 0.61m deep -----	40
9	Soil temperature 1.8m from the basement wall and 0.3m to 2.13m deep -----	41
10	Ground isotherms for the Base Case (July 14) ---	45
11	Ground isotherms for the Base Case (Aug. 13) ---	46
12	Ground isotherms for the Base Case (Sept. 12) --	47
13	Ground isotherms for the Base Case (Oct. 12) ---	48
14	Ground isotherms for the Base Case (Nov. 11) ---	49
15	Ground isotherms for the Base Case (Dec. 11) ---	50
16	Ground isotherms for the Base Case (Jan. 10) ---	51
17	Ground isotherms for the Base Case (Feb. 9) ----	52
18	Ground isotherms for the Base Case (March 11) --	53

19	Ground isotherms for the Base Case (April 10) --	54
20	Ground isotherms for the Base Case (May 25) ----	55
21	Ground isotherms for the Base Case (June 24) ---	56
22	Annual heat loss for soil thermal conductivity = 1.56 W/M K -----	59
23	Annual heat loss for soil thermal conductivity = 2.42 W/M K -----	60
24	Annual heat loss for soil thermal conductivity = 3.69 W/M K -----	61
24.1	Annual heat loss for three different soil thermal conductivities -----	63
25	Annual heat loss with a structure 6m from the wall -----	66
26	Annual heat loss with a structure 3m from the wall -----	67
27	Annual heat loss for isothermal boundary 4m below the floor -----	69
28	Annual heat loss for isothermal boundary 1m below the floor -----	70
29	Annual heat loss with snow cover on the ground -	75
30	Annual heat loss with an asphalt cover on the ground -----	77
30.1	Far field soil temperatures below asphalt and grass covered surfaces -----	79
31	Ground isotherms under an Asphalt cover (July 20)	80
32	Ground isotherms under an Asphalt cover (Aug. 29)	81
33	Ground isotherms under an Asphalt cover (Oct. 8)	82

34	Ground isotherms under an Asphalt cover (Nov. 17)	83
35	Ground isotherms under an Asphalt cover (Dec. 27)	84
36	Ground isotherms under an Asphalt cover (Feb. 5)	85
37	Ground isotherms under an Asphalt cover (Mar. 17)	86
38	Ground isotherms under an Asphalt cover (Apr. 26)	87
39	Ground isotherms under an Asphalt cover (Jun. 5)	88
40	Ground isotherms under an Asphalt cover (Jul. 15)	89
41	Annual heat loss with half length insulation ---	91
42	Annual heat loss with full length insulation ---	92
43	Ground isotherms for full length insulation (July 20) -----	93
44	Ground isotherms for full length insulation (August 29) -----	94
45	Ground isotherms for full length insulation (October 8) -----	95
46	Ground isotherms for full length insulation (November 17) -----	96
47	Ground isotherms for full length insulation (December 27) -----	97
48	Ground isotherms for full length insulation (February 5) -----	98
49	Ground isotherms for full length insulation (March 17) -----	99
50	Ground isotherms for full length insulation (April 26) -----	100
51	Ground isotherms for full length insulation (June 5) -----	101

51.1	Annual heat loss for a basement maintained at 22 C -----	104
52	Basement model showing boundary conditions -----	110
53	Wall heat loss for Model 1 -----	112
54	Floor heat loss for model 1 -----	112
55	Wall heat loss for Model 2 -----	114
56	Floor heat loss for Model 2 -----	114
57	Basement Model 3 -----	116
58	Wall heat loss for Model 3 -----	117
59	Floor heat loss for model 3 -----	117

LIST OF TABLES

Table		Page
1a	Building and Soil properties -----	33
1b	Surface convection film coefficients -----	33
2	Comparison of monthly average below grade wall heat loss using HEATING 5 and values calculated by McBride -----	42
3	Snow cover in inches for Ohio -----	74
4	Snow cover in centimeters for Ottawa -----	107
5	Building and soil thermal properties -----	108

NOMENCLATURE

SYMBOL	DESCRIPTION	UNITS
K	thermal conductivity	W/M K
Q	heat loss	W
A	area	m ²
L	path length	m
T _a	ambient air temperature	°C
T _b	basement air temperature	°C
T _s	soil temperature	°C
T	temperature	°C
t	time	hrs.
h(e)	convective coefficient between the ground surface and ambient air	W/m ² K
h(i,w)	convective coefficient between the basement wall and the inside air	W/m ² K
h(i,f)	convective coefficient between the basement floor and the inside air	W/m ² K

Chapter I

INTRODUCTION

In an era of uncertain energy supplies, interest in building energy conservation has increased steadily during the past few years. Historically there has been a lack of interest in the below grade portion of buildings even though the heat loss can be 10-20% [1] of the total heat loss of an average North American home. But with the advent of super-insulated buildings, the above-grade heat losses have been reduced significantly thereby making the below grade heat loss a more significant component of the total heat loss.

Blich [2] has reported on the benefits of building underground shelters. Earth sheltering uses the earth as a barrier and a moderator. The earth moderates temperature extremes in the air and acts as a barrier to storm and wind effects. An underground building can effect an energy saving of 75% or more.

To date, the only widely accepted procedure for calculating below grade heat loss from basements is that recommended by ASHRAE [3] which is directed towards winter design heat loss for conventional basements. The circular heat flow pattern is assumed to be the only path of heat flow between the basement and ground surface. For insulated

basement walls the same circular heat transfer paths are assumed with the resistance of the insulation added to that of each path.

This approach has some major drawbacks. It is based on a steady-state approximation and does not consider the storage capacity of the soil. When insulation is added to the wall, the heat flow paths are distorted and no longer circular. The ASHRAE method cannot distinguish between the interior and exterior insulation applications.

With the increasing cost of energy, accurate modelling of each component of a building's thermal envelope is necessary. Therefore a more detailed and accurate understanding of the transient heat transfer from basements is needed.

The following sections present a response to these needs. A literature survey investigates previous studies on the factors which effect below grade building heat transfer. A detailed description of the model used to study the transient heat transfer in basements, its validation and a parametric study obtained from it are also presented.

1.1 LITERATURE SURVEY

This survey is divided into two parts. The first is a study of the factors influencing the soil temperatures and soil thermal properties and subsequently basement heat loss. The second is a study of some of the methods used to calculate basement heat loss and ground temperature distribution.

1.1.1 SOIL-TEMPERATURES-

The ground temperature is one of the most important parameters effecting heat transfer in Underground Installations. The ground temperatures are dependant on a number of variables. They may be classified as [4]:-

1. Geographic, including latitude, altitude and solar radiation.
2. Meteorological, including snow cover, rainfall, cloud cover, local air temperature, and wind speed.
3. Site-specific, including topography, surface cover, and shading effects of nearby trees.
4. Subsurface, including the thermal and physical properties of soil, and the level and movement of ground water in the soil.

Geographic distribution of the ground climate has received very little attention from the building industry, which has been concerned mainly with the depth of frost penetration for foundation design. Since no private or public agency has sponsored a national program of ground temperature measurement, existing ground temperature records are scattered and few, collected by individual researchers for their own work, or by state agricultural research stations on their own initiative.

The first recorded measurement of soil temperature studies in Canada were made at McGill University in Montreal (1882-1883) and reported by Callender [5] and Callender and

McLeod [6]. Electric resistance thermometers were installed to a depth of 2.74 m and observations were made on the temperature equalizing effect of rainfall and the insulating effect of snow cover on the soil temperatures near the surface. They showed that daily variations in temperatures occur only to depths of a few centimeters, while changes below 25.4 cm follow an annual cycle. The range of temperature variation decreases with depth below the surface and a nearly constant temperature is reached at about 6.1 m. The respective temperature variations at a depth of 2.54, 10.16, 25.4 and 50.8 cm. were 13.33 C, 10 C, 3.33 C, 1.67 C and 0.56 C. The mean annual soil temperature was shown to be 2.26 C higher than the mean annual air temperature.

Crabb et al [7] studied the influence of vegetative cover on soil temperatures at East Lansing, Michigan. Their studies indicated that solar radiation is an influencing factor on the soil temperatures. But vegetal cover tends to reduce the receipt of solar heat in proportion to the density of that cover. They also showed that the effect of vegetative cover is more widespread than its solar shielding effect. It markedly influences each of the following :-

1. Moisture content at different soil depths:
2. Porosity, permeability, and the aeration of the soil.
3. The length of time snow will remain on the soil surface.

Comparison of air and soil temperatures at depths of 1, 12, 18 and 33 inches were made. Temperatures at the 1 and 12 inch levels showed the hourly effect of atmospheric temperatures and insolation, but at lower depths these effects are negligible. They concluded that soil temperature variations, at the lower depths, are not the result of hourly, or even daily air temperatures, but of accumulations of the heat gradually stored in the soil profile.

Crawford [8] measured ground temperatures and showed that ground surface temperatures are significantly effected by the surface conditions (snow cover etc.) and solar radiation.

Gold [9] demonstrated the influence of snow cover and size of the convective coefficient on the difference between average air and corresponding ground surface temperatures. Observations were made at Ottawa on ground temperatures under a grassed surface and two nearby parking lots, one snow covered in winter and the other cleared. In winter, the monthly average surface temperature of the snow covered parking lot was about 8 C warmer than the lowest monthly average air temperature while that of the grassed site was about 10 C warmer. At the grassed site, the monthly average surface temperature in summer was a little warmer than the average air temperature, but was always within 1.7 C of it. The average surface temperatures of the parking lots were, on the other hand, upto 15 C warmer.

The reflectivity of the surfaces of the parking lots with respect to solar radiation was about the same as that for the grassed surface (about 90% of the incoming solar radiation was absorbed). As the parking lots did not have a cover of vegetation and were well drained, no heat was dissipated by transpiration and evaporation.

In an earlier study at the grassed site, Gold and Boyd [10] showed that during a period of April 1 to September 30 about 48% of the net solar radiation, absorbed by the ground, was dissipated by evapotranspiration, about 42% by longwave radiation, and about 7% by convection, and that only 3% was conducted into the ground.

Soil surface temperatures in six one-meter square plots with different soil covers were studied by Johnson and Davis [11]. The maximum surface temperatures for tarmac, bare ground and grass soil covers were 53.33 C, 47.78 C and 38.33 C, respectively, with a corresponding maximum air temperature of about 26.57 C.

Kusuda [12] studied soil temperatures under five different soil covers. The summer month asphalt covered surface was 8.3 C warmer than the average air temperature, while the grass cover remained consistently below ambient conditions by about 0.6 C to 3.9 C. The asphalt covered surface eliminates the effect of transpiration and evaporation and this accounts for the higher temperatures of the asphalt surface.

Gilpin and Wong [13] have developed a model to predict the effects of variable surface covers on the surface temperatures.

The most influential ground climate work has been performed by T. Kusuda and P.R. Achenbach of the National Bureau of Standards [14]. The work was commissioned by the Department of Civil Defence in order to obtain a method for estimating the natural ground temperature, which would provide a basis for determining the equipment requirements for ventilation, air conditioning and heating of various size fall-out shelters. They collected available ground temperature records for forty-seven different locations in the United States. The data for each station were analyzed by a least square procedure to obtain a best fit to a simplified sinusoidal temperature model.

Chang [15,16] has prepared global maps of estimated ground temperature at depths of 4 inches, 12 inches and 4 feet. The annual amplitude of the 4 inch depth is almost identical with that of the surface, so Chang's map of North America has been used for calculating basement heat losses by ASHRAE (1977).

1.1.2 SOIL THERMAL PROPERTIES

An understanding of the fundamental mechanisms involved in heat flow through the soil is required before accurate prediction techniques can be developed for determining the

heat transfer from basements. Soil thermal properties are very difficult to define precisely because of the influence of density, porosity, moisture content, soil type and temperature, which are all functions of time and depth. Considerable work has been done by researchers to better define these parameters.

Smith [17] determined the thermal conductivities of a number of soils using a guarded hot box method under steady-state conditions. The soil samples were disintegrated and repacked during the testing. The thermal conductivities were considerably decreased when the soils were reduced to a finely fragmented state.

Kersten [18] used a steady-state method for determining thermal conductivities in which a heating element is placed in the center of a cylindrical soil container. He concluded that the thermal conductivity increases almost linearly with an increase in moisture content, provided the soils were below the saturation point.

De Vries [19,20] presented a theoretical treatment of the influence of moisture vapour diffusion on the apparent thermal conductivity of soils. The apparent thermal conductivity of the soil was composed of two components; the real conductivity and a vapour migration term. The main factor which increases the vapour conductivity term is the temperature.

Kimbell et al [21] provided a summary of this procedure and examined the accuracy of the theory by comparing it with measurements and with a survey of empirical investigations. By doing this, it was observed that the soil heat flux prediction is not improved by the inclusion of the isothermal vapour flux for intermediate and low-moisture contents and that a good prediction of the soil heat flux can be obtained based on conduction.

Rollins et al [22] studied the relative amounts of liquid and vapour moisture migration under a thermal gradient under steady-state conditions. He concluded that the predominant method of soil moisture movement is not in the liquid state.

Kersten [23] carried out tests on 19 different soils which represented a wide textural variety, gravel, sand, sandy loam, silt loam, and clay, as well as some crushed rocks and a fibrous peat. Moisture contents for the test varied from air-dry to values greater than the optimum moisture content. The densities varied from a loosely poured condition to the maximum obtainable by heavy ramming. He found that density affects the thermal conductivity in about the same manner for all soils, at any moisture content, and for either frozen or unfrozen conditions. On the average, each one pound per cubic foot increase in density increases the thermal conductivity by about three percent. An increase in moisture content causes an increase

in the thermal conductivity. This is true up to the point of saturation. The thermal conductivity of a soil, at a given density and moisture content, varies in general with the texture of the soil, being relatively high for coarse textured soils and relatively low for fine textured soils. The mineral composition of the soil also affects the conductivity. Quartz tends to give high values whereas minerals such as plagioclase feldspar and pyroxene, which are constituents of basic rocks, tend to give low values of thermal conductivity.

Baladi et al [24] used a one-dimensional (spherical) transport model to predict the coupled heat and moisture migration phenomena in soils under truly transient conditions. Solutions for theoretical calculations were compared to experimental measurements. He concluded that soil energy transport is aided by higher moisture content and that dry soils, and slightly less accurately well-graded soils, can be modelled quite accurately by using pure heat conduction.

It is seen from this portion of the literature survey that the uppermost levels of the soil are greatly affected by the irregularities of radiation, surface cover, wind and rain. This complicates the thermal processes and makes thermal modelling very difficult. Despite the thermal irregularities of the surface regime, thermal processes in the soil below a depth of 2 or 3 feet can be described

remarkably well over the course of a year by the heat conduction theory. The development of a semi-infinite solid with periodic temperature variation at the surface is discussed in texts by Carslaw and Jaeger [25], Ingersoll [26], and Junikas [27].

1.1.3 BASEMENT HEAT LOSS STUDIES

One of the earliest methods for calculating basement heat loss was derived from research performed by Houghten et al. [28] at the ASHVE Research Laboratory. Houghten constructed a totally earth covered room, 4.57 x 4.57 x 2.44m in dimension with the walls and floor constructed of concrete, and two walls and the roof covered with 2.54cm thick structural insulation board. Based on his work, the resulting accepted design practice for determining heat loss through the walls of a basement was to determine the basement floor heat loss prior to calculating the wall heat loss. The floor heat loss was based solely on the deep ground temperature, which was equated with the ground water temperature, with no further provision for depth, soil type, climate, or seasonal variations. An overall transmission coefficient for the heat conduction path from the basement air to the deep ground temperature was taken as 0.57 w/m C. The below grade wall heat loss was assumed to be twice the basement floor heat loss. This method was adopted by ASHRAE to estimate winter design heat losses and is given in the pre - 1977 ASHRAE Fundamentals.

A very thorough analysis of an underground survival shelter using a transient three-dimensional finite difference analysis was presented by Kusuda and Achenbach [29]. Comparisons of calculated and experimental data showed good agreement. But this study was limited to a small structure and was carried out for a short-term occupancy (14 days). The soil was considered to be homogeneous with no soil moisture movement.

Boileau and Latta [30] devised an approximately graphical procedure to determine winter heat loss from basements. In this procedure the heat flow from the basement wall is assumed to travel along circular paths centered on the intersection of the ground surface and basement wall. For the floor these paths are continued around circular arcs centered on the intersection of the basement floor and wall. The heat flow paths are shown in Figure 1. The basic heat flow equation used is:-

$$dQ = K \Delta T dA/L \quad \text{----- (1)}$$

The length of the heat flow path, L , is the circular arc length centered on the intersection of the ground surface and the face of the basement wall, plus an allowance to express the thermal resistance of the wall, internal wall and external soil surface air films and insulation as equivalent thickness of the soil. The total basement wall heat loss is determined by integrating equation (1) over the full depth of the wall.

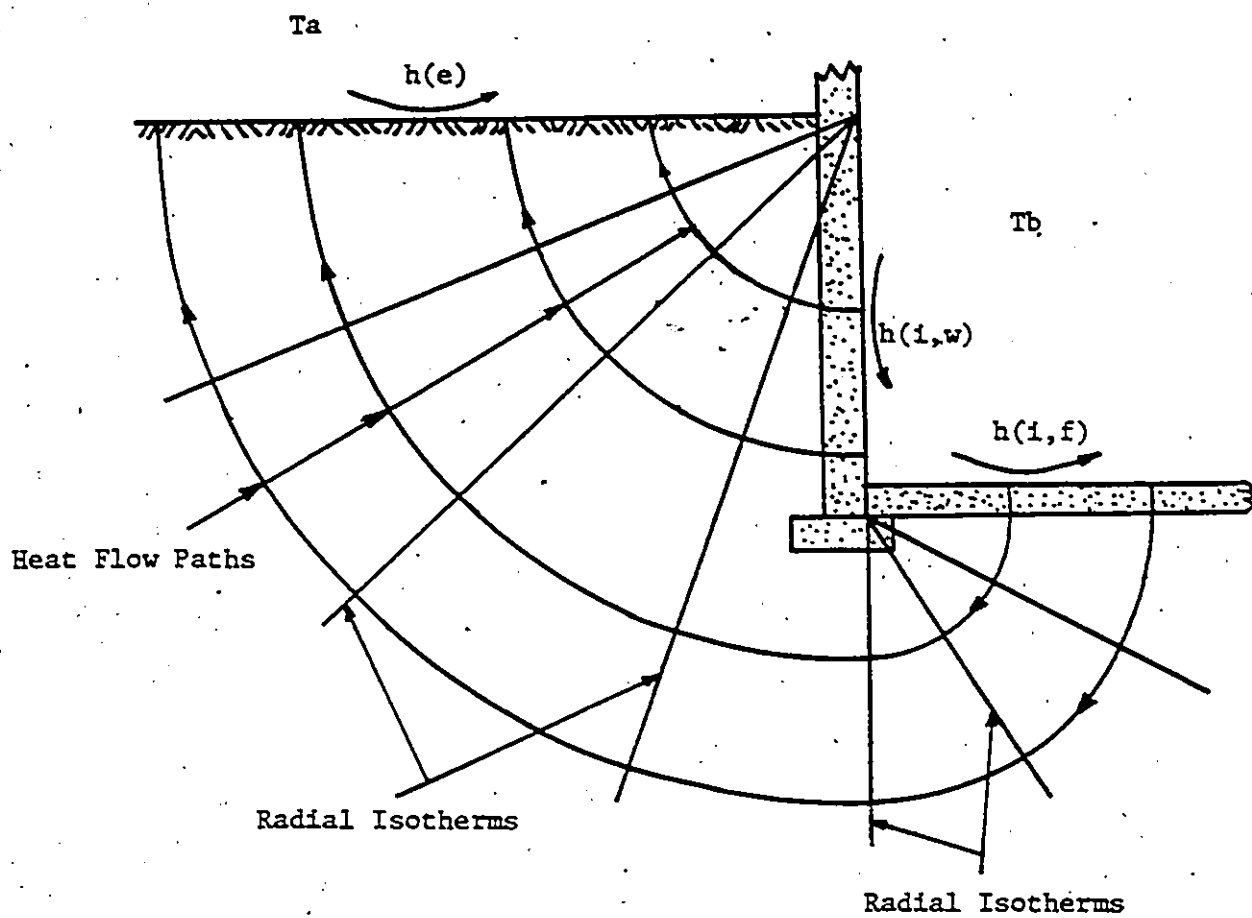


Fig.1. Heat flow from basement to ground surface.

This procedure has been recommended by ASHRAE and is published in the ASHRAE Handbook of Fundamentals (1977,1981). This procedure is based on the assumption that during the course of the winter months a steady-state condition is developed. The ground surface is considered the only sink. Deep ground temperatures are disregarded on the basis that the walls are more closely coupled to the surface than to the deep ground, and that most of the floor area of a residential basement is also more closely coupled to the surface than to the deep ground. This assumption would not be true if the basement were located below ground water characterized by an appreciable flow.

McBride et al [31] instrumented a basement and recorded data during one complete year. A transient two-dimensional finite difference calculation procedure was developed for determining the hourly heat loss from the basement. The comparison of calculated results and experimental data showed very good agreement. Soil thermal conductivity variations throughout the year were modelled by periodic changes in the soil thermal conductivity during the model operation. Solar radiation intensity at the ground surface, the freezing and thawing of the soil and moisture migration was neglected in an effort to reduce the complexity of the model. McBride's experimental results have been used in the present study to validate HEATING 5.

Szydlowski et al [32] developed a transient two dimensional finite difference technique to calculate basement heat losses. The basement used by McBride was used as the test basement. Their model considered different types of below grade configurations, the effects of earth berming, and analysis of the thermal impact of varying level of interior and exterior insulations on conventional basements, earth-bermed walls, and earth covered structures. An economic analysis was also done to indicate the cost-effectiveness of the insulation levels analyzed. Changes in soil thermal conductivity caused by variations in the soil moisture content were approximated by including time-varying soil thermal properties in the model. The latent heat of fusion of soil moisture under freezing and thawing conditions and the latent heat of vapourization during surface drying were not considered.

Wang [33] developed a two-dimensional finite element computer program and studied the effects of insulation placement on the basement heat losses. He concluded that:-

1. Exterior wall insulation applications are 25 to 32% more efficient than interior applications.
2. Box sill and sill plate insulation have a significant impact on foundation heat loss. They may reduce the heat loss through the foundation wall by 20 to 36%.
3. Insulation located near the top half of the wall is more beneficial than insulation placed at the bottom of the wall.

Meixel et al [34] developed a transient, finite difference computer program to study the impact of insulation placement on the seasonal heat loss through basement and earth sheltered structures. They presented evidence for the possibility of freeze/thaw or frost-heave damage due to inappropriately insulated basement walls and demonstrated the benefits to the annual energy balance that can be achieved through appropriate insulation to take the maximum advantage of both the thermal buffering characteristics of the soil mass and its potential as a heat sink.

Ship et al [35] developed a transient two-dimensional finite difference analysis to predict the thermal characteristics of a large earth sheltered building that penetrated beyond a single storey below the ground surface. Data from Williamson Hall (at the University of Minnesota) were successfully used to validate the model. The effect of wall insulation depth and thickness, pavement versus sod covered ground cover, effect of soil berms and soil property changes were presented in their study.

According to Swinton and Platts [36], there are many variables to be determined while calculating basement heat losses. These variables have defeated all attempts of mathematical analysis and computer based modelling. They have developed an engineering method for estimating basement heat losses and insulation performance. This method is

offered as a fit against monitored cold-country conditions. The engineering method can be used directly when the soil is not very wet or subject to moving water in winter, and where snow cover is present over much of the winter.

G.P. Mitalas [37] of the National Research Council, Ottawa, has devised an empirical method for predicting monthly values of the basement heat losses. This method is based on actual measurements and computer simulations of actual basements. He concluded that the basement temperature, soil thermal conductivity, and ground water level significantly influence the basement heat losses.

Raff [38] has suggested the possibility of altering the ground temperatures to suit the needs of an underground structure. This can be achieved by having different soil covers, paving, south facing slope or glazing.

1.2 OBJECTIVES

In view of the literature survey, it is seen that there has been very little transient thermal modelling of basements in which annual time spans are considered. Most of the techniques are capable of handling limited geometries.

In an effort to provide some added insight on the thermal response of earth sheltered structures, a transient finite - difference computer program sufficiently general to accommodate numerous earth sheltering configurations was acquired. This HEATING 5 [39] computer program was selected

on the basis of its versatility and ease in programming. This program was validated against one complete year of experimental data acquired from an actual residence basement by McBride [31] in Ohio.

Several assumptions are made to simplify the basement analysis. Changes in the moisture content and heat transfer by moisture movement are not explicitly calculated. These effects are incorporated by including time-varying thermal properties of the soil. All soil/air interface boundary heat transfer is characterized by associated uniform convective coefficients. The heat transfer from the basement is assumed to be two-dimensional. This assumption is valid throughout the basement wall except for regions near the corners. This has been assumed by Wang [33], Mitalas [37], and Szydlowski [32].

A parametric study was made to investigate the effects of the following parameters on the basement heat losses. They are:-

- 1) Soil thermal conductivity
- 2) Proximity to adjacent structures
- 3) Ground water level
- 4) Ground surface conditions
 - a) Snow cover
 - b) Asphalt cover
- 5) Insulation placement
 - a) Full length placement on exterior wall
 - b) Half length placement on exterior wall

6) Basement Temperature

Such an analysis is important because the effect of most of the above-mentioned parameters, except for insulation placement, have not been studied by other researches. Their effects have only been speculated.

It is common practice to assume a constant thermal conductivity for the soil surrounding the basement. If exact values are not known the mid-range values are chosen. The effect of choosing mid-range values or incorrect values of the soil thermal conductivity on basement heat loss are studied. The effect of adjacent structures, different ground water levels, and ground surface conditions are quantified in this study. This study is limited to relatively shallow basements (i.e. basements that extend to about 2 meters below grade).

This work is essential because it presents a better understanding of basement heat losses. It defines the important parameters which have to be considered while calculating basement heat losses.

Chapter II

HEATING 5 COMPUTER PROGRAM

This program has been developed at the Oak Ridge National Laboratory by W.D. Turner, D.C. Elrod and I.I. Siman-Tov. It is designed to solve steady-state and/or transient heat conduction problems in one-, two-, or three-dimensional coordinates. The thermal conductivity, density, and specific heat may be both spatially and temperature dependant. Materials may undergo a change of phase. The boundary condition parameters may be time and/or temperature dependant. The mesh spacing can be variable along each axis.

It includes a temperature distribution plotting program, HEATPLOT, which can be used with the plotting data set produced by HEATING 5, to plot temperature contours (isotherms), temperature - time profiles, and temperature - distance profiles.

The steady-state finite difference equations are solved by the point successive overrelaxation iterative method and a modification of the Aitken delta **2 extrapolation process.

The transient problem may be solved by an implicit technique or an explicit method. The solution of the

equations arising from the implicit technique is accomplished by the point successive overrelaxation iteration, and includes procedures to estimate the optimum acceleration parameter.

HEATPLOT approximates contour plots by using the quadrilaterals formed by four nodes. The temperature at the center of the quadrilateral is taken as the average of the temperatures at the four nodes. The quadrilateral is then divided into four triangles, and each side of the triangle is tested to determine if the contour line passes through that side.

The HEATING 5 computer program has the following limitations:-

- a) 3700 lattice points per 1 megabyte of core
- b) 100 regions
- c) 50 materials
- d) 50 boundary conditions
- e) 5 materials with change of phase capabilities.

All of the above-mentioned features were not used during this analysis. A two-dimensional analysis was selected along with time varying thermal properties and boundary conditions. A variable mesh spacing was chosen so that accurate results could be obtained in a shorter time period. The transient problem was solved by the implicit (Crank Nicolson) technique. HEATPLOT was also invoked to get the temperature-time (isotherms) profiles.

2.1 SIMULATION PROCEDURE

This chapter explains how the HEATING 5 program accepts the input to the heat transfer problem. It will explain how to represent the geometric configuration of the problem with a lattice of points. In preparing the input data, any consistent set of units may be used in the program except for problems involving radiation. Then, all temperature units must be in either degrees centigrade or Fahrenheit.

2.1.1 REGIONS

The configuration of the problem is approximated by dividing it into regions, depending on the shape, material, indentations, cutouts and other deviations from the general geometry. In some cases, zoning into regions must be done in order to describe a specific boundary condition or a material whose thermal conductivity, density or specific heat is a function of position. There are three rules governing the region division. They are:-

1. Boundary lines or planes must be parallel to the coordinate axis (two points, four lines, or six planes are required to enclose a region in one-, two-, or three-dimensional geometry, respectively).
2. A region may contain only one material. However the same material may be contained in a number of regions.

3. When a boundary condition is defined along the boundary of a region, it must apply along the full length of the boundary line for a two-dimensional problem and over all of the boundary plane for a three-dimensional problem.

The three rules for defining a region may be better understood if we are to refer to Figures 2a & 2b. A two-dimensional rectangular model is considered. There are two materials, material 1 and material 2. The various boundary conditions on those materials are shown in Figure 2b.

It is seen the boundary lines are parallel to the coordinate axis. To satisfy the second rule, the configuration can be divided into 2 regions (on the basis of the materials only). If the upper right corner of the material is omitted as is in Figure 2a, three regions are required, although regions 2 and 3 contain the same material.

Now the boundary conditions are considered and zoning is done on the basis of rule 3. The left boundary of the left-most rectangle contains 2 different boundary types. Therefore zoning is done to satisfy rule 3. The region 1 is now divided into 2 regions, i.e. 1 and 4. The regional description of the two-dimensional model is shown in Figure 2b.

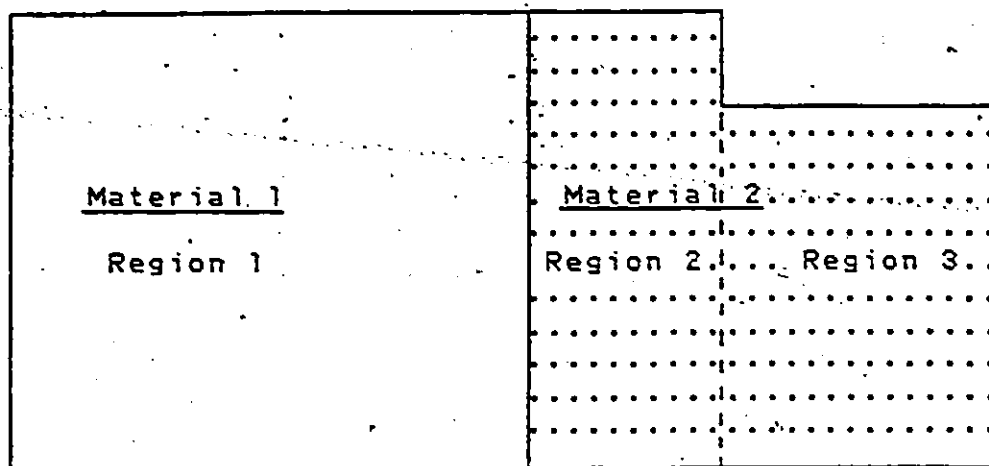


Fig. 2a. Region division according to rule 1 and 2

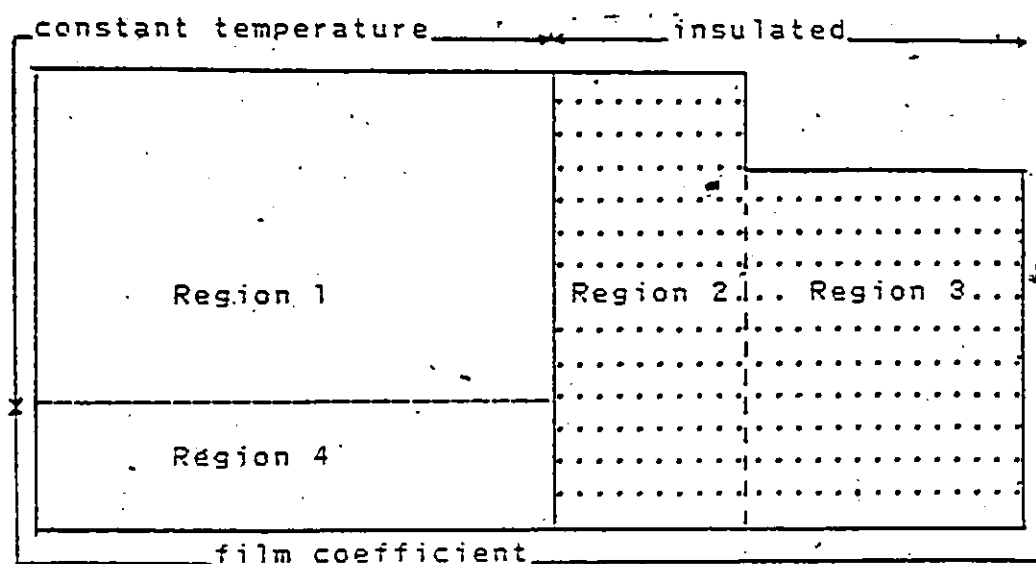


Fig. 2b. Region division according to boundary conditions

2.1.2 LATTICE ARRANGEMENT

The second requirement for describing the overall configuration is to construct a set of lattice lines perpendicular to each axis and extending the entire length of the remaining co-ordinates. The lattice lines are actually points, lines, or planes for a one-, two-, or three-dimensional problem. The lattice is defined in the following manner. The lattice lines are divided into two classes: gross lattice lines and fine lattice lines. A gross lattice line must be specified at both region boundaries along each axis. Fine lattice lines, which are equally spaced, may appear between two consecutive gross lattice lines to create a finer mesh. If unequal mesh spacing is desired within a particular region, then gross lattice lines may appear within that region. A nodal point is defined by each lattice point in one-dimensional problems, by each intersection of two lattice lines in two-dimensional problems, and by each intersection of three lattice planes in three-dimensional problems.

2.1.3 ANALYTICAL AND TABULAR FUNCTIONS

The analytical and tabular functions are built in functions which may be used to aid in the description of some of the input parameters. The analytical function in this program is:-

$$P(v) = A_1 \cos(X) + A_2 \cos(2X) + A_3 \cos(2X) - A_4 \cos(3X)$$

$$+A_5 \cos(3X) + A_6 \sin(X) - A_7 \sin(2X) + A_8 \sin(3X) \\ - A_9 \sin(3X) + A_{10} \sin(3X)$$

where $X = 2\pi (v/24 + A_{11})/365$, and $A_1 - A_{11}$ are constants that are inputted into the program to describe the analytical function.

A tabular function is defined by a set of ordered pairs, where the first element of a pair is the independent variable and the second is the corresponding value of the function. In order to evaluate the tabular function at some point, the program uses linear interpolation in the interval containing the point. A set of ordered pairs must be chosen so that the independent variable is arranged in ascending order.

2.1.4 BOUNDARY CONDITIONS

HEATING 5 possesses a variety of boundary conditions to enable the modelling of the physical problem as accurately as possible. The boundary condition is applied along a surface of a region and heat is transferred from a surface node to a boundary node or to the corresponding node on the opposing parallel surface. The boundary conditions which can be applied over the surface of a region are listed below:-

1. The temperature on the surface of a region can be specified as a constant or a function of time.

2. The heat flux across the surface of a region can be specified directly as a constant or a function of time and/or surface temperature.
3. The heat flux across the surface of a region can be specified indirectly by defining the heat transfer mechanism to be forced convection, radiation and/or natural convection.

Simulation is not required for insulated boundaries. Heat is not allowed to cross the surface. The boundary conditions are classified as either surface-to-boundary (type 1), isothermal (type 2), or surface-to-surface (type 3). Boundary conditions of the surface-to-boundary type are used to define heat transfer between a surface node and a boundary node. The temperature of the boundary node is specified and can be a function of time. Surface nodes are actually internal nodes which are located on the edge of the region. Boundary nodes are dummy nodes and their temperatures are not calculated by the program but are specified as an input to the model. Surface-to-surface boundary conditions are used to define heat transfer between parallel surfaces. In this case heat is transferred between a node on one surface to the corresponding node on the opposing surface. A more detailed description of the simulation technique can be referred to from the Reference Manual prepared by the Union Carbide Corporation, Nuclear Division [39].

A description of the Numerical technique used by the HEATING 5 program is listed in Appendix A and a reference manual has been compiled to use HEATING 5 for basement heat loss calculations and is listed in Appendix B. A sample problem along with the job control cards required to run the program on an IBM 3031 System are presented on Appendix C. Appendix D contains the instructions required to run HEATPLOT (the plotting program) and also contains an example along with the job control cards required to run this program on the ZETTA plotter (Model 1453SX).

Chapter III

MODEL ASSUMPTIONS

Several initial simplifying assumptions have been made to develop a manageable and reasonably accurate model. Changes in the moisture content and heat transfer by moisture movement are not explicitly calculated. These effects are approximated by including time-varying thermal properties in the model. The latent heat of fusion of soil moisture under freezing and thawing is not considered. All soil/air interface boundary heat transfer is characterized by associated uniform convective coefficients. In all calculations except one, radiation and evapo-transpiration are neglected. It is assumed that the heat gained by solar insolation at the ground surface is offset by the heat loss due to evapo-transpiration and long wave radiation from soil to air. The deep ground water flow is assumed to be such that the temperature remains constant throughout the year.

The model considers a two-dimensional cross-section, bounded by a vertical adiabatic center line and a second vertical adiabatic boundary sufficiently removed to minimize its impact on the basement heat loss.

A variable grid size has been chosen to get accurate results in shorter time periods. The grid spacing near the

basement wall is about 15 cm. and that near the the basement floor is about 20 cm. A grid size of 444 nodes was chosen. A similar analysis was performed with 880 nodes (with a closer grid spacing away from the basement walls and floor). There was no significant change in the wall and floor heat loss. Therefore the use of 444 nodes can be justified in an effort to save computer time.

The lower horizontal boundary consists of an isothermal sink (set at the deep ground water temperature) and the upper horizontal boundary is set by a seasonally varying convective film coefficient.

The forcing functions for the heat conduction model are the temperatures of the ground water table, basement air and ambient air.

3.1 MODEL VALIDATION

The HEATING 5 computer program is validated against data acquired from an actual basement in Columbus, Ohio, by McBride [31] who instrumented a basement and recorded data for a complete year. The residence selected for the study was an unoccupied house that was built specifically for extensive testing purposes as a part of a research project. A description of the residence can be found in references [40,41,42]. Instrumentation of the test basement consisted of temperature probes located at different levels along an outside basement wall and at distances of 0.91m and 1.83m

from the basement wall. Figure 3 shows the location of the temperature probes. Since the house was built before instrumentation began, temperatures below the basement floor could not be measured. Temperatures at two locations in the soil, outside surface of the basement wall, ambient air and interior basement air were recorded daily at 4.00 p.m. by McBride. The basement wall (concrete blocks) and floor (poured concrete) thermal properties were extracted from ASHRAE. Earth thermal properties were extracted from Smith [43]. The thermal conductivity of earth in the Columbus region ranges from 0.69 to 2.42 W/m C depending on the soil density, moisture content and composition. McBride selected a mid-range value of the thermal conductivities and varied them to account for moisture effects. These values were considered in the model analysis.

The thermal properties of the basement floor, wall and soil are listed in Table 1a. The surface film coefficients are listed in Table 1b. Figure 4 shows a diagram of the assumed model.

Fourier curve fits of the ambient air and basement air temperatures are used as inputs to the model. The third order Fourier fit of the ambient air temperature according to Szydlowski [32] is :-

$$T_a = 13.65 + 1.321\cos(Z) + 1.072\cos(2Z) + 0.8706\cos(3Z) \\ + 4.271\sin(Z) + 0.425\sin(2Z) - 1.181\sin(3Z)$$

and the Fourier fit of the basement air temperature is:-

$$T_b = 22.355 + 3.328\cos(Z) + 0.548\cos(2Z) - 0.735\cos(3Z)$$

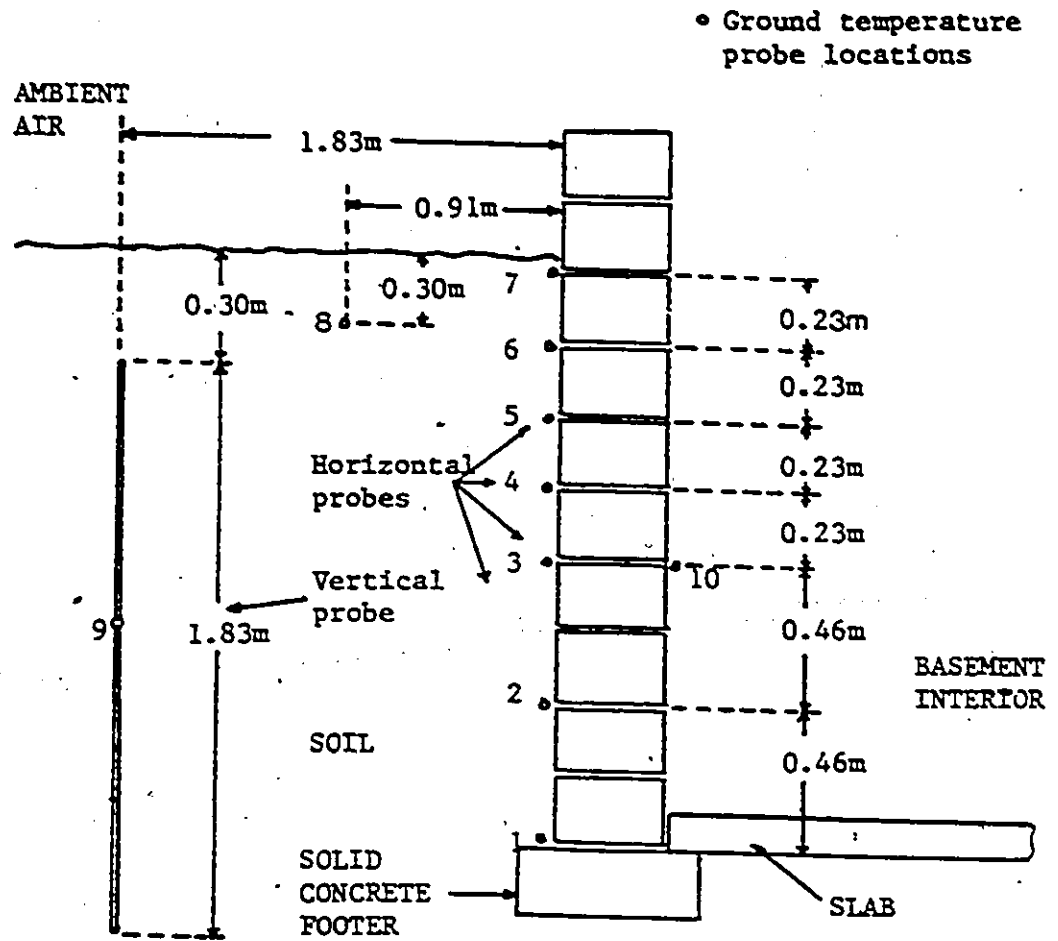


Fig.3. Ground temperature locations for The Ohio house.

Table 1a. BUILDING AND SOIL PROPERTIES

ELEMENT	DENSITY (kg/m ³)	SPECIFIC HEAT (KJ/kg C)	THERMAL CONDUCTIVITY (W/m C)
Basement Wall	977	0.84	1.16
Basement Floor	2243	0.84	1.73
Soil (Nov.-Mar)	1922	1.67	1.99
Soil (Apr)	1922	1.67	1.38
Soil (May-Sept)	1922	1.67	1.21
Soil (Oct)	1922	1.67	1.38

Table 1b. SURFACE CONVECTION FILM COEFFICIENTS

BOUNDARY	CONVECTIVE COEFFICIENT (W/m ² C)
Soil/Ambient Air	
November-March	34.07
April	28.39
May-September	22.71
October	28.39
Building Interior	
Floor	6.13
Wall	8.29

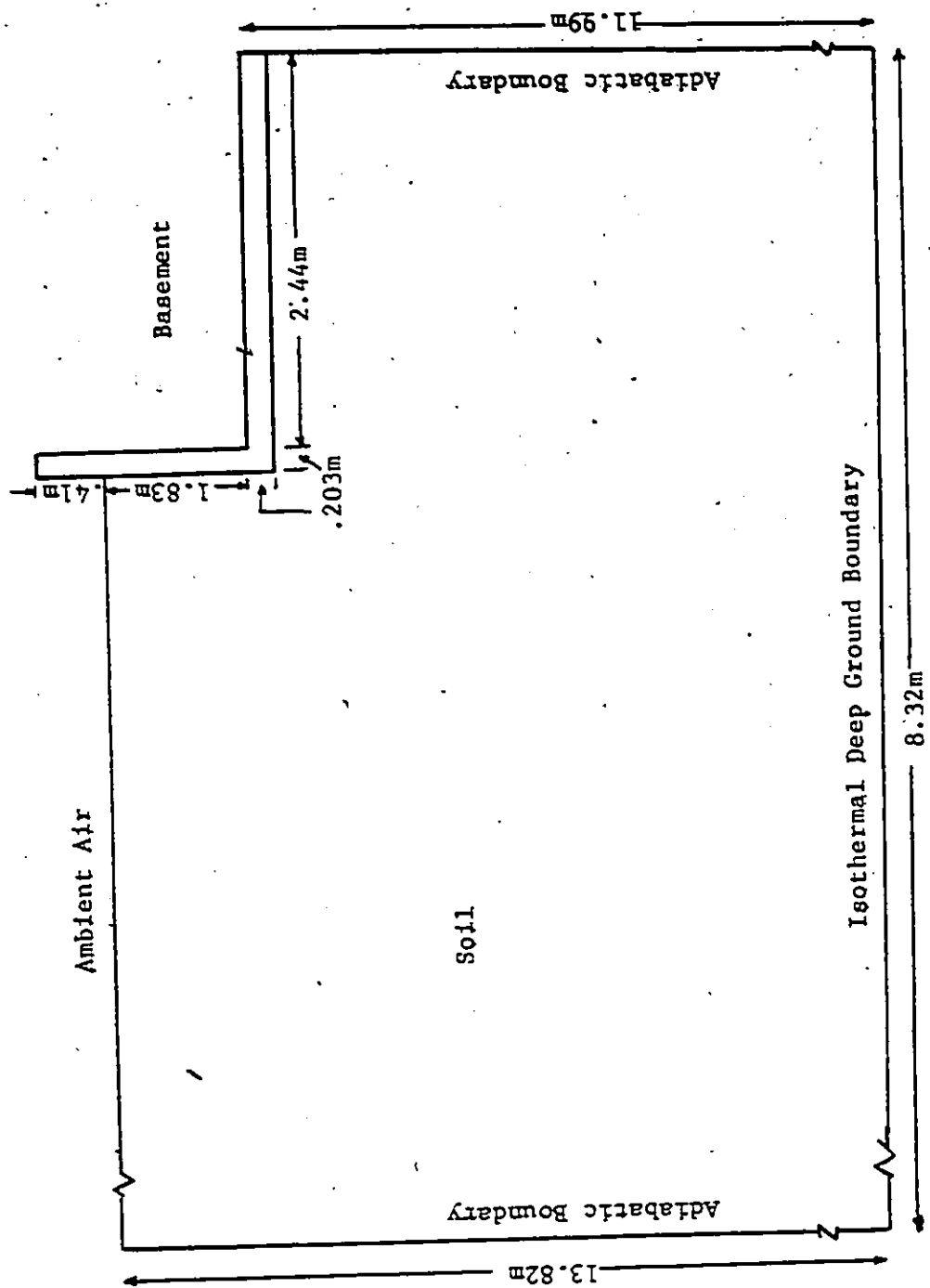


Fig. 4. Basement model showing boundary conditions.

$$+1.263\text{SIN}(Z) -0.334\text{SIN}(2Z) +0.8\text{SIN}(3Z)$$

where $Z = 2\pi(t/24 + 183)/365$ and t is in hours starting from January 1.

Figures 5 and 6 show the measured and Fourier fit of the measured ambient air and basement air temperatures respectively.

A variable grid size has been chosen to better predict the basement heat loss. The grid spacing near the basement wall is about 15 cms and the grid spacing near the basement floor is about 20 cms. A time step of 5 days is used for the model analysis. The simulation procedure involves the use of both the steady-state and transient models. The steady-state model is used to obtain a temperature distribution which is then used as an input to the initial temperature distribution for the transient model. Studies by Szydlowski [32] have shown that this type of analysis reduces the transition period between the initial steady-state solution and the transient solution to about 4 months (i.e. it takes about 4 months for the soil to warm up to actual conditions). During this analysis a 6 month warming period is assumed and the results for the first 6 months are discarded. The Crank Nicolson method is used because it is stable for all time steps.

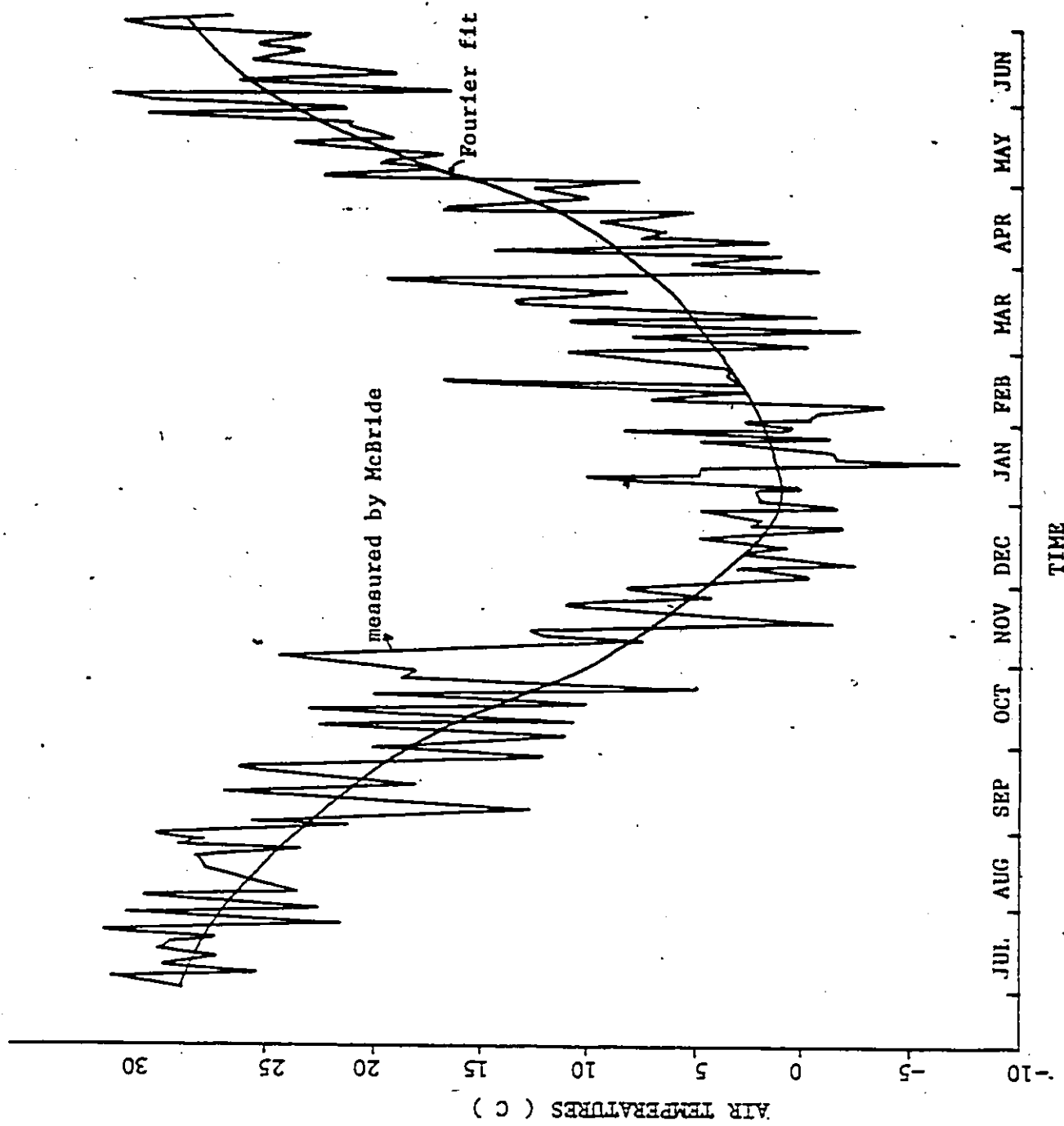


Fig.5. Dry bulb air temperatures.

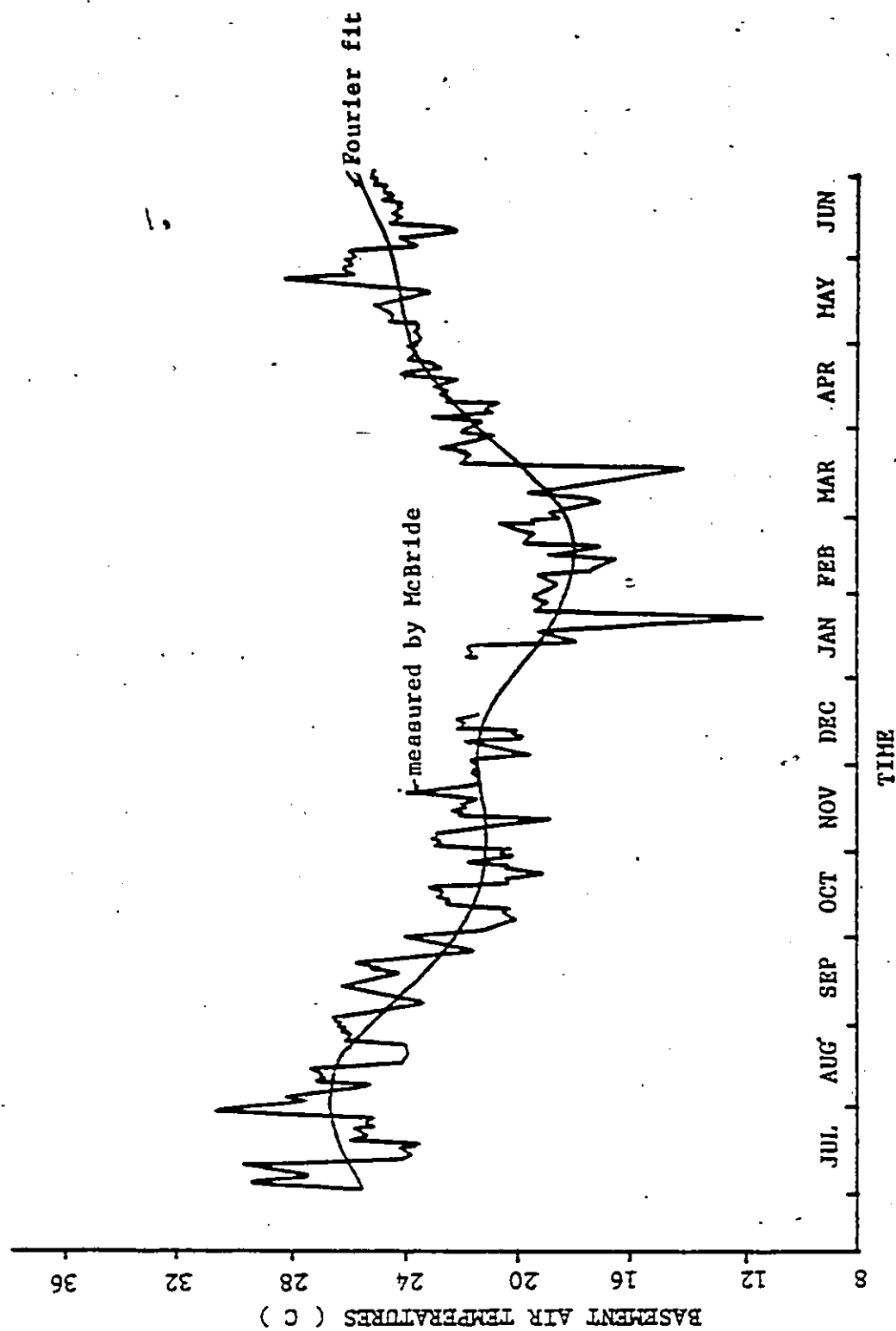


Fig.6. Basement air temperatures.

3.1.1 RESULTS

Figure 7 illustrates the relationship of the calculated average basement wall outside surface temperature and a third order Fourier curve fit of the corresponding recorded data. Results for the two locations in the soil (0.91m from the basement wall and 0.61m deep, and 1.83m from the basement wall and 0.3m to 2.13m deep). are also presented in Figures 8 and 9. Table 2 lists the monthly average below grade wall heat loss calculated by McBride from the measured temperatures and those calculated by HEATINGS 5. The maximum monthly below grade wall heat loss during the heating season is within 8% of that calculated by McBride. But the average yearly agreement is excellent. It is within 1.1% of that calculated by McBride. Considering the simplifying assumptions incorporated in the model, the results are in very good agreement.

The ASHRAE procedure was then used to calculate the below grade wall heat loss using the actual soil thermal conductivities for Columbus, Ohio. It overpredicted the wall heat loss by 32.9% and 25.5% for the months of January and February. The method presented by the 1981 ASHRAE Fundamentals [3] assumes a soil thermal conductivity of 1.38 W/m K. The design heat loss calculated by this method is 7% higher than that reported by McBride (for the month of February).

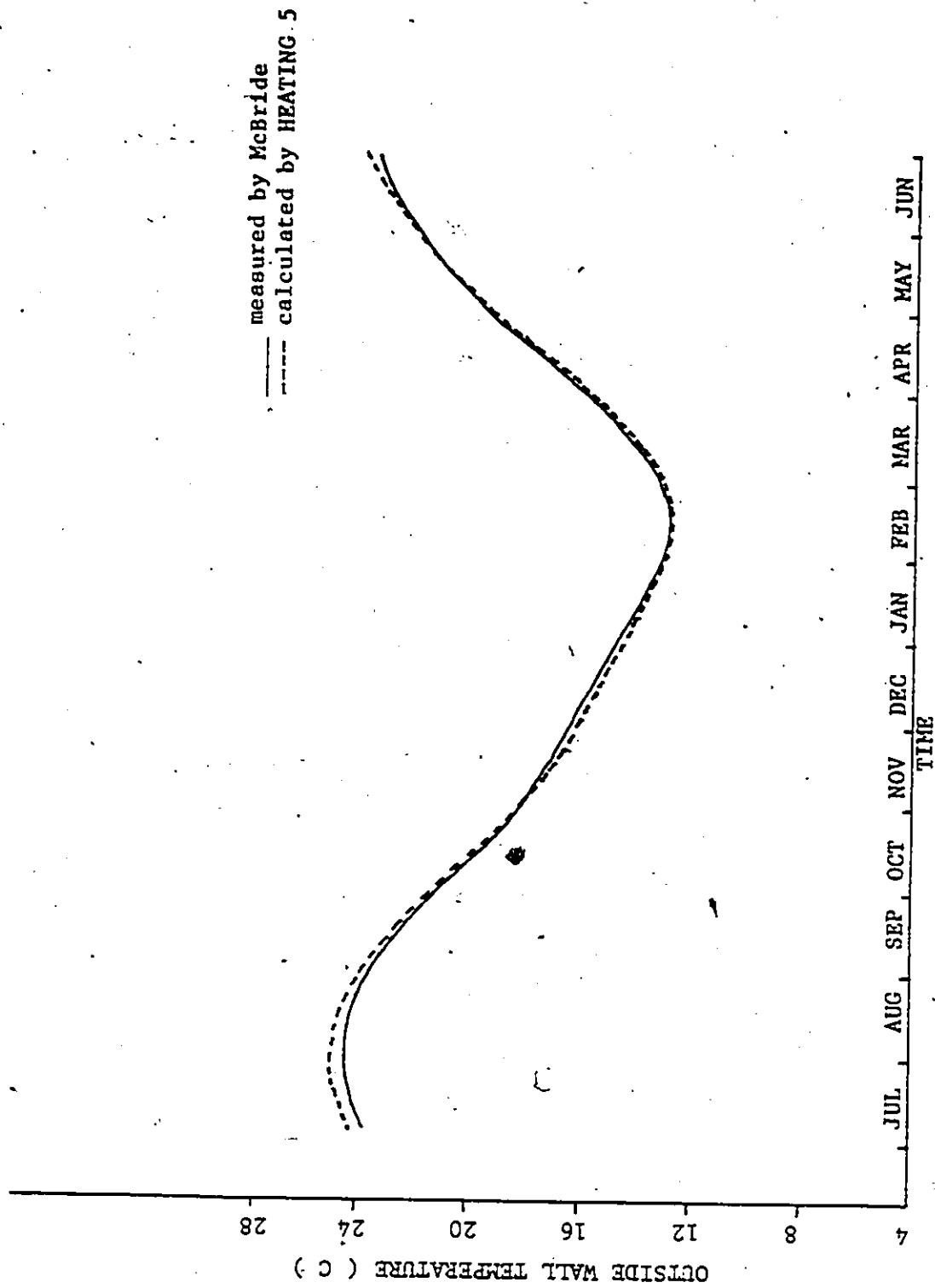


Fig.7. Average outside basement wall temperatures.

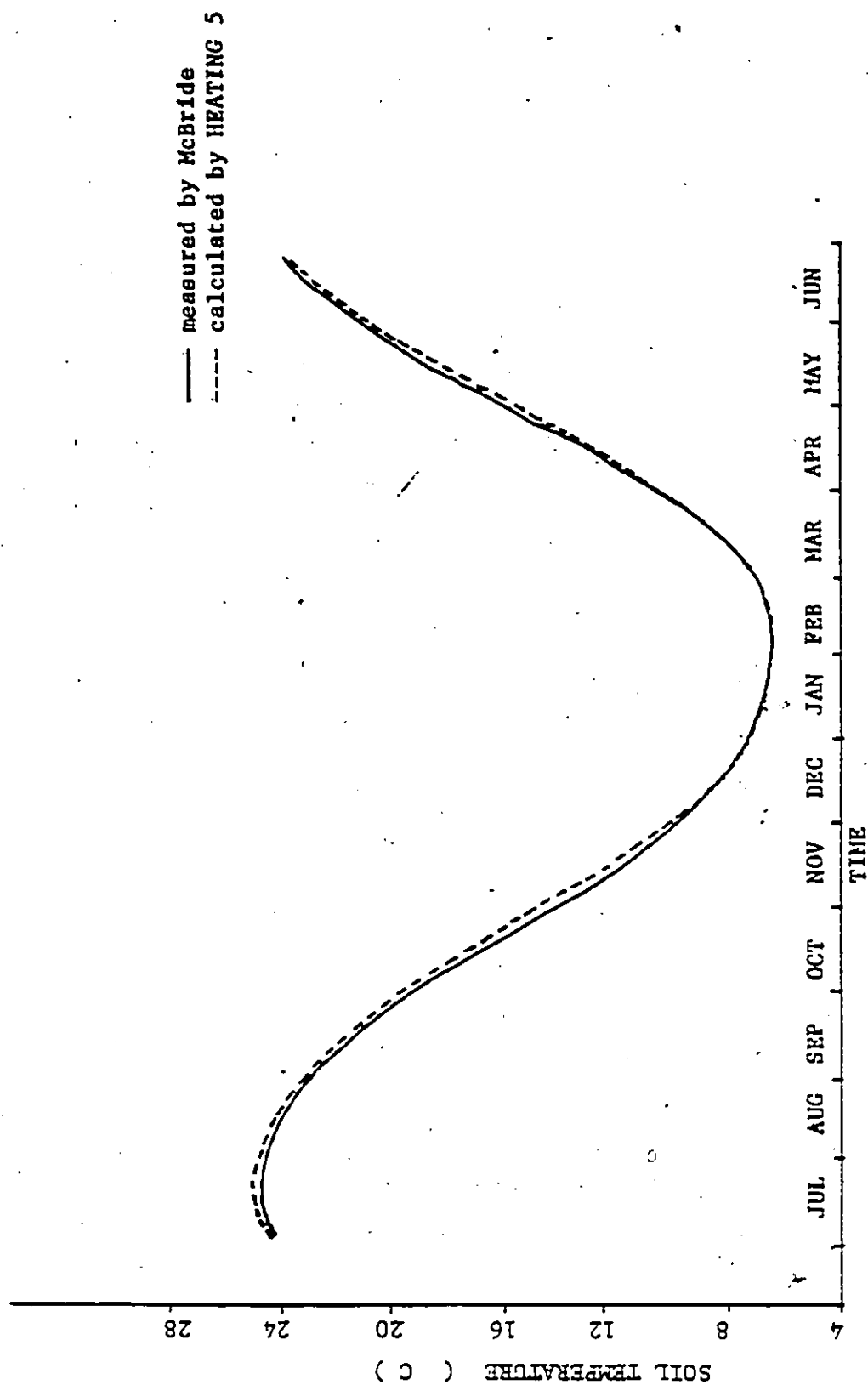


Fig. 8. Soil temperature at 0.9m away from the basement wall and 0.6m deep.

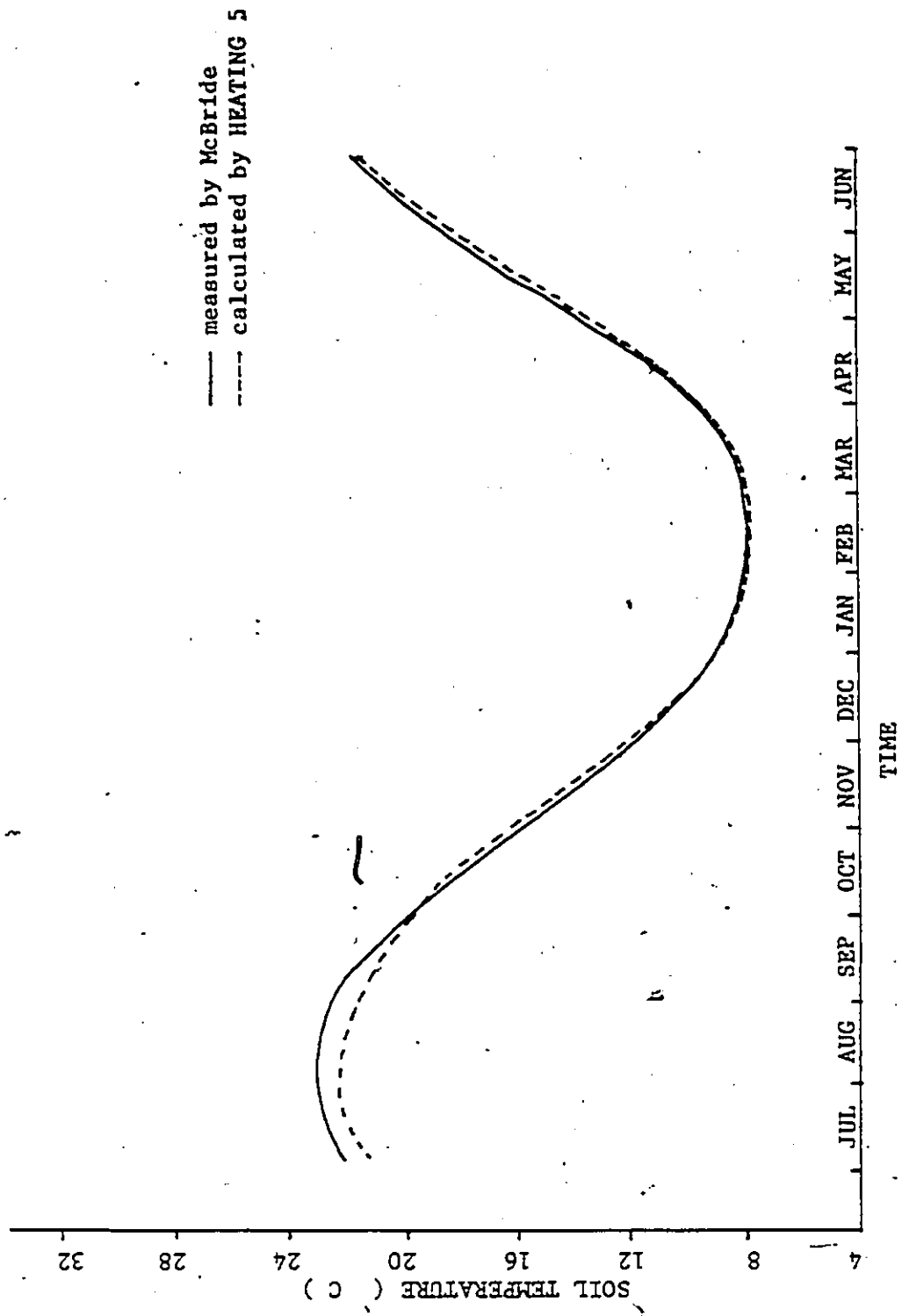


Fig.9. Soil temperature 1.8m from the basement wall and 0.3m to 2.13m deep.

Table 2. Comparison of monthly average below grade wall heat loss using HEATING 5 and values calculated by McBride.

MONTH	CALCULATED BY MC BRIDE FROM MEASURED TEMPERATURES (W/M ²)	CALCULATED BY HEATING 5 (W/M ²)
JULY	8.42	6.17
AUGUST	5.08	5.23
SEPTEMBER	4.13	4.84
OCTOBER	5.08	4.68
NOVEMBER	11.86	12.81
DECEMBER	17.70	17.73
JANUARY	16.03	16.40
FEBRUARY	17.13	16.88
MARCH	17.51	18.12
APRIL	17.32	17.64
MAY	11.29	10.93
JUNE	5.46	4.22
YEARLY AVERAGE	11.42	11.30

HEATPLOT is then used to plot the temperature profiles near the basement. The temperature profiles are shown in Figures 10 - 21. It is seen that during the months of January, February and March, the isotherms are somewhat radial. The assumption made by ASHRAE can be valid only during this period.

The storage effects of the soil can be observed from Figures 10 - 21. During the cooling season i.e. the latter part of May to early October the soil gains heat from the atmosphere, while the soil starts losing heat to the atmosphere during the heating season i.e. early October to late May. The heat flow paths from the basement wall extend downwards into the soil (i.e. away from the ground surface) during the cooling season, while the heat flow paths during the heating season extend towards the ground surface.

The soil acts as a heat sink during the summer months. This effect can be seen by referring to Figure 10. The upper portion of the basement wall (down to about 0.5 m below grade) gains heat from the outside air and the surrounding soil, while the rest of the basement wall loses heat to the soil. This effect assists in reducing the energy required to cool the basement during the summers. The floor heat losses are quite significant during the summer months as is evidenced from the closely spaced isotherms below the floor, indicating a large thermal gradient.

During the heating season the floor heat loss decreases while there is a significant increase in the wall heat loss. Figure 16 (for January 10) shows the closely spaced isotherms in the upper portion of the walls. The insulating effect of the soil can be seen from this figure. The lower portions of the wall, as well as the floor, have a significantly lower heat loss than the upper portions of the wall.

GROUND ISOOTHERMS FOR THE BASE CASE

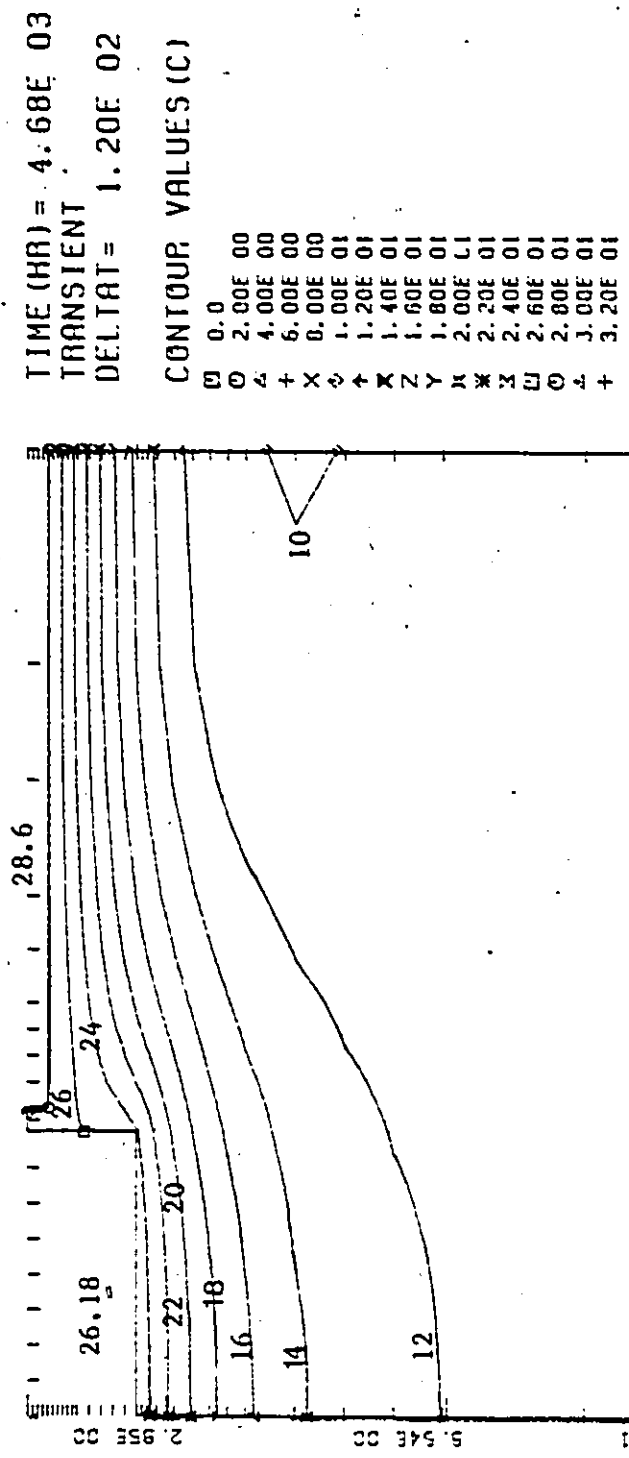


Fig.10. Ground Isotherms for July 14.

GROUND ISOTHERMS FOR THE BASE CASE

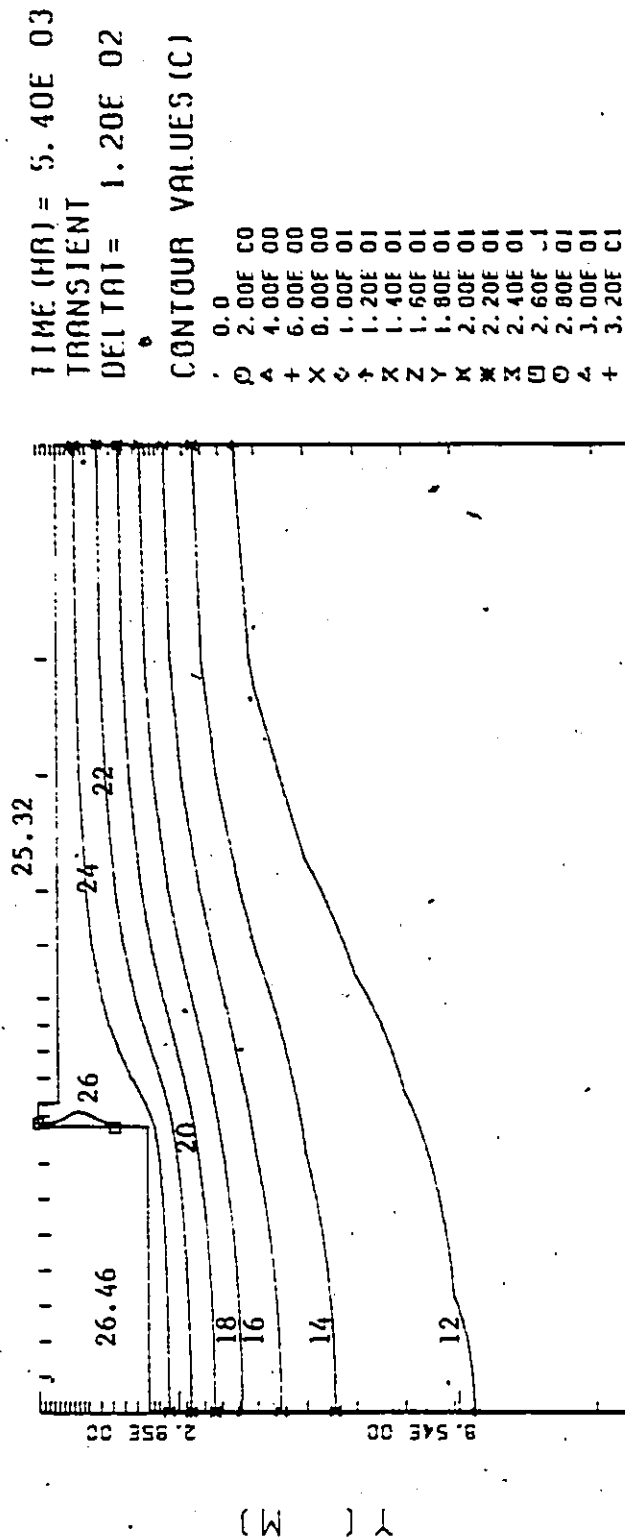


Fig.11. Ground isotherms for August 13.

GROUND ISOOTHERMS FOR THE BASE CASE

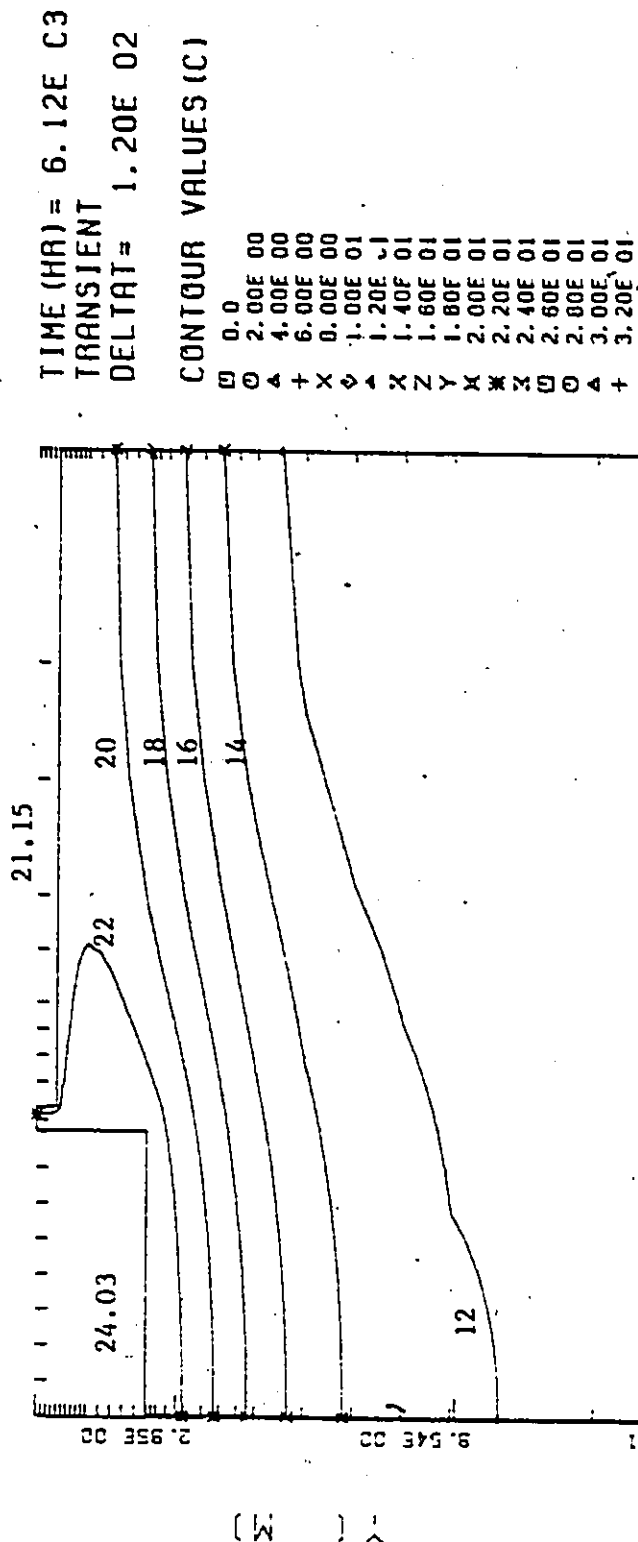
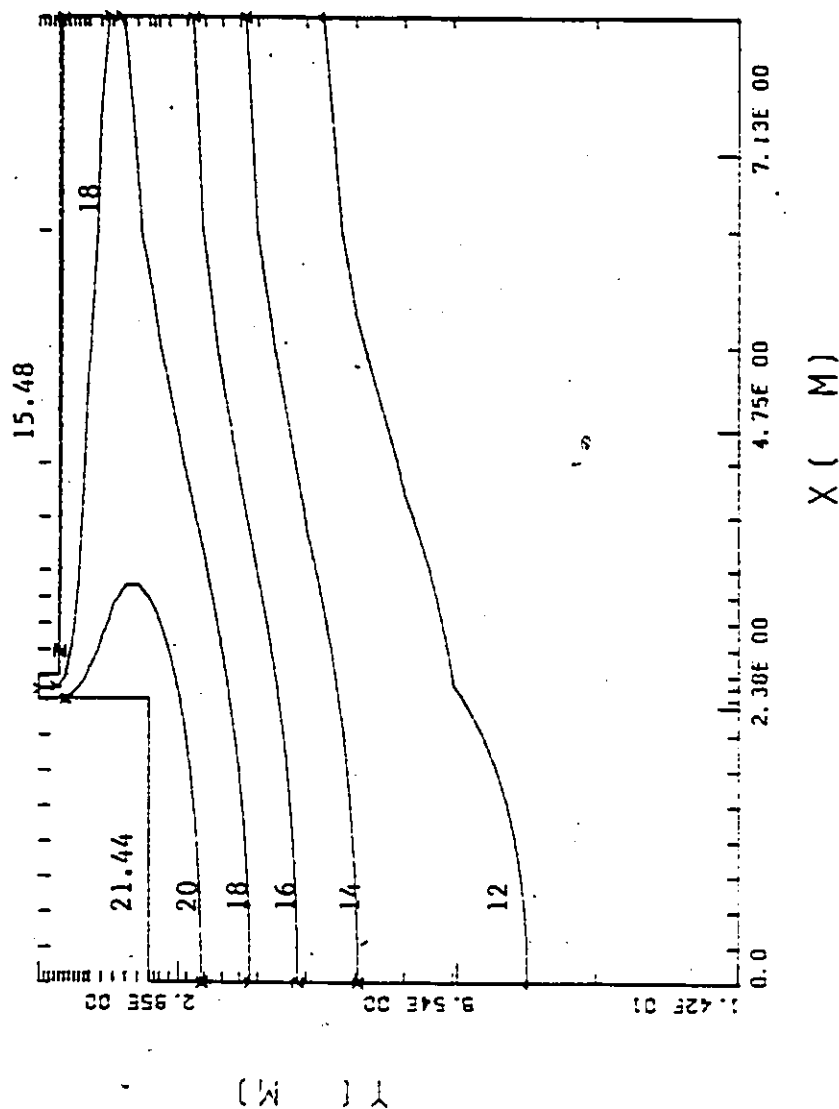


Fig.12. Ground isotherms for Sept.12.

GROUND ISOTHERMS FOR THE BASE CASE



TIME (HR) = 6.84E 03

TRANSIENT

DELTA T = 1.20E 02

CONTOUR VALUES (C)

0	0.0
1	2.00E 00
2	4.00E 00
3	6.00E 00
4	8.00E 00
5	1.00E 01
6	1.20E 01
7	1.40E 01
8	1.60E 01
9	1.80E 01
10	2.00E 01
11	2.20E 01
12	2.40E 01
13	2.60E 01
14	2.80E 01
15	3.00E 01
16	3.20E 01

Fig.13. Ground isotherms for Oct.12.

GROUND ISOOTHERMS FOR THE BASE CASE

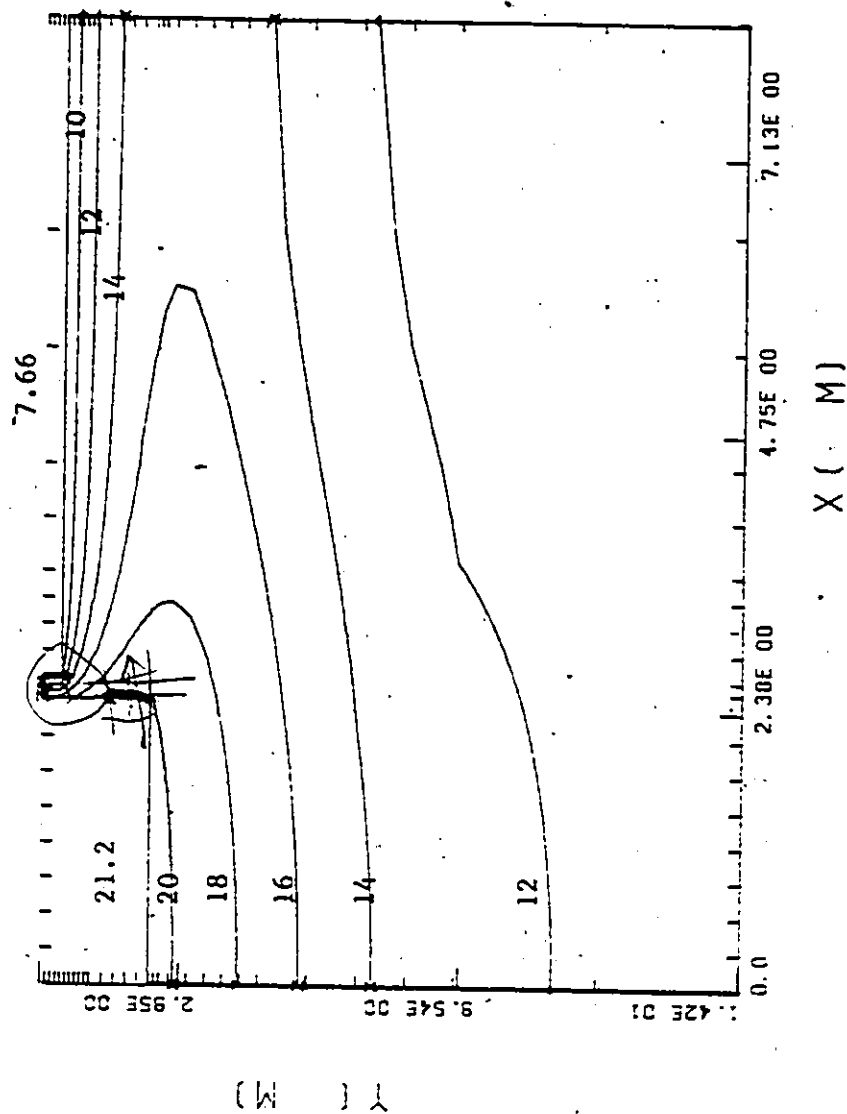
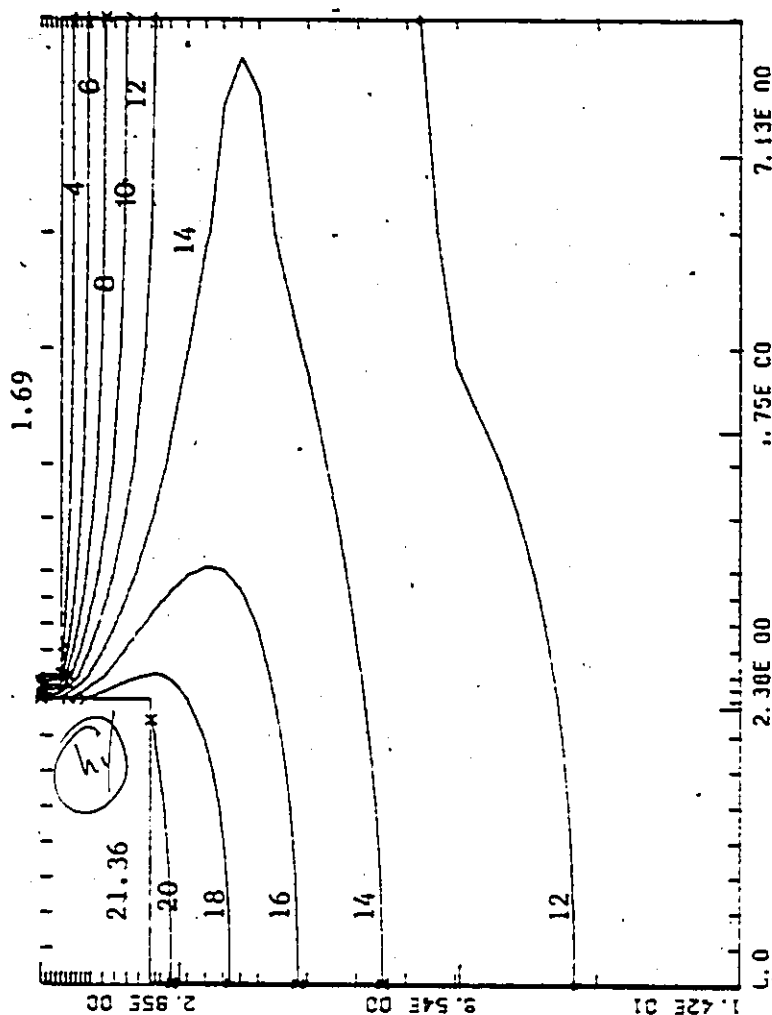


Fig. 14. Ground isotherms for Nov. 11.

GROUND ISOTHERMS FOR THE BASE CASE



TIME (HR) = 8.28E 03
 TRANSIENT
 DELTAT = 1.20E 02

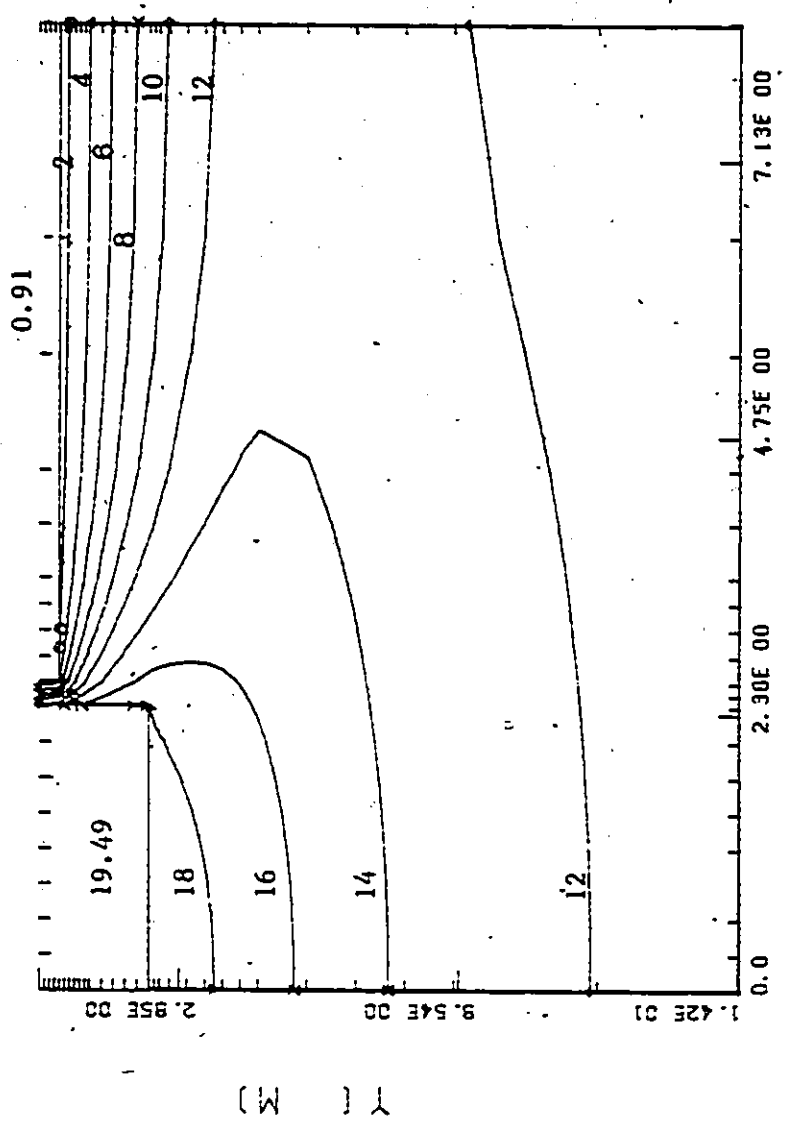
CONTOUR VALUES (C)

0 0.0
 1 2.00E 00
 2 4.00E 00
 3 6.00E 00
 4 8.00E 00
 5 1.00E 01
 6 1.20E 01
 7 1.40E 01
 8 1.60E 01
 9 1.80E 01
 10 2.00E 01
 11 2.20E 01
 12 2.40E 01
 13 2.60E 01
 14 2.80E 01
 15 3.00E 01
 16 3.20E 01

X (M)

Fig.15. Ground isotherms for Dec.11.

GROUND ISOOTHERMS FOR THE BASE CASE



TIME (HR) = 9.00E 03
TRANSIENT
DELTA T = 1.20E 02

CONTOUR VALUES (C)

- 0 0.0
- 0 2.00E 00
- 4 4.00E 00
- + 6.00E 00
- X 8.00E 00
- 0 1.00E 01
- + 1.20E 01
- X 1.40E 01
- Z 1.60E 01
- Y 1.80E 01
- X 2.00E 01
- X 2.20E 01
- X 2.40E 01
- 0 2.60E 01
- 0 2.80E 01
- 4 3.00E 01
- + 3.20E 01

9.51E 00

X (M)

Fig.16. Ground Isotherms for Jan.10.

GROUND ISOTHERMS FOR THE BASE CASE

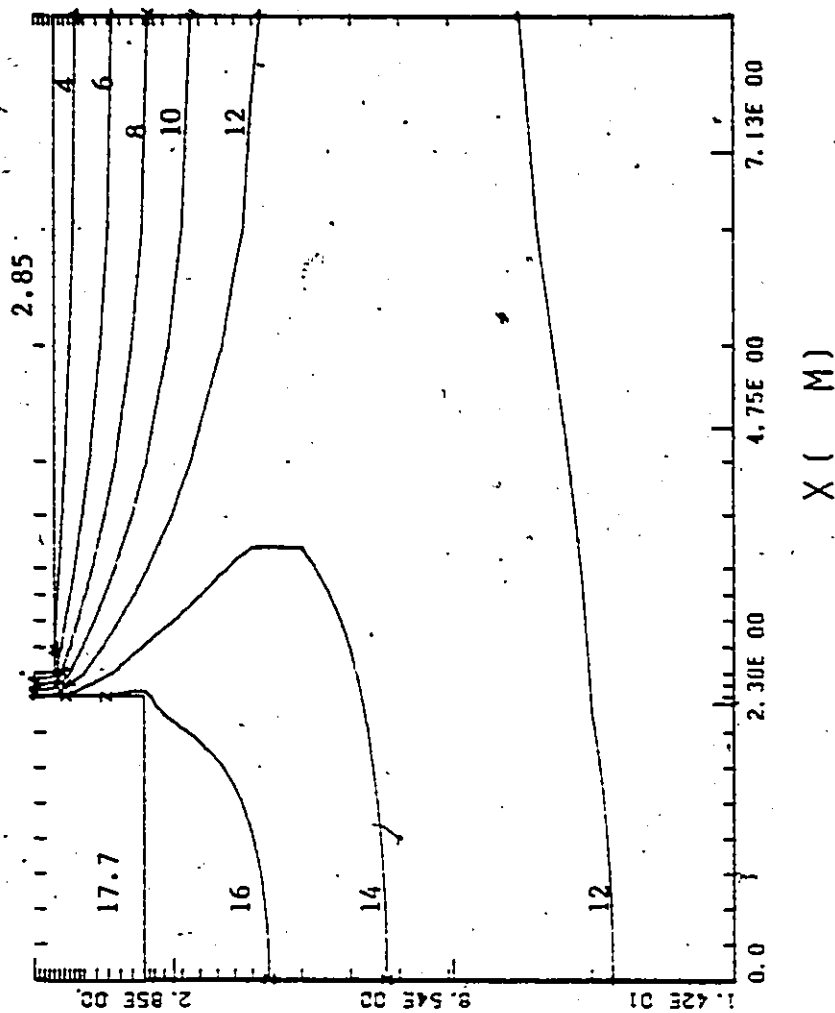


Fig.17. Ground Isotherms for Feb.9

GROUND ISOTHERMS FOR THE BASE CASE

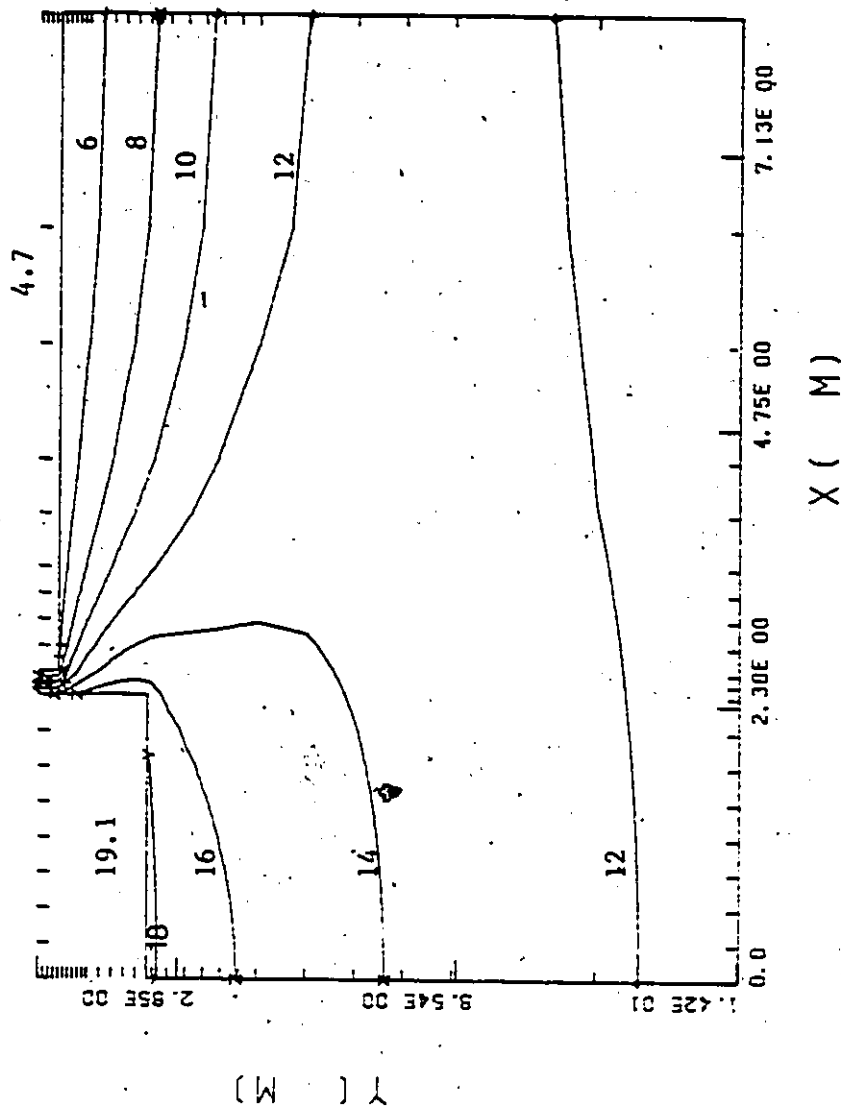


Fig.18. Ground isotherms for March 11.

GROUND ISOTHERMS FOR THE BASE CASE

TIME (HR) = 1.08E 04
TRANSIENT
DELTA T = 1.20E 02

CONTOUR VALUES (C)

- 0.0
- 2.00E 00
- 4.00E 00
- 6.00E 00
- 8.00E 00
- 1.00E 01
- 1.20E 01
- 1.40E 01
- 1.60E 01
- 1.80E 01
- 2.00E 01
- 2.20E 01
- 2.40E 01
- 2.60E 01
- 2.80E 01
- 3.00E 01
- 3.20E 01

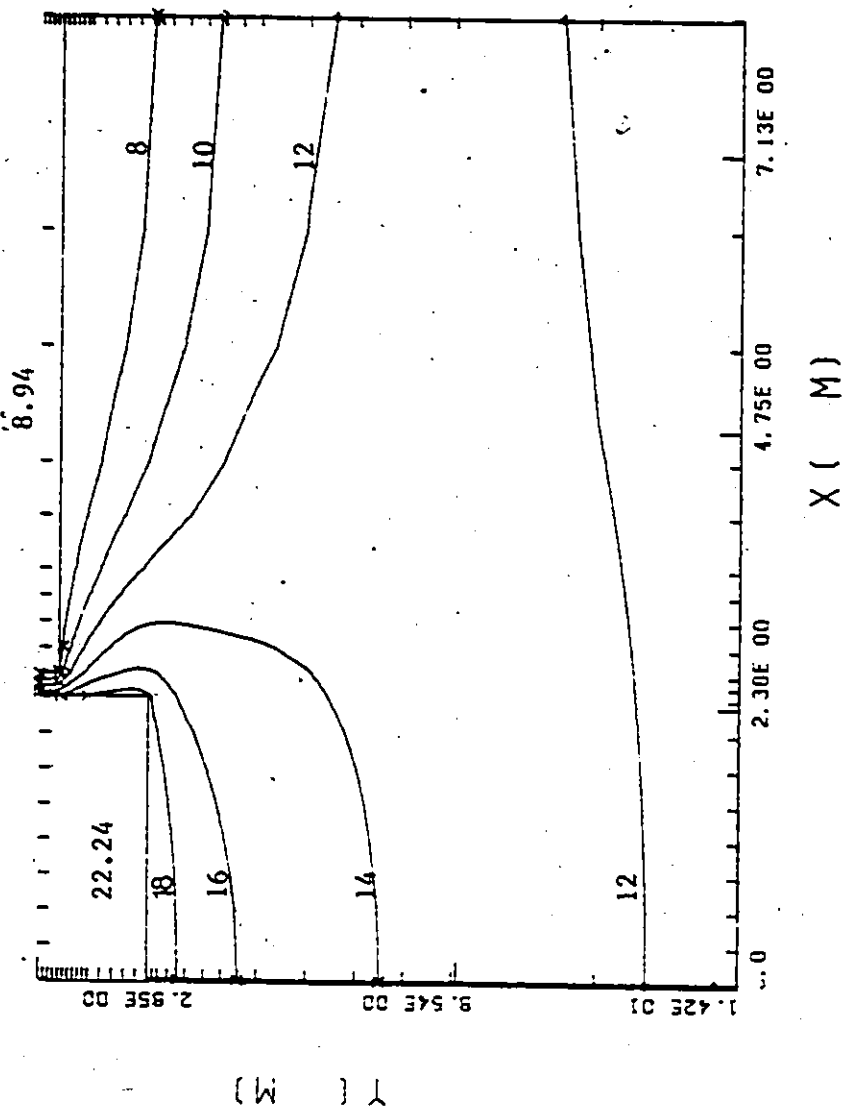


Fig.19. Ground Isotherms for April 10.

GROUND ISOOTHERMS FOR THE BASE CASE

TIME (HR) = 1.22E 04
 TRANSIENT
 DELTAT = 1.20E 02
 CONTOUR VALUES (C)

0	0
2	2.00E 00
4	4.00E 00
6	6.00E 00
8	8.00E 00
10	1.00E 01
12	1.20E 01
14	1.40E 01
16	1.60E 01
18	1.80E 01
20	2.00E 01
22	2.20E 01
24	2.40E 01
26	2.60E 01
28	2.80E 01
30	3.00E 01
32	3.20E 01

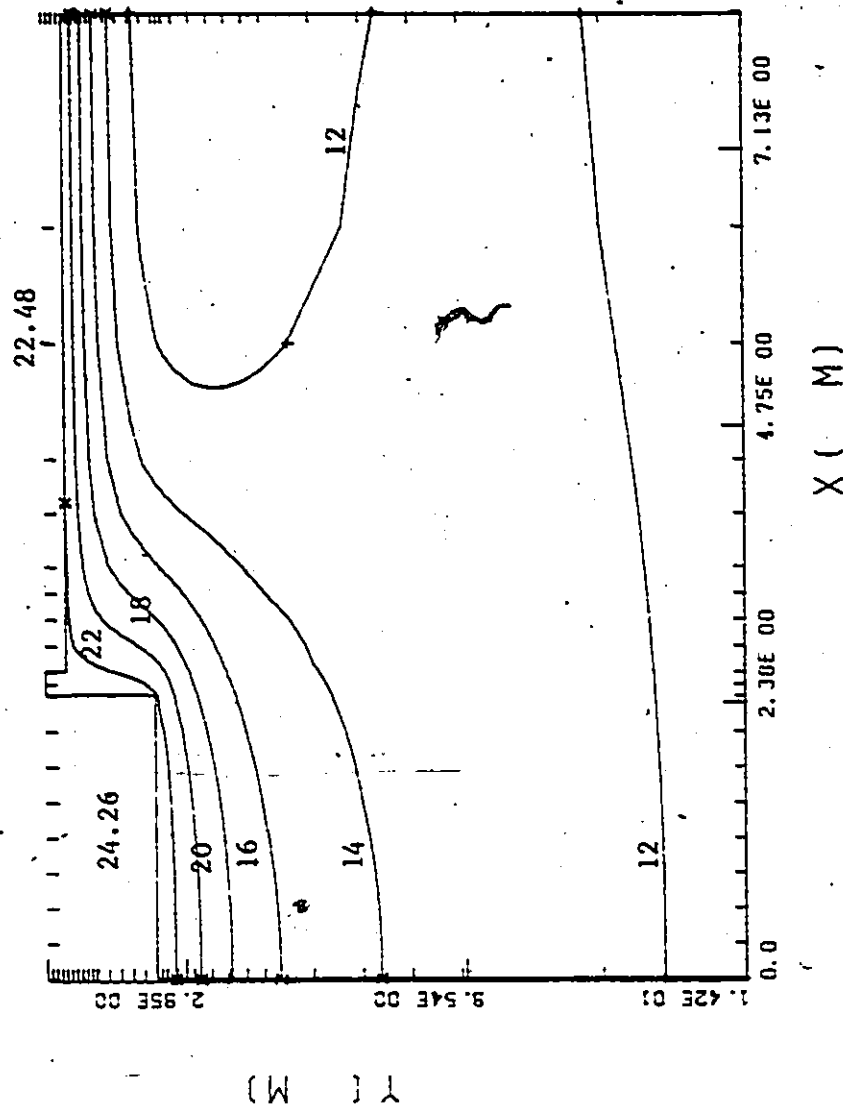


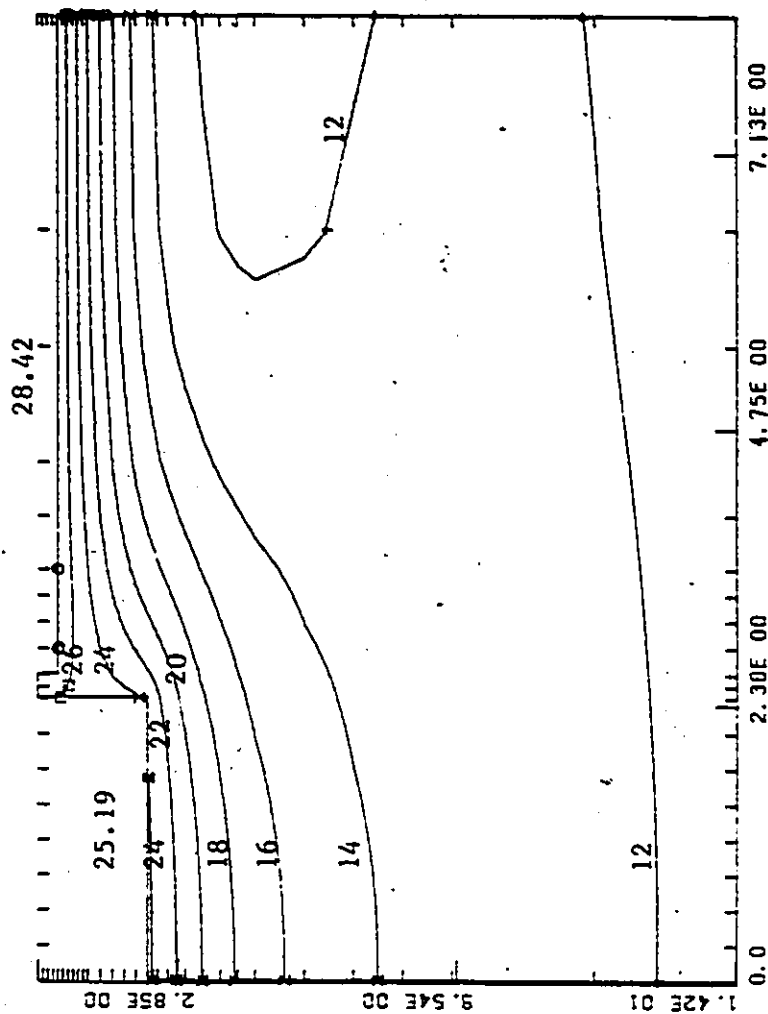
Fig.20. Ground isotherms for May 25.

GROUND ISOTHERMS FOR THE BASE CASE

TIME (HR) = 1.30E 04
TRANSIENT
DELTA T = 1.20E 02

CONTOUR VALUES (C)

0	0.0
1	2.00E 00
2	4.00E 00
3	6.00E 00
4	8.00E 00
5	1.00E 01
6	1.20E 01
7	1.40E 01
8	1.60E 01
9	1.80E 01
10	2.00E 01
11	2.20E 01
12	2.40E 01
13	2.60E 01
14	2.80E 01
15	3.00E 01
16	3.20E 01



X (M)

Fig.21. Ground isotherms for June 24.

Chapter IV

RESULTS AND DISCUSSIONS OF THE PARAMETRIC STUDY

The same basement configuration, ambient air and basement air temperatures that have been used for validation purposes will be used for the parametric study. The soil thermal conductivities vary with time. The model that has been validated will be referred to as the Base Case throughout this thesis.

4.1 SOIL THERMAL CONDUCTIVITY

It is known that the local surface conditions can exert a dominant influence on the heat loss of an underground structure. As is evidenced from the literature survey, soil properties can vary greatly with climate and soil type. Therefore it is worthwhile to examine the extent to which soil properties can influence basement heat losses. If the soil thermal conductivity of a particular location is not known, the normal procedure is to take the mid-range value of the soil thermal conductivity of that region. Since this range may be quite large, it is essential to know how much of an effect this approximation can make on the basement heat loss. This analysis is presented in two parts:-

4.1.1 SEASONAL-VARIATION COMPARED-TO-FIXED SOIL-CONDUCTIVITIES

The soil thermal conductivity in the Columbus, Ohio area ranges from 0.69 to 2.42 w/m K. The mid-range value for that area is 1.56 w/m K. The HEATING 5 computer program was run for these three soil thermal conductivities and the basement heat losses are compared against the base case. The base case considers seasonally varying soil thermal conductivities (whose average value is 1.56 w/m K) and represents the actual basement. The other three thermal conductivities are constant throughout the year and represent the errors that can be induced taking incorrect soil thermal conductivities. The comparisons are shown in Figures 22 - 24. It is seen that the mid-range values of the soil thermal conductivity can cause a wall heat reduction by as much as 8.3% during February and a corresponding reduction in the floor heat loss by 50%. The average wall and floor heat loss during the heating season is reduced by about 5.4% and 17.9% respectively.

A soil thermal conductivity of 2.42 w/m K, which is the upper end of the range, can increase the wall heat loss by 6.25% and the floor heat loss by about 20% during the month of February. The wall and floor heat loss during the heating season is increased by about 6.2% and 62.2% respectively.

Soil with a thermal conductivity of 0.69 w/m K, which is the lower end of the range, can reduce the wall and

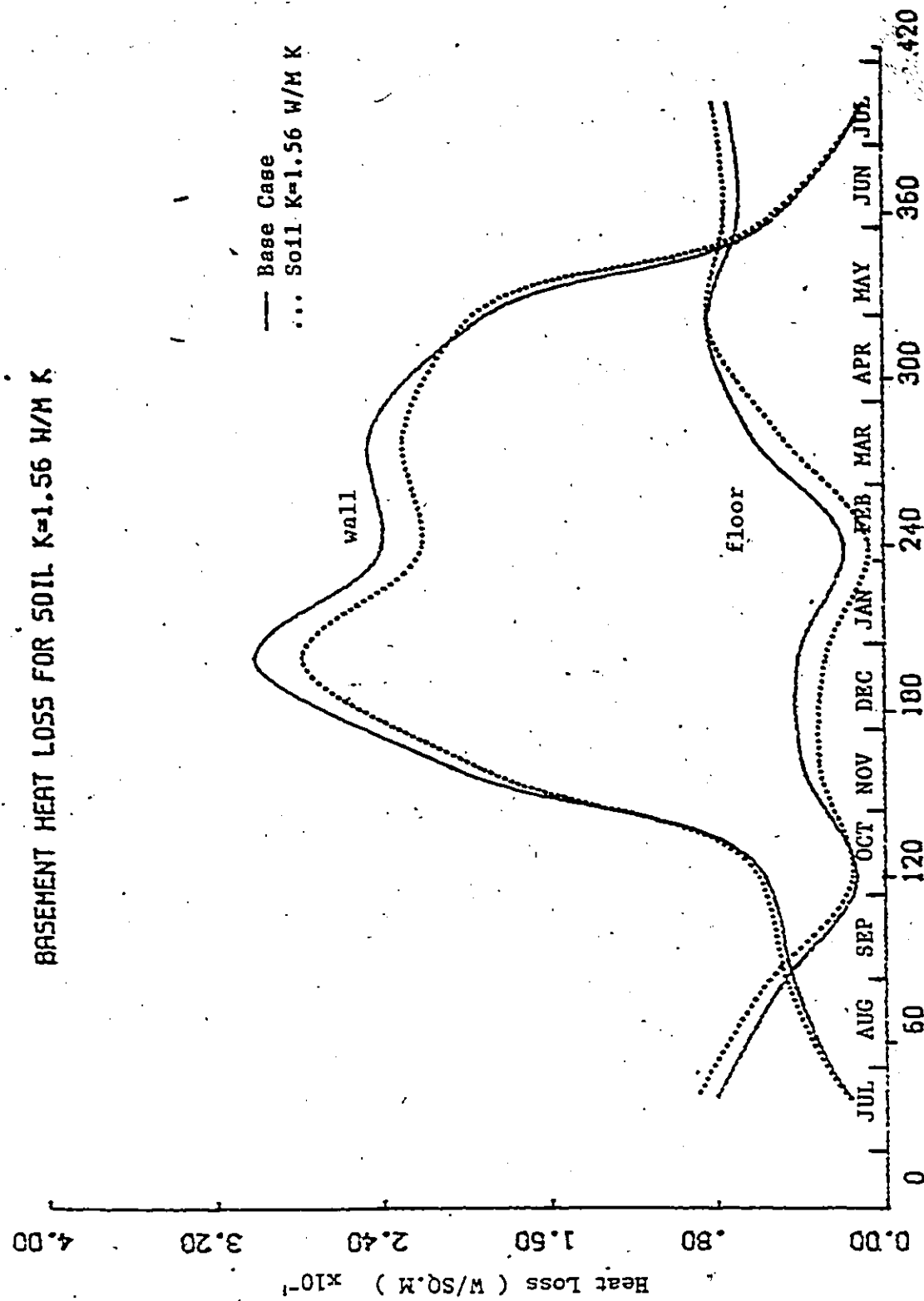
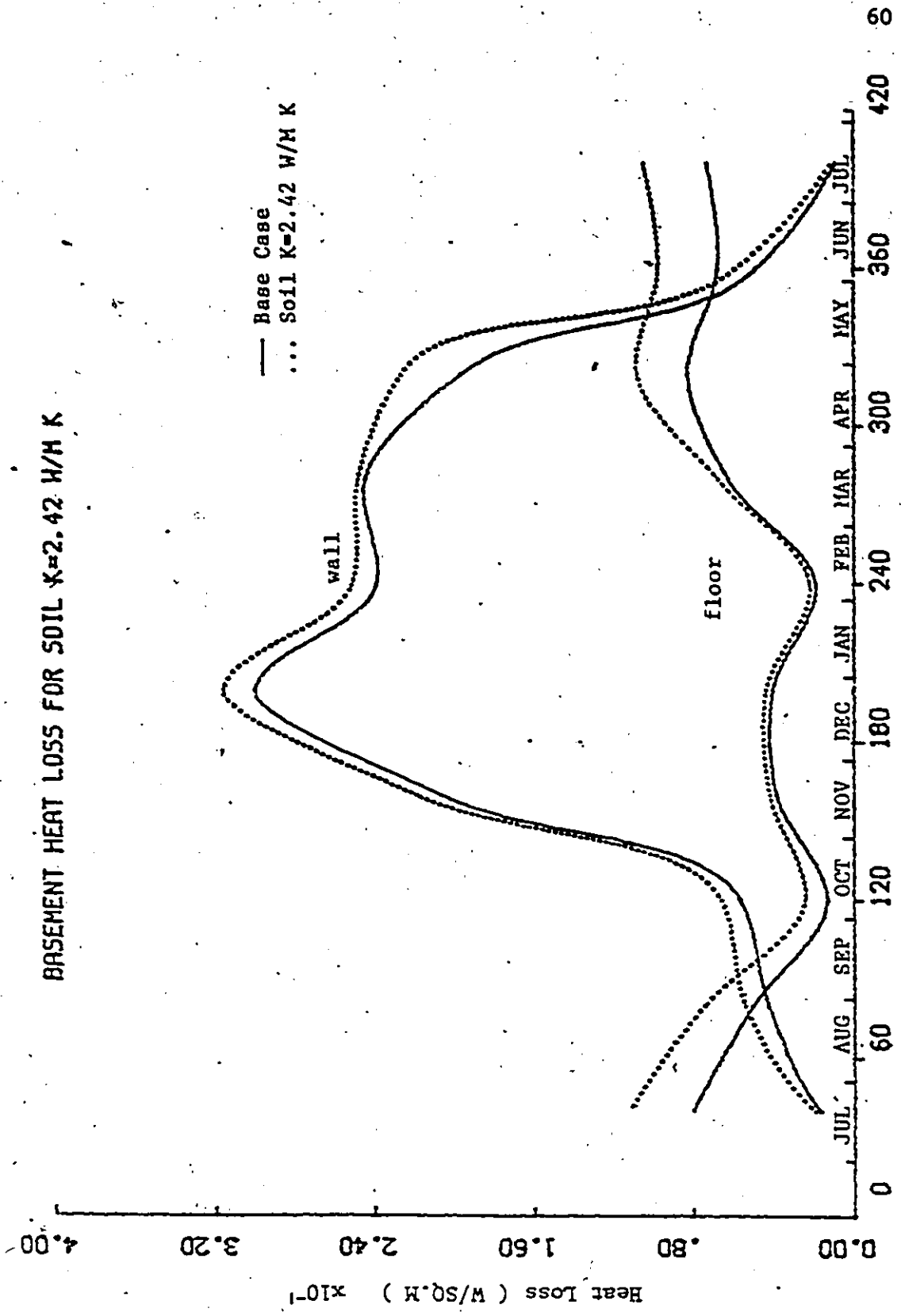


Fig.22. Annual heat loss for soil thermal conductivity= 1.56 W/M K.

BASEMENT HEAT LOSS FOR SOIL $\kappa=2.42$ W/M K



Time In Days From June 10

Fig.23. Annual heat loss for soil thermal conductivity= 2.42 W/M K.

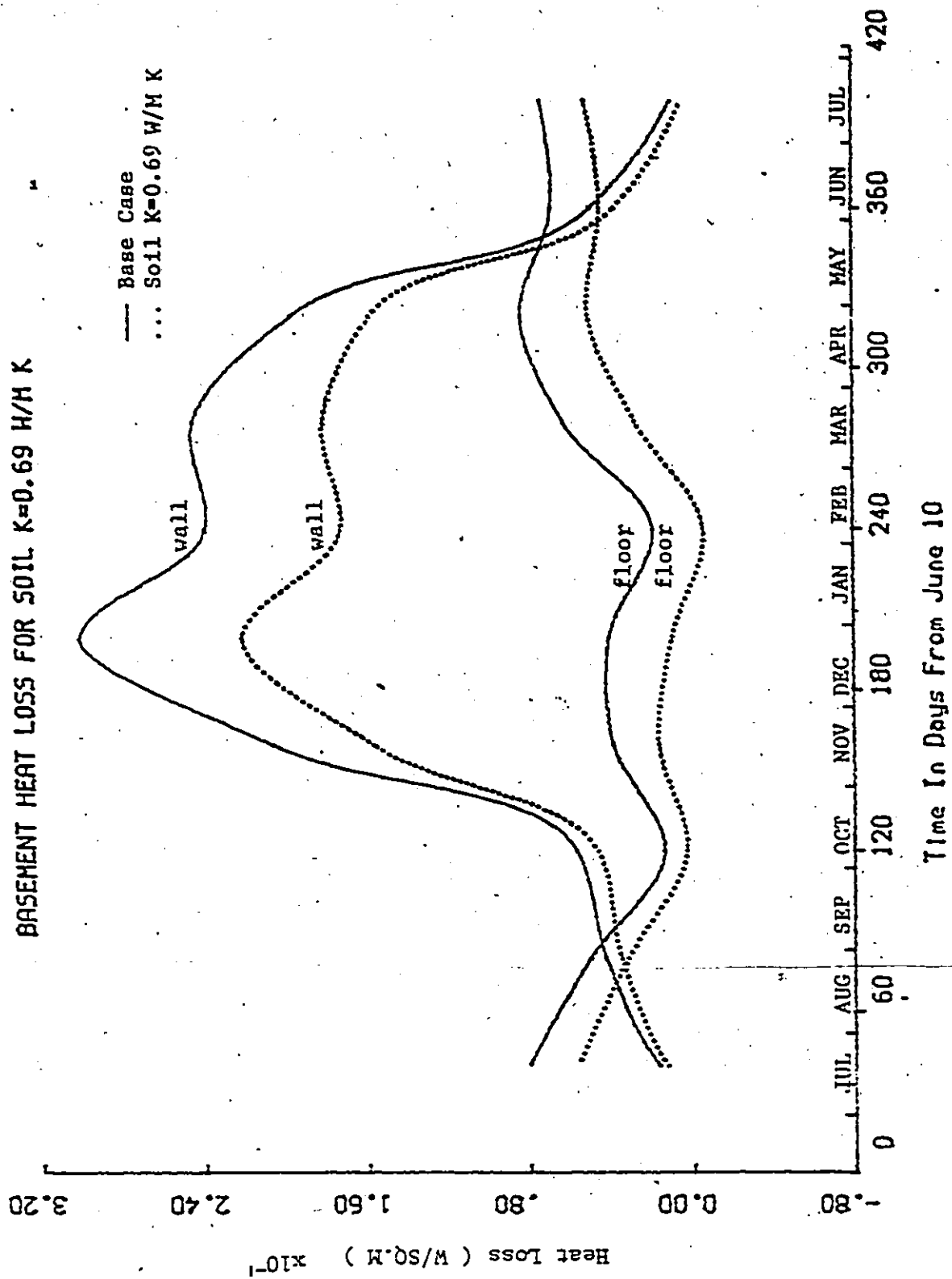


Fig. 24. Annual heat loss for soil thermal conductivity = 0.69 W/M K.

floor heat loss by about 27% and 125% respectively during the month of February. This means that the floor is gaining heat during this period. The average wall and floor heat loss during the heating season is reduced by about 24.3% and 54% respectively.

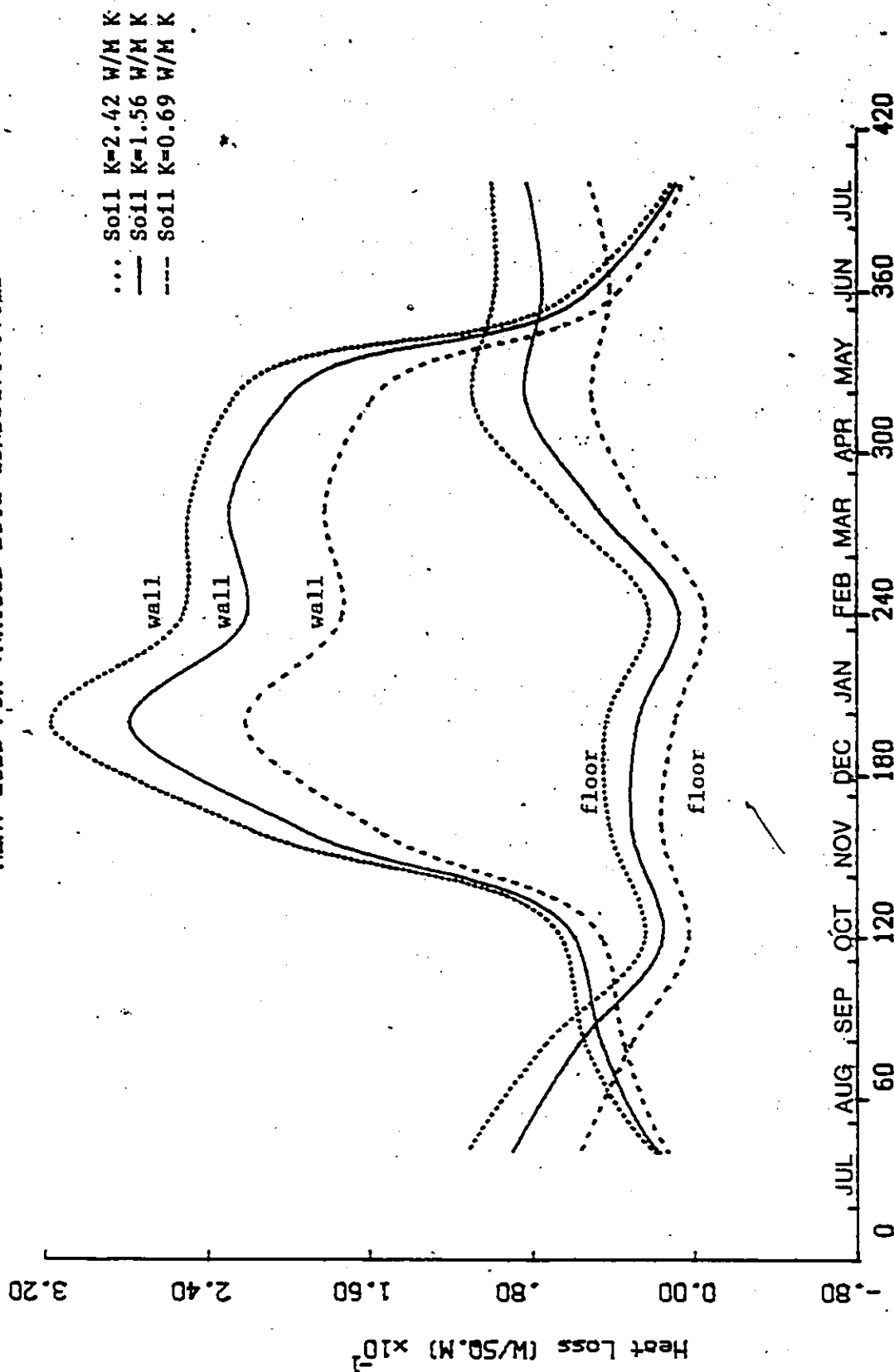
It is seen that the amount and direction of heat flow can be affected by the soil thermal conductivity. Although both the wall and floor heat losses are affected by the soil thermal conductivity, the floor heat losses, on a percentage basis, are more susceptible to soil thermal conductivity changes. It is essential that values close to the actual soil thermal conductivities be used for heat loss calculations and not the mid-range values.

4.1.2 COMPARISON OF FIXED SOIL THERMAL CONDUCTIVITIES

A comparison is made between the basement wall and floor heat loss for three different soil thermal conductivities - 0.69 w/m K, 1.56 w/m K and 2.42 w/m K. The soil thermal conductivities were assumed to be constant throughout the year and the corresponding basement heat losses are shown in Figure 24.1.

It is seen that by increasing the soil thermal conductivity from 1.56 w/m K to 2.42 w/m K the wall and floor heat loss increases by 37.7% and 36.5% during the heating season. But if the soil thermal conductivity is reduced from 1.56 w/m K to 0.69 w/m K, the basement wall

HEAT LOSS FOR VARIOUS SOIL CONDUCTIVITIES



Time In Days From June 10

Fig.24.1. Annual heat loss for three different soil thermal conductivities.

and floor heat loss is reduced by about 17.4% and 44.4% during the heating season.

It can also be observed from Figure 24.1 that the variation of the soil thermal conductivities have a greater influence on basement wall heat loss during the winters than during the summers. On the other hand, the variation of the soil thermal conductivities effect the basement floor heat loss throughout the year (in summer as well as winter).

It can be concluded that the basement heat losses are dependant on the soil thermal conductivity, but no mathematical relationship could be made from this analysis.

4.2 PROXIMITY OF ADJACENT STRUCTURES

In all the basement analysis done till now, it has always been assumed that the basement is isolated from any adjacent heat source. But in actual cases it is very likely that the basement will not be isolated and a similar structure could be as close as 2 or 3 meters away from the test basement.

It was decided to find out the effect of adjacent structures on the basement heat loss. During the course of this analysis it was assumed that the adjacent structure is similar to the test basement. The effect of this adjacent basement can be inputted by restricting the distance of the vertical adiabatic boundary from the basement wall.

The boundary was first restricted to 3 meters (i.e the adjacent basement was 6 meters) from the wall. The result

of the basement wall and heat loss for this condition is shown in Figure 25. The maximum wall heat loss, which occurs in January, is reduced by about 2% while at the same time the floor heat loss is reduced by about 23%. On an average, the wall and floor heat loss during the heating season is reduced by about 3.2% and 20.2% respectively.

The adiabatic boundary was then restricted to a distance of 1.5m (i.e. the adjacent basement was 3 meters) away from the basement wall. The wall and floor heat losses for this condition are shown in Figure 26. The maximum wall heat loss, which occurs during January, is reduced by about 5% while the floor heat loss is reduced by about 50%. The average wall and floor heat loss during the heating season is reduced by 8% and 42% respectively.

Although the adjacent basement does increase the ground temperatures around the test basement, the decrease in wall heat loss is quite small in comparison to the floor heat loss. This is due to the fact that the wall heat loss is more dependant on the ground surface conditions than to the proximity of the adjacent basement. Since the basement floor heat loss is coupled to a lesser extent with the ground surface, the effect of the adjacent basement is more pronounced. The temperatures are noted at four positions. The basement wall/ground surface temperature increases by about 0.03 C and 0.01 C due to restricting the adiabatic boundary at 1.5m and 3.0m from the wall, while the

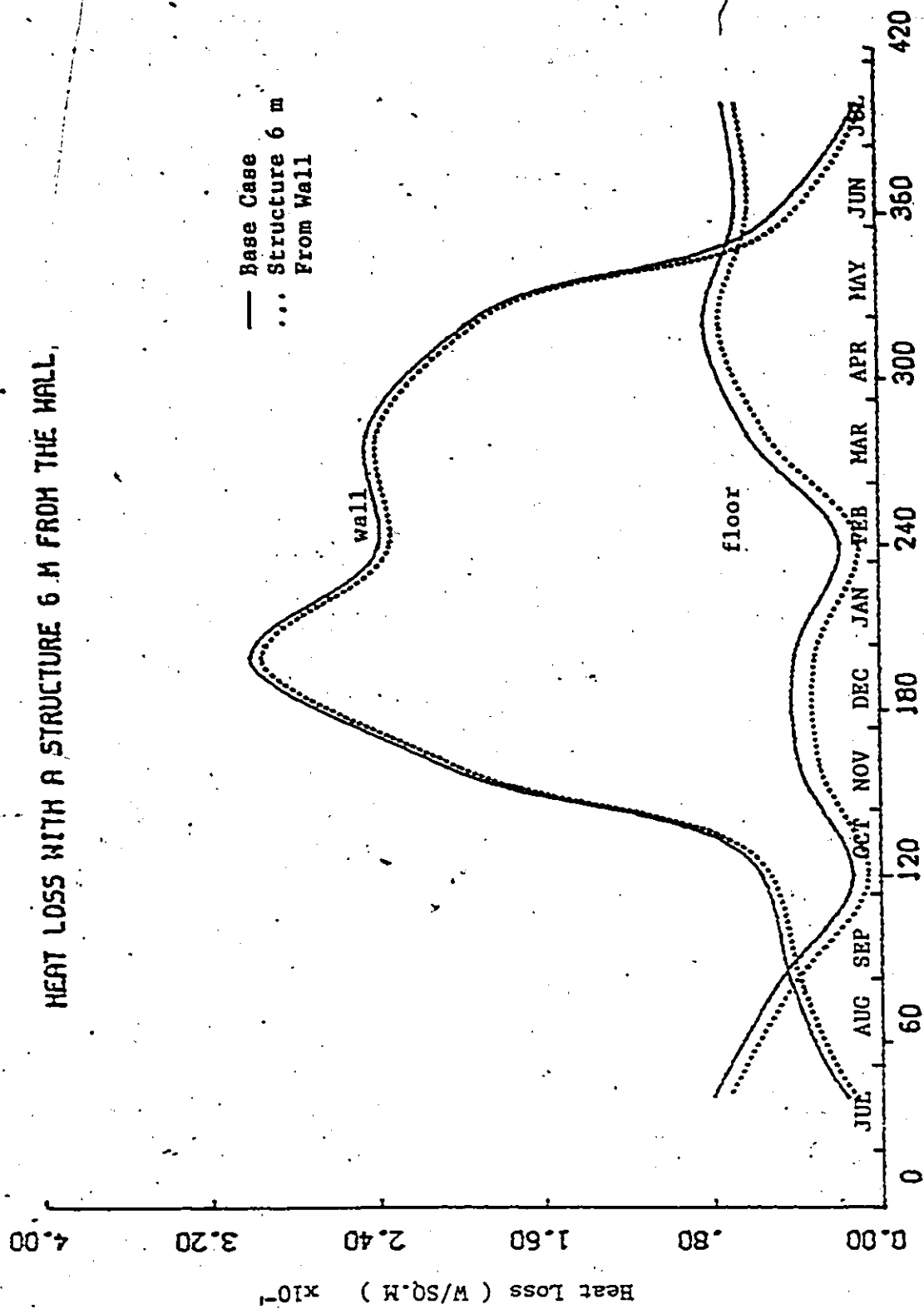


Fig.25. Annual heat loss with a structure 6m from the wall

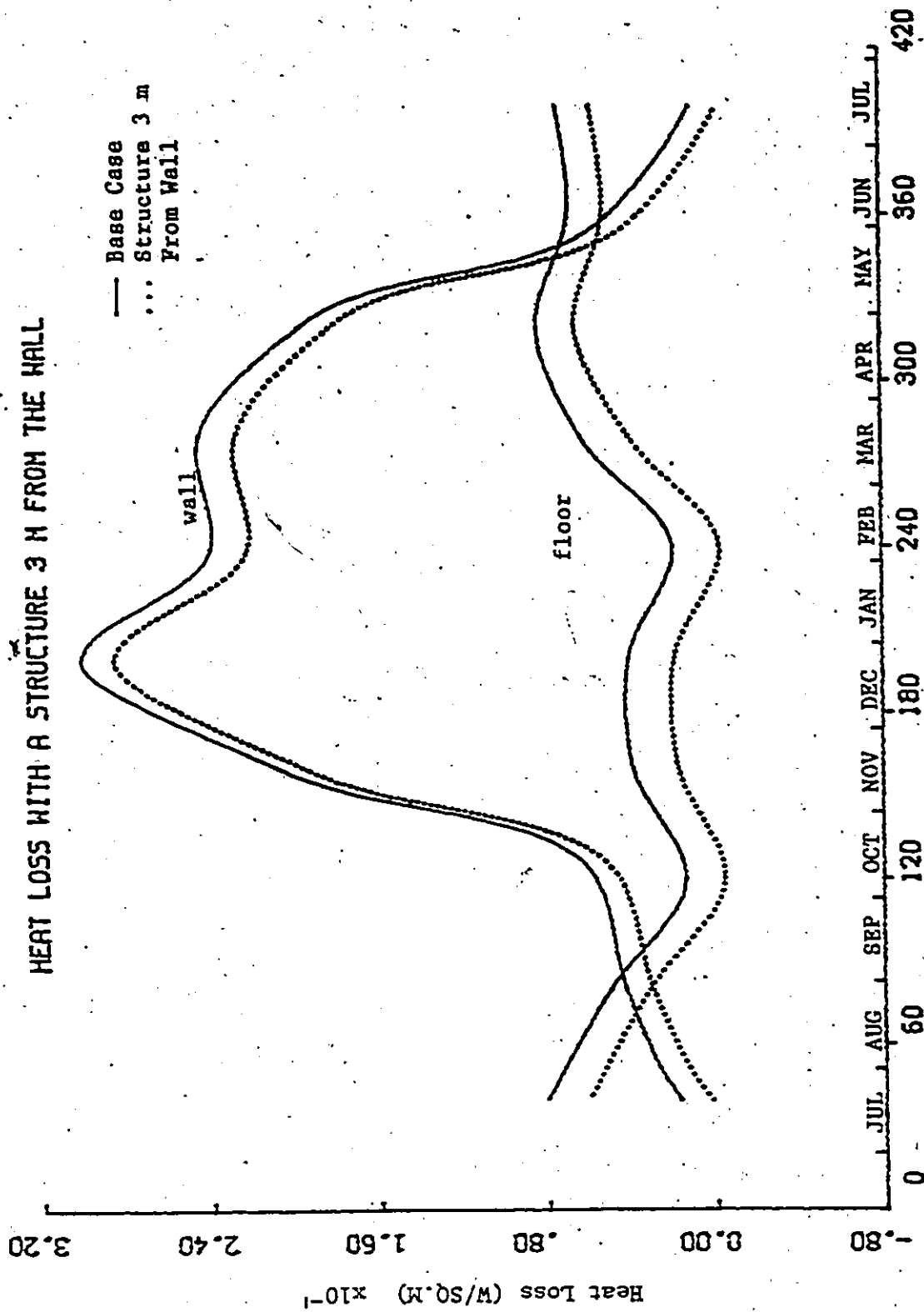


Fig.26. Annual heat loss with a structure 3m from the wall.

wall/ground temperature at a depth of 1.833m increases by about 1.1 C and 0.4 C respectively. The temperatures at the ground surface at a distance of 0.91m from the wall are increased by about 0.1 C and 0.02 C for the restricted boundary being at 1.5m and 3.0m from the wall, while the ground temperature at a distance of 0.91m from the wall and 1.833m deep increases by as much as 2.5 C and 0.8 C respectively. This means that if the basement is deeper into the ground, the effect on the wall heat loss would be more significant.

4.3 GROUND WATER LEVEL

The level and flow of ground water affects the ground temperatures beneath the basement. This is because wet soil has a larger thermal conductivity than dry soil and that moisture migration effects are more pronounced due to the ground water flow. The ground water flow is assumed to be abnormally high during the analysis. The effect of different levels of ground water can be simulated by varying the deep ground isothermal boundary. During the model validation, the ground water level was 11.67m below the basement floor. This level was then reduced to 4 meters and 1 meter below the basement floor. The resulting wall and floor heat losses are shown in Figures 27 - 28. When the ground water level is 4 meters below the floor, the floor heat loss during the heating season increases by as much as

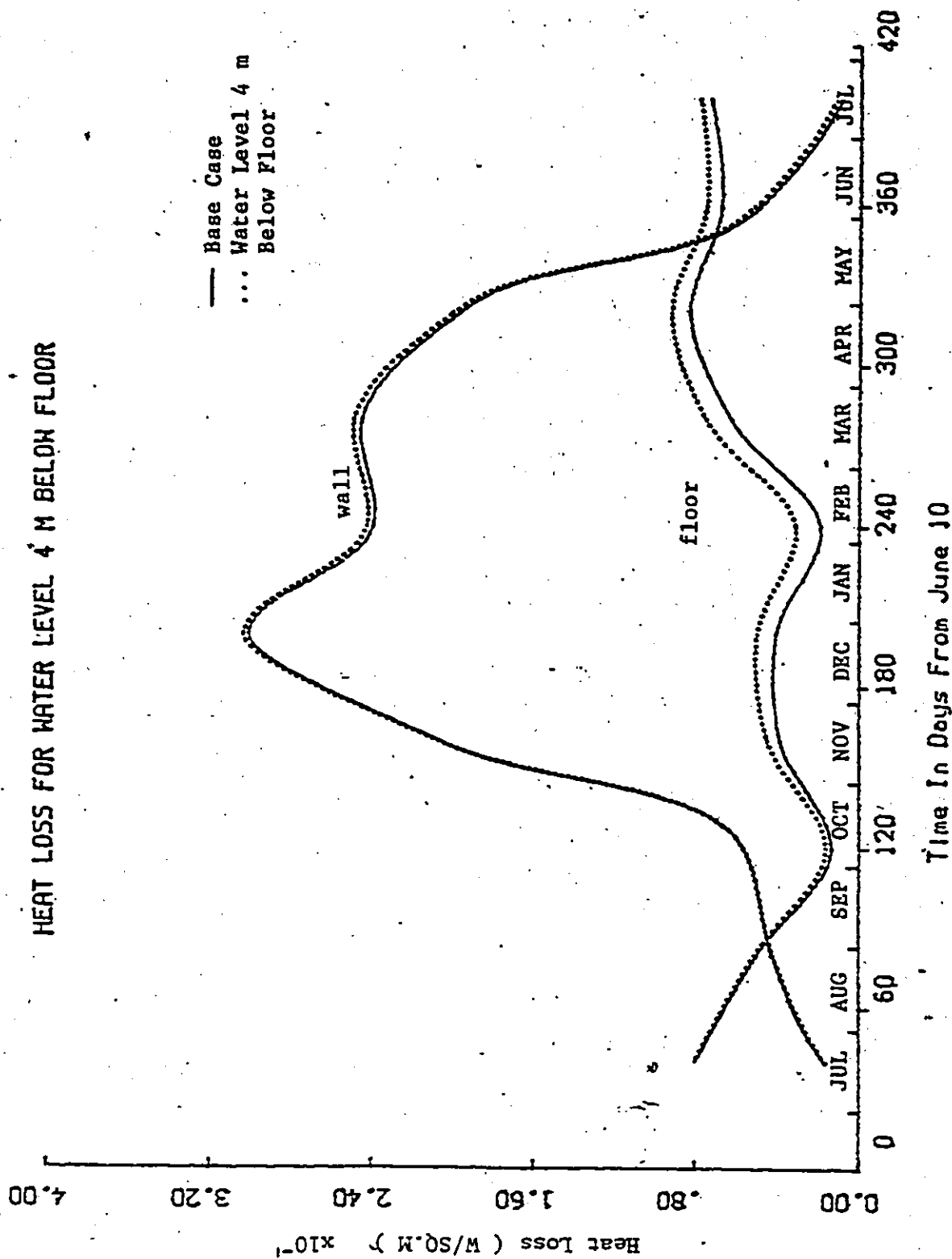


Fig.27. Annual heat loss for isothermal boundary 4m below the floor

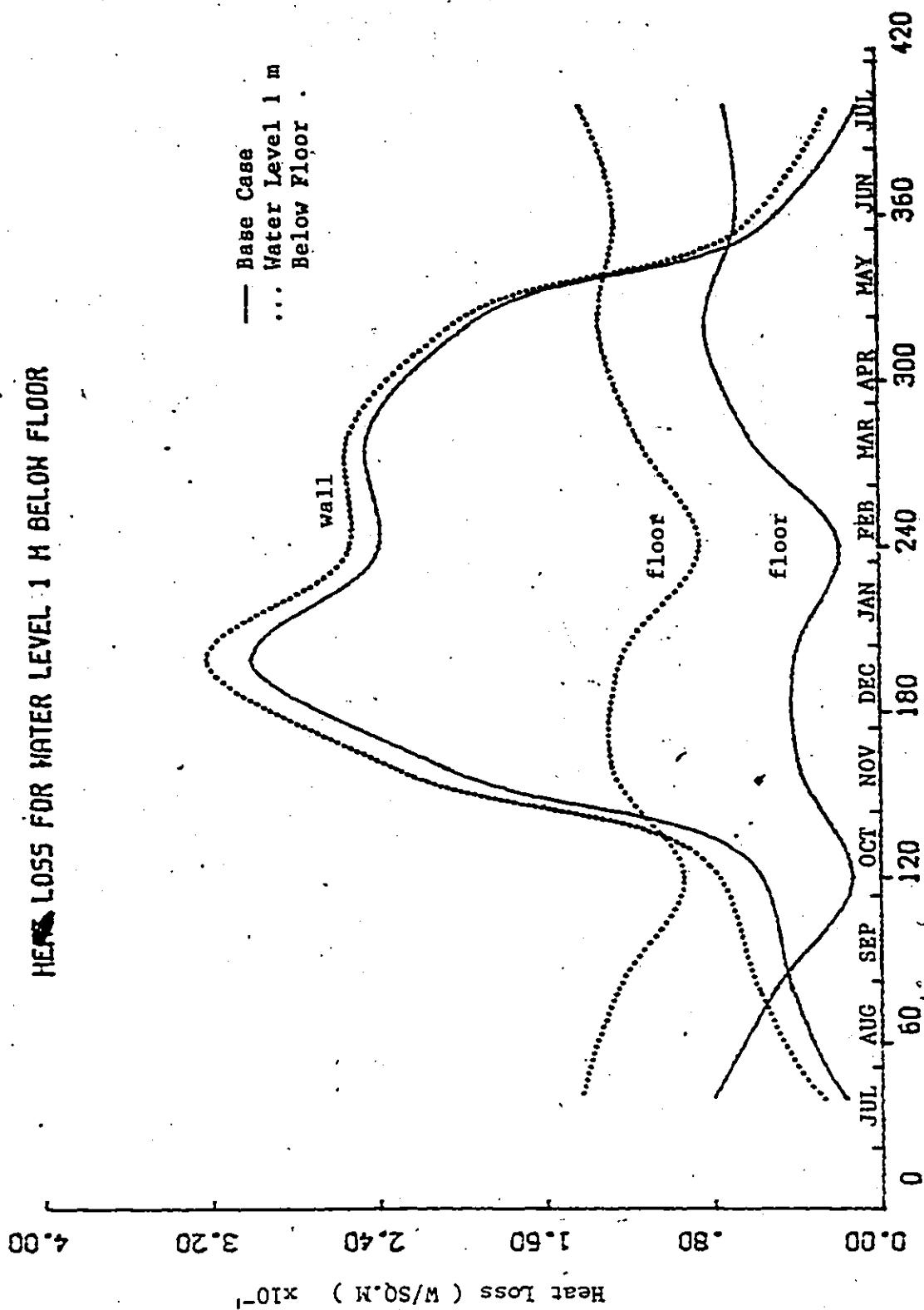


Fig.28. Annual heat loss for isothermal boundary 1m below the floor

18.8% while the wall heat loss increases by about 1% only. When the water level is 1m below the floor, the floor heat loss during the heating season increases by as much as 150% while the wall heat loss increases by about 6%. It can be concluded that the ground water level plays an important role in the basement floor heat loss. Its effect on the wall heat loss is almost negligible.

It was decided to use HEATING 5 to calculate the heat loss from an actual basement with an abnormally high ground water table. After careful evaluation of the literature available, the basement maintained by the Division of Building Research, National Research Council of Canada (DBR/NRC) was selected for evaluation purposes. The ground water level was 0.5m below the basement floor. A more detailed description of the DBR/NRC basement and the results of the study are presented in Chapter V.

4.4 GROUND SURFACE CONDITIONS

It is known that the ground temperatures are sensitive to changes in the surface cover. The surface cover determines the amount of solar radiation absorbed, the availability of water for evaporation, and the amount of heat to be dissipated by convection. At the ground surface, the heat transfer mechanisms taking place are:- direct and diffuse radiation absorbed by the ground, heat loss by evaporation and transpiration from the ground, heat loss by long wave

radiation from the ground and heat loss or gain by convection. In some cases the heat gained by solar radiation is balanced by the heat lost by evaporation, transpiration and long wave radiation from the ground surface to the air [9].

Snow cover tends to decouple the air temperatures from the ground temperatures due to the insulating blanket that it forms on the ground. It insulates the ground during periods of time when the air is colder than the ground and the heat flow is upwards.

The effect of paving the ground is significant because it causes all the precipitation to run off and prevents the movement of moisture to the surface. The heat loss due to evaporation and transpiration from the ground can be ignored if a paved surface is considered.

The effect of these two conditions on basement heat loss will be studied.

4.4.1 SNOW COVER

Monthly snow cover data for the Columbus, Ohio region was taken from Meteorological records [44] for that region. These values were then converted to effective convective coefficients and added as inputs to the model. The snow thermal conductivity value was taken to be 0.598 w/m K (ASHRAE Fundamentals). The thermal capacity of snow was neglected. The monthly snow cover thickness for the Ohio

region is listed in Table 3. The wall and floor heat losses for these conditions are shown in Figure 29. It is seen that about 5.7 inches (14.478 cms.) of snow cover can reduce wall heat losses by as much as 33% (during the month of February) while the corresponding floor heat losses are reduced by 8%. The snow cover acts as an insulator and causes the ground temperatures to be higher than those without snow cover. The far field ground surface temperatures (below the snow cover) for the months of January, February and March increase by about 0.15 C, 0.89 C and 0.14 C respectively as compared to the base case. The wall/ground surface temperatures (below the snow cover) are higher by about 0.72 C, 4.37 C and 1.92 C for the months of January, February and March respectively as compared to a similar basement without snow cover. On an average, the wall and floor heat loss during the heating season decreases by about 11% and 2.4% respectively due to the snow cover.

4.4.2

ASPHALT COVER

The ground near the half basement was assumed to be covered by an asphalt surface. It was assumed that the asphalt surface was on the south facing side of the basement and there was no shale over the pavement, and that the boundary at the center of the basement remained adiabatic. The thickness of the asphalt cover was assumed to be 4 inches and its thermal properties were taken from the ASHRAE

SNOW COVER IN INCHES					
DAYS	NOVEMBER	DECEMBER	JANUARY	FEBRUARY	MARCH
1	-	-	T	7	4
2	-	-	T	7	4
3	-	-	T	6	7
4	-	-	-	5	7
5	-	-	-	5	5
6	-	T	1	7	7
7	-	1	T	7	7
8	-	1	-	7	5
9	-	3	5	7	7
10	-	3	5	7	6
11	-	3	4	6	4
12	-	3	4	6	2
13	-	2	5	6	1
14	-	-	5	7	T
15	-	-	6	7	T
16	-	-	6	7	T
17	-	-	10	6	T
18	-	-	12	6	T
19	-	-	11	6	-
20	-	-	15	6	-
21	-	T	17	6	-
22	-	T	17	5	-
23	-	T	17	5	-
24	-	-	14	6	-
25	-	-	5	5	-
26	T	T	5	5	-
27	T	T	6	5	T
28	2	T	7	4	-
29	1	T	6	-	-
30	-	-	6	-	-
31	-	-	7	-	-
AVERAGE	0.102	0.523	5.746	5.714	2.069

T= Trace. (assumed to be 0.025inches)

Table 3. Snow Cover in Inches For Ohio (1977-78).

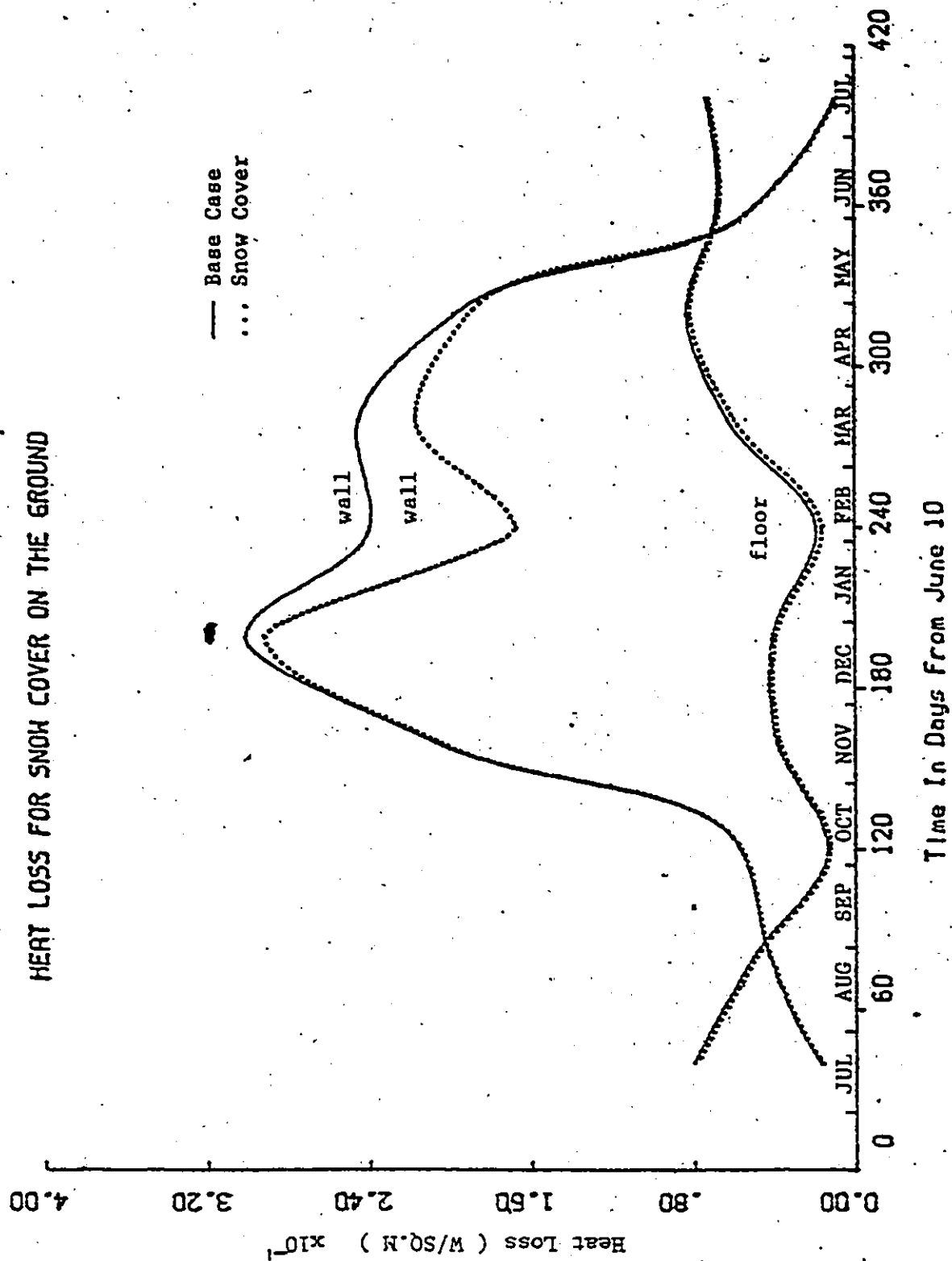


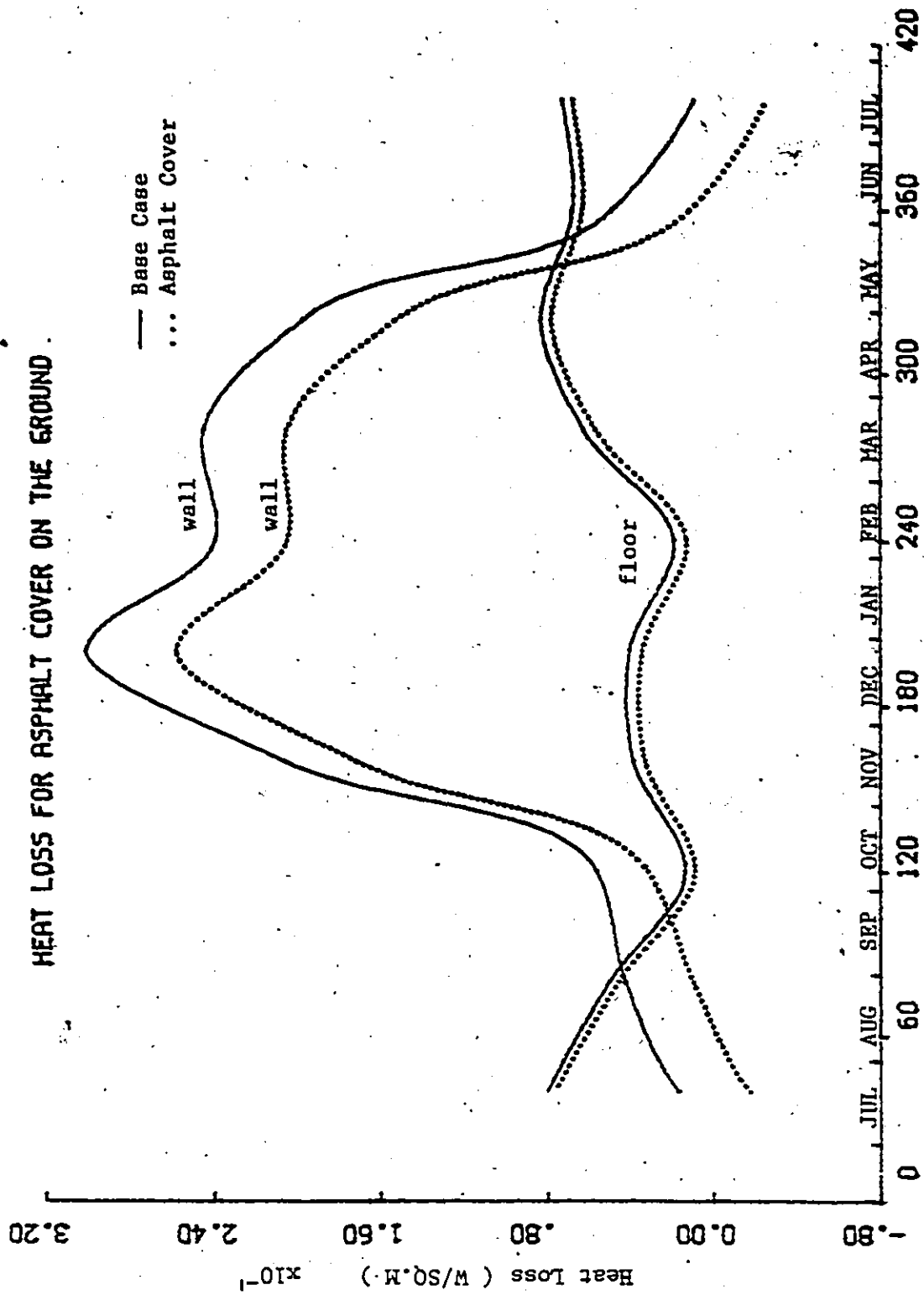
Fig.29. Annual heat loss with snow cover on the ground

Fundamentals. The density, specific heat and thermal conductivity of asphalt are:- 2110 kg/m^3 , 0.92 KJ/kg C and 0.74 W/m C respectively. The solar absorbtivity of asphalt was taken to be 0.9 [45]. The amount of heat absorbed due to solar radiation was taken from 'Physical Climatology' by Sellers [46]. A Fourier curve fit of the solar heat was developed and sol-air temperatures were then calculated from this fit. The equivalent ambient air temperature can be expressed by the following Fourier equation:-

$$T_a = 16.3224 + 16.7181 \cos(Z) + 1.401 \cos(2Z) + 0.6967 \cos(3Z) \\ + 3.3961 \sin(Z) + 0.1725 \sin(2Z) - 1.1878 \sin(3Z)$$

where $Z = 2\pi(t/24 + 183)/365$ and t is in hours starting from January 1.

The asphalt surface was assumed to be cleared of snow during the winter. The basement wall and floor heat losses were calculated using HEATING 5 and are shown in Figure 30. It is seen that during the winter months, the south wall heat loss is reduced by about 18% (during the month of February) while the floor heat loss is reduced by about 25%. On an average, the wall and floor heat loss during the heating season is reduced by about 19% and 9.4% respectively. During the summer months (i.e. the middle of June to the middle of August) the south basement wall heat loss is negative and the walls are actually gaining heat. This is because in addition to the above grade portion of the wall,



Time In Days From June 10

Fig.30. Annual heat loss with an asphalt cover on the ground

the below grade walls receive heat down to a depth of 1.01m below the ground. In this analysis it was assumed that the asphalt cover reduces the evaporation and hence the heat loss by evaporation and transpiration from the ground surface to zero. The ground gains heat due to the absorption of solar radiation.

The calculated surface temperatures far from the basement are about 6 C warmer than the air temperatures during the summer months (mid June to mid August). Gold [9] measured an average ground air temperature difference of 15 C during the summer months for a parking lot in Ottawa.

Raff [38] estimated that eliminating the evaporative heat loss would result in a yearly average ground to air temperature difference of 3.2 C (for the Washington, D.C. - Baltimore area). The yearly average ground to air temperature difference for surfaces far from the test basement is 3.1 C.

The wall/ground surface temperatures (below the asphalt cover) for the months of May, June, July, January, February and March increases by about 4.2 C, 2.2 C, 2 C, 4.95 C, 3.84 C and 4.29 C respectively as compared to a basement without an asphalt cover. The far field ground surface temperature (below the asphalt surface) increases for the above mentioned months are 3.4 C, 4.18 C, 4.36 C, 1.47 C, 0.88 C, 1.89 C respectively. The far field soil temperatures below the asphalt covered surface and the grass covered surface

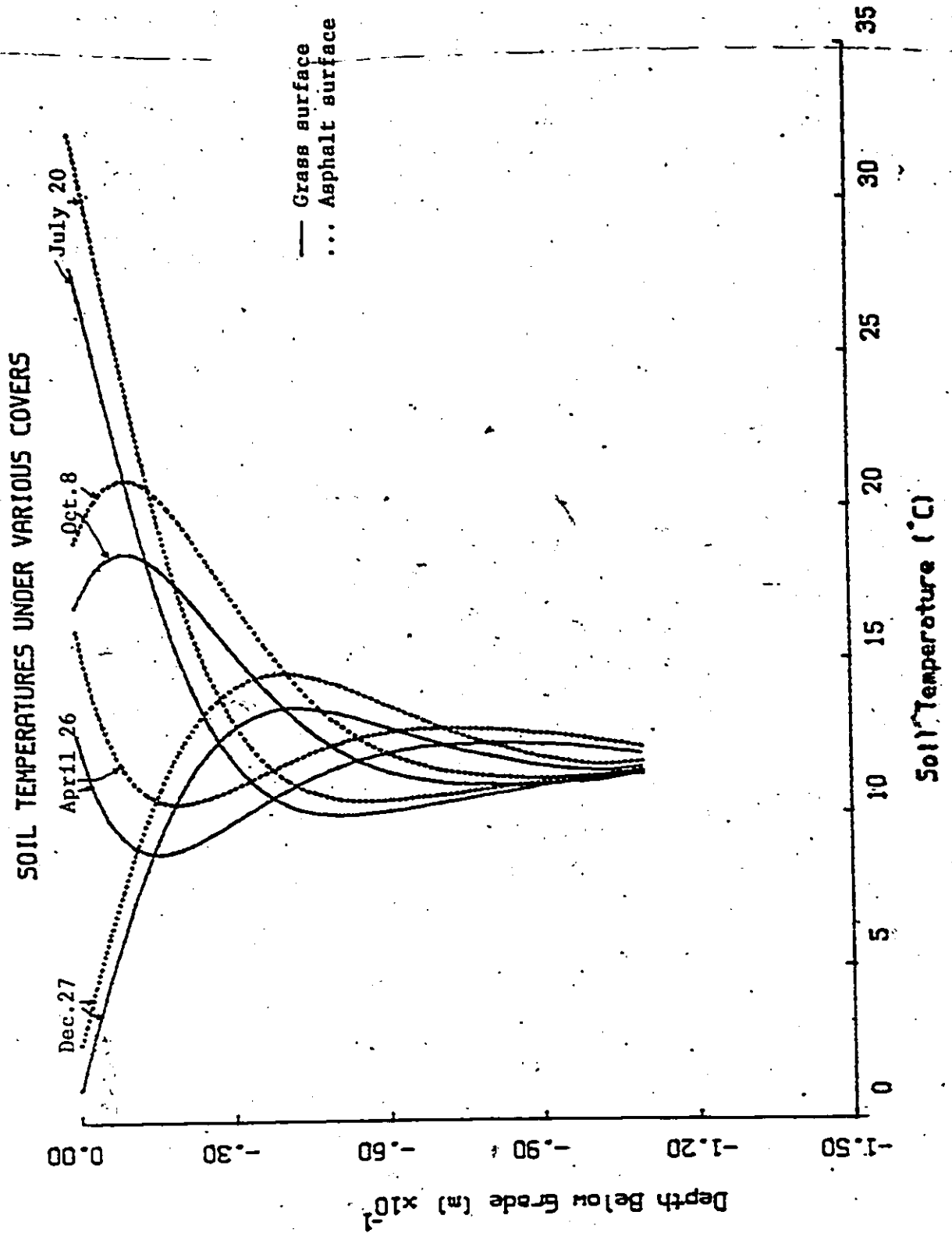


Fig. 30.1. Far field soil temperatures below asphalt and grass covered surfaces.

THE GROUND IS COVERED BY AN ASPHALT PAVEMENT

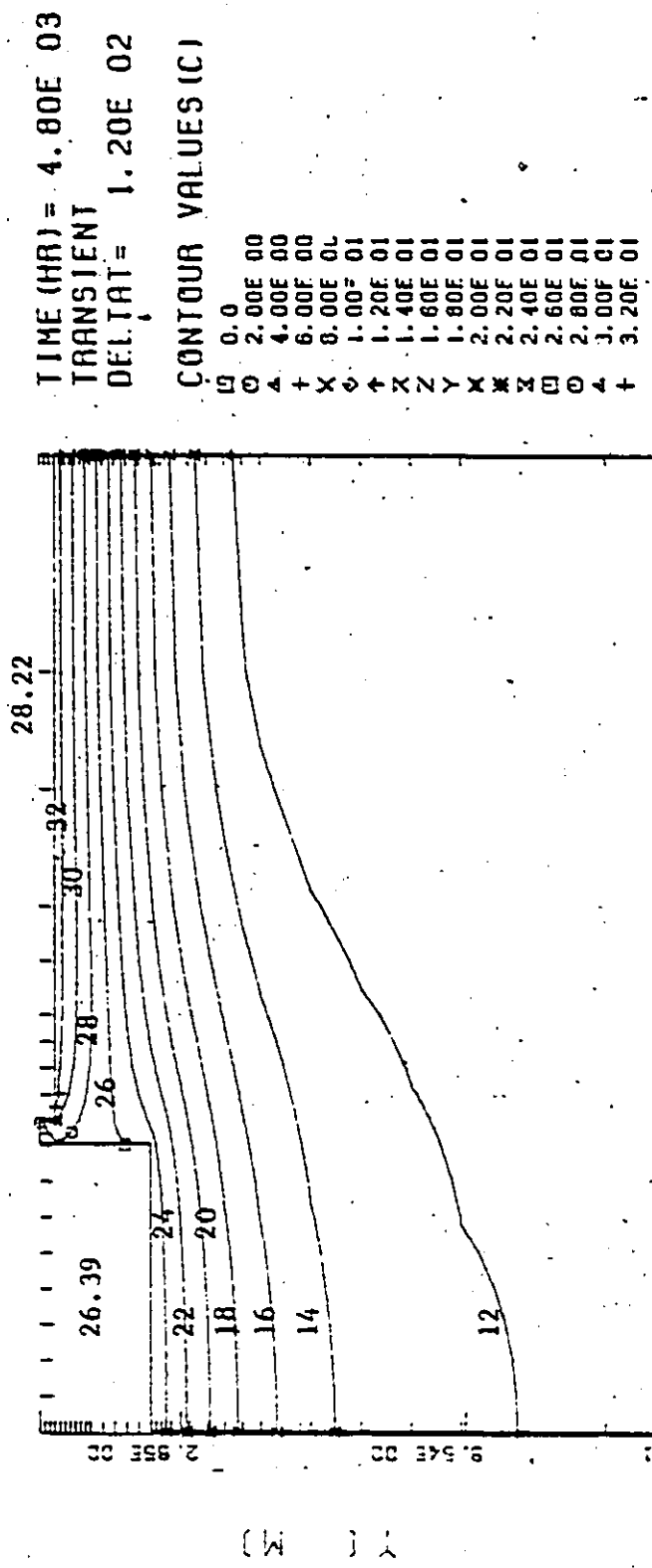


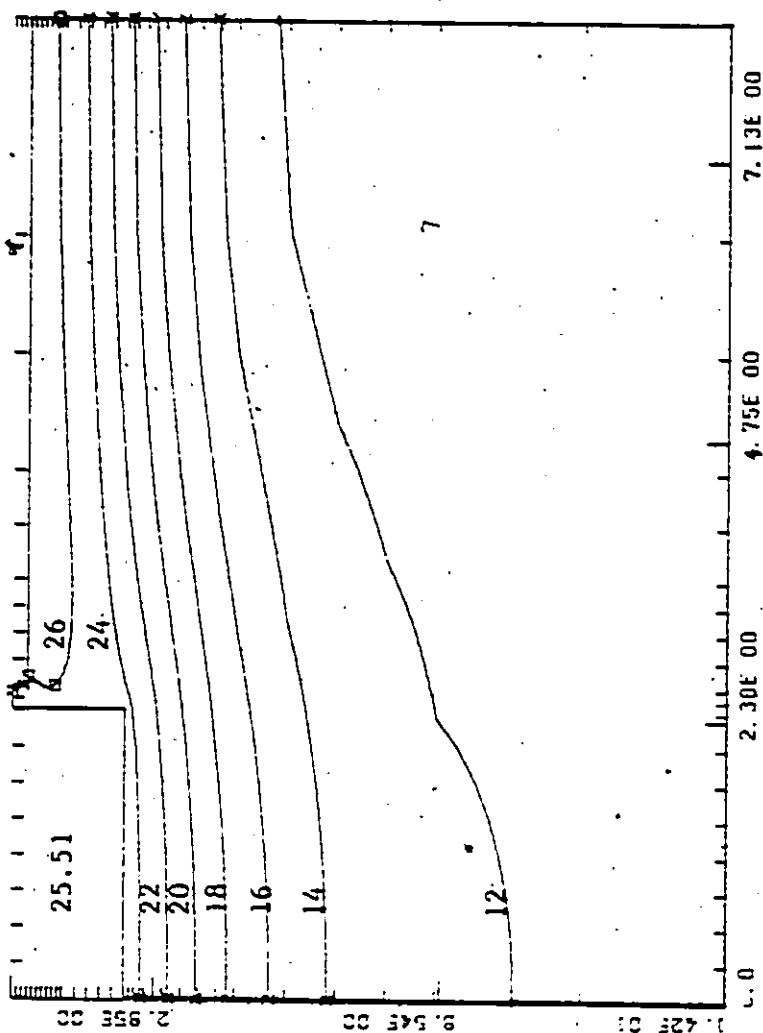
Fig.31. Ground isotherms for July 20.

THE GROUND IS COVERED BY AN ASPHALT PAVEMENT

TIME (HR) = 5.76E 03
TRANSIENT
DELTA T = 1.20E 02

CONTOUR VALUES (C)

0	0.0
1	2.00E 00
2	4.00E 00
3	6.00E 00
4	8.00E 00
5	1.00E 01
6	1.20E 01
7	1.40E 01
8	1.60E 01
9	1.80E 01
A	2.00E 01
B	2.20E 01
C	2.40E 01
D	2.60E 01
E	2.80E 01
F	3.00E 01
G	3.20E 01



X (M)

Fig. 32. Ground Isotherms for Aug. 29

THE GROUND IS COVERED BY AN ASPHALT PAVEMENT

TIME (HR) = 6.72E 03,
TRANSIENT
DELTA T = 1.20E 02

CONTOUR VALUES (C)

0.0
2.00E 00
4.00E 00
6.00E 00
8.00E 00
1.01E 01
1.20E 01
1.40E 01
1.60E 01
1.80E 01
2.00E 01
2.20E 01
2.40E 01
2.60E 01
2.80E 01
3.00E 01
3.20E 01

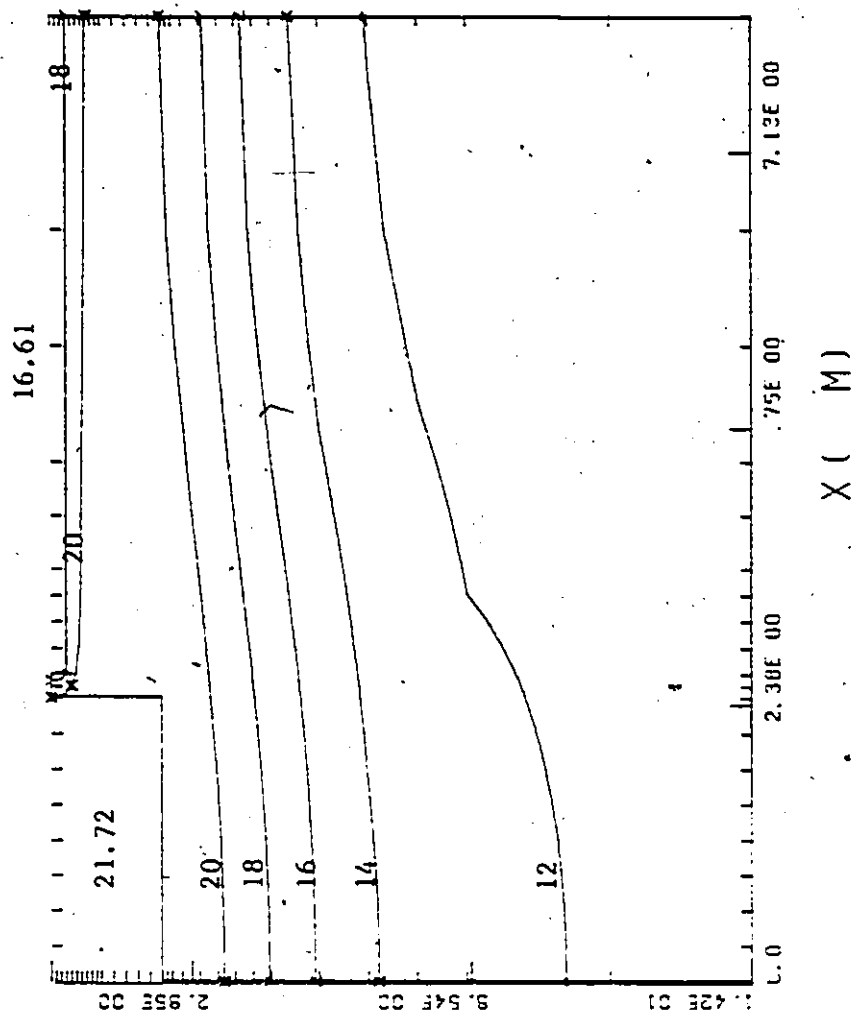


Fig.33. Ground isotherms for Oct.8

THE GROUND IS COVERED BY AN ASPHALT PAVEMENT
6.39

TIME (HR) = 7.68E 03
TRANSIENT
DELTA T = 1.20E 02

CONTOUR VALUES (C)

0 0.0
1 2.00E 00
2 4.00E 00
3 6.00E 00
4 8.00E 00
5 1.00E 01
6 1.20E 01
7 1.40E 01
8 1.60E 01
9 1.80E 01
10 2.00E 01
11 2.20E 01
12 2.40E 01
13 2.60E 01
14 2.80E 01
15 3.00E 01
16 3.20E 01

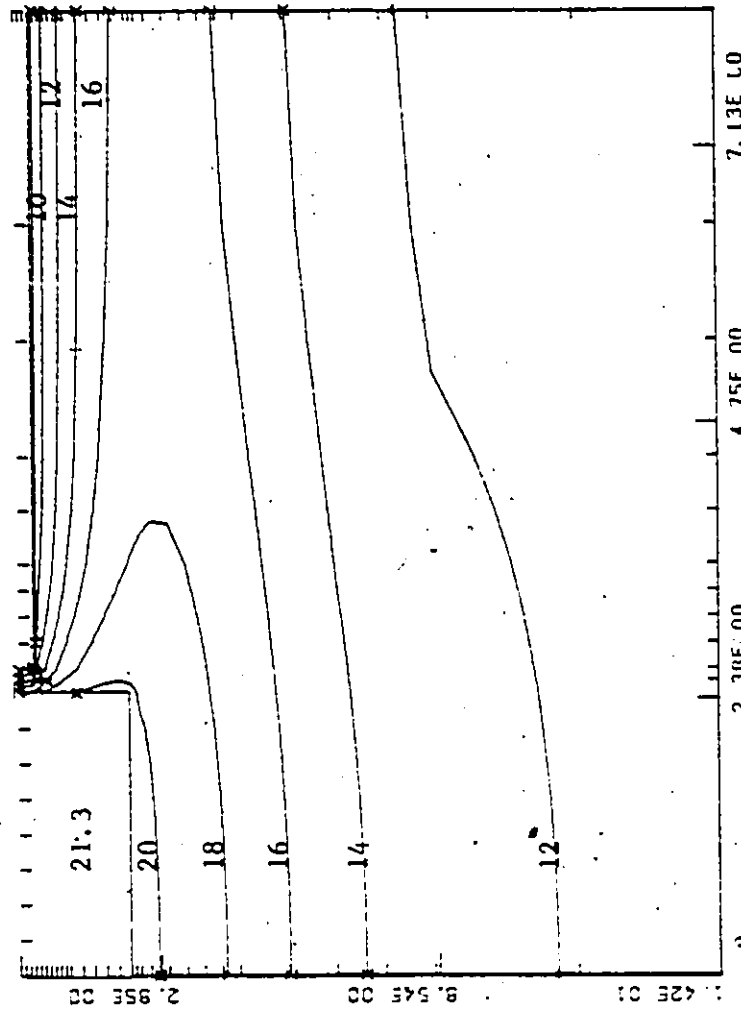


Fig.34. Ground isotherms for Nov.17

THE GROUND IS COVERED BY AN ASPHALT PAVEMENT

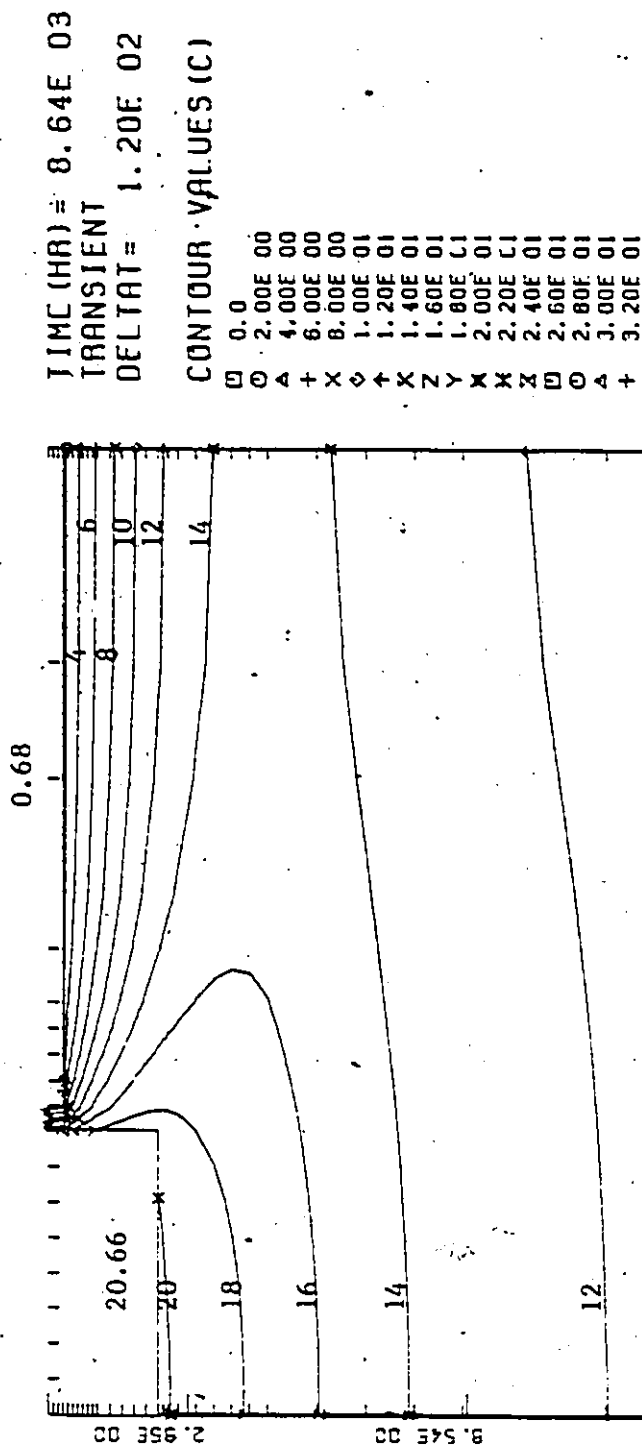


Fig.35. Ground isotherms for Dec.27

THE GROUND IS COVERED BY AN ASPHALT PAVEMENT

2.52

TIME (HR) = 9.60E 03
TRANSIENT
DELTA T = 1.20E C2

CONTOUR VALUES (C)

0 0.0
1 2.00E 00
2 4.00E 00
3 6.00E 00
4 8.00E 00
5 1.00E 01
6 1.20E 01
7 1.40E 01
8 1.60E 01
9 1.80E 01
10 2.00E 01
11 2.20E 01
12 2.40E 01
13 2.60E 01
14 2.80E 01
15 3.00E 01
16 3.20E 01

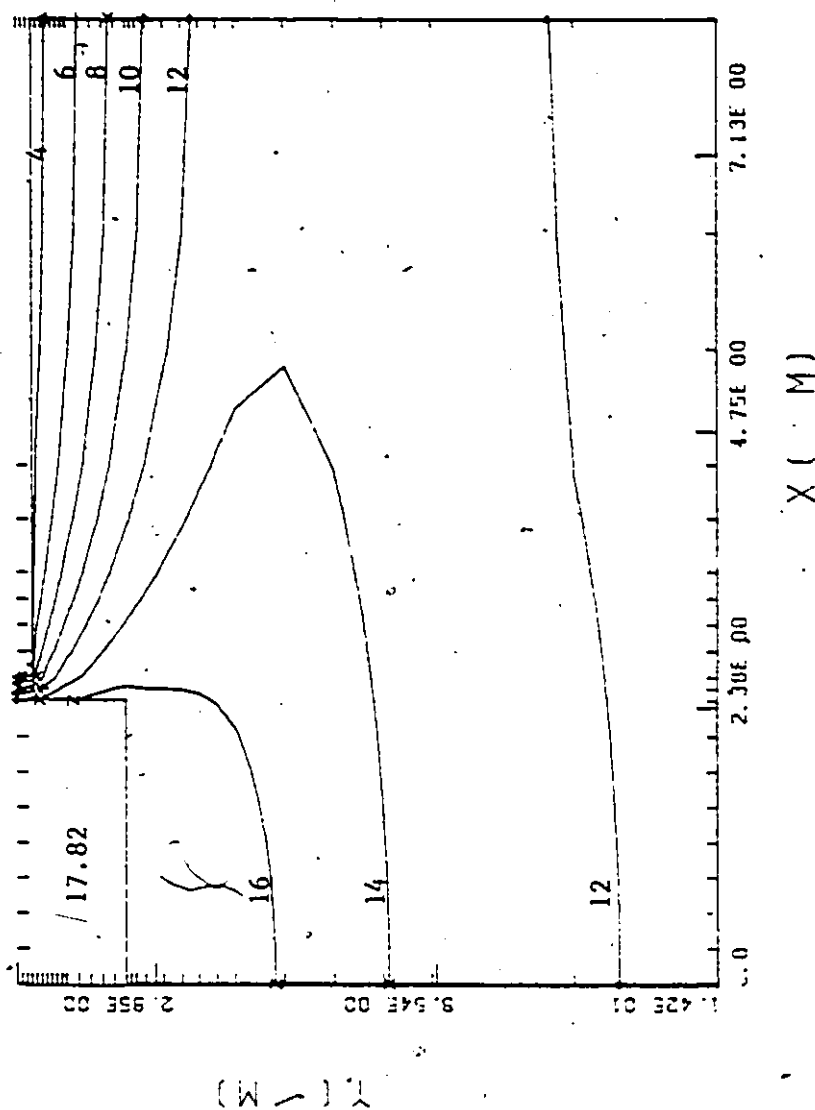


Fig. 36. Ground isotherms for Feb. 5

THE GROUND IS COVERED BY AN ASPHALT PAVEMENT

5.13

TIME (HR) = 1.06E 04
 TRANSIENT
 DELTAT = 1.20E 02
 CONTOUR VALUES (C)

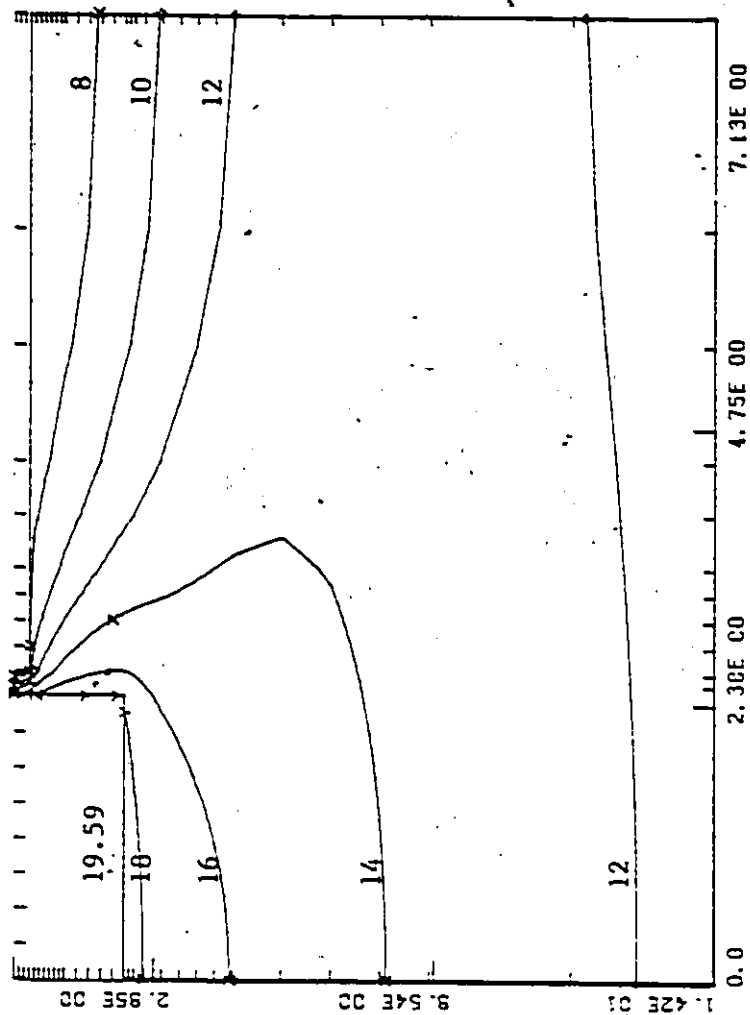


Fig. 37. Ground isotherms for March 17.

THE GROUND IS COVERED BY AN ASPHALT PAVEMENT

TIME (HR) = 1.15E 04
TRANSIENT
DELTA T = 1.20E 02

CONTOUR VALUES (C).

0 0.0
0 2.00E 00
4 4.00E 00
+ 6.00E 00
X 8.00E 00
0 1.00E 01
+ 1.20E 01
X 1.40E 01
Z 1.60E 01
Y 1.80E 01
X 2.00E 01
X 2.20E 01
X 2.40E 01
0 2.60E 01
0 2.80E 01
4 3.00E 01
+ 3.20E 01

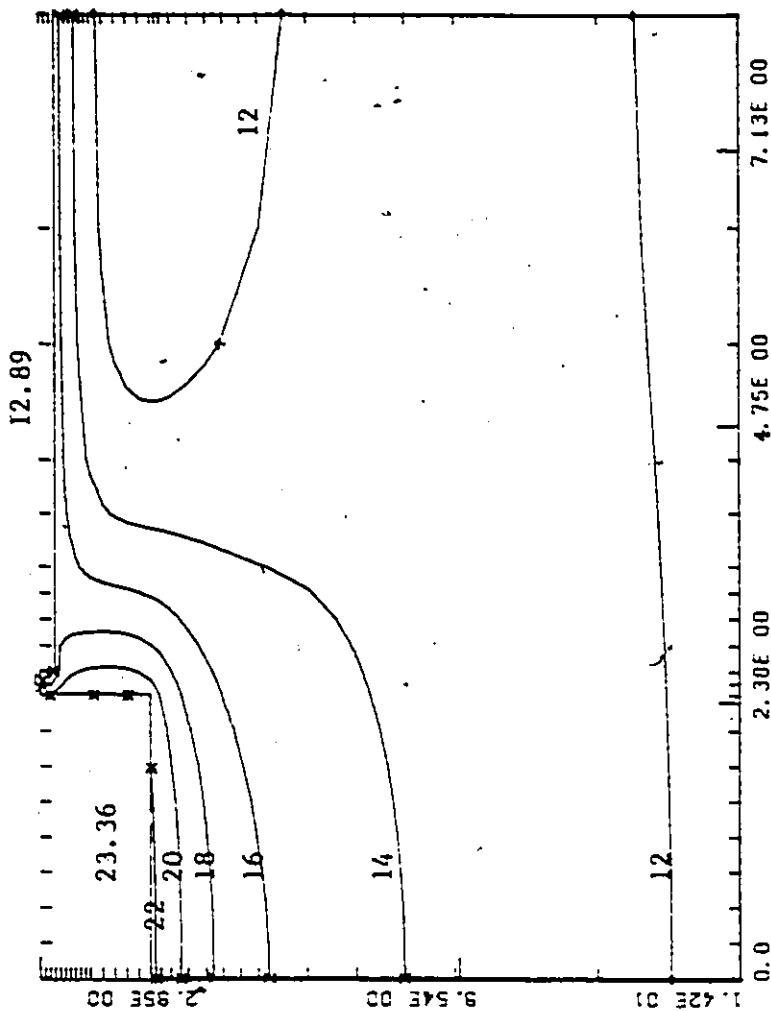
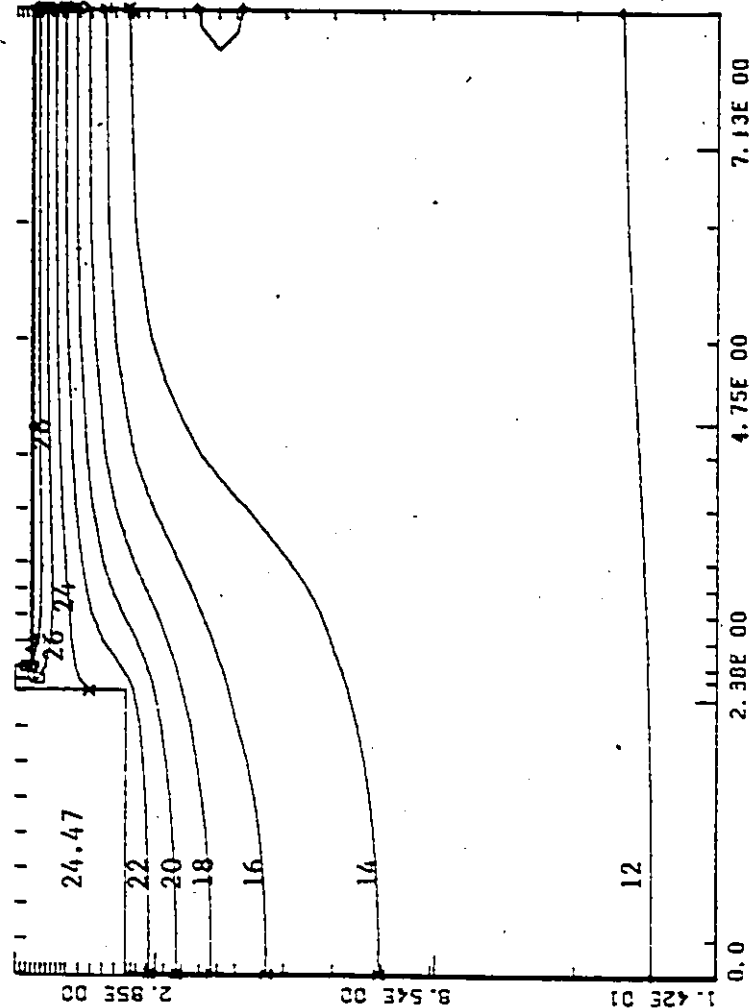


Fig.38. Ground isotherms for April 26.

THE GROUND IS COVERED BY AN ASPHALT PAVEMENT

25.18



TIME (HR) = 1.25E C4
TRANSIENT
DELTA T = 1.20E 02

CONTOUR VALUES (C)

- 0 0.0
- 1 2.00E 00
- 2 4.00E 00
- 3 6.00E 00
- 4 8.00E 00
- 5 1.00E 01
- 6 1.20E 01
- 7 1.40E 01
- 8 1.60E 01
- 9 1.80E 01
- A 2.00E 01
- B 2.20E 01
- C 2.40E 01
- D 2.60E 01
- E 2.80E 01
- F 3.00E 01
- G 3.20E 01

9.51E 00

X (M)

Fig.39. Ground isotherms for June 5.

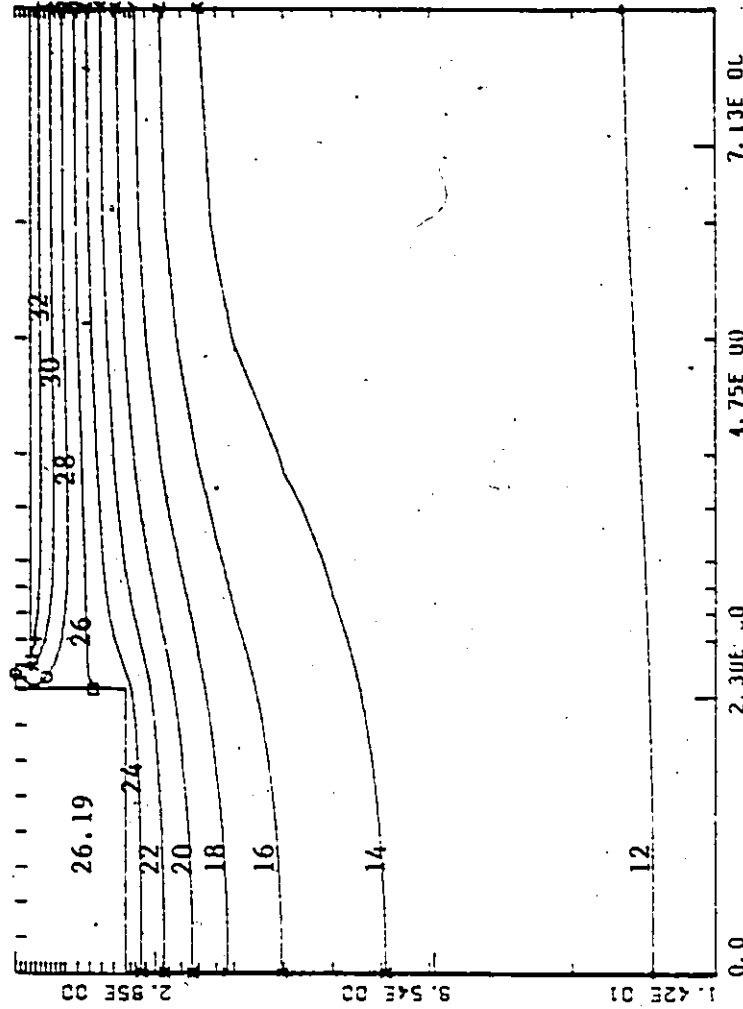
THE GROUND IS COVERED BY AN ASPHALT PAVEMENT

28.56

TIME (HR) = 1.34E 04
TRANSIENT
DELTA T = 1.20E 02

CONTOUR VALUES (C)

0	0.0
1	2.00E 00
2	4.00E 00
3	6.00E 00
4	8.00E 00
5	1.00E 01
6	1.20E 01
7	1.40E 01
8	1.60E 01
9	1.80E 01
A	2.00E 01
B	2.20E 01
C	2.40E 01
D	2.60E 01
E	2.80E 01
F	3.00E 01
G	3.20E 01



X (M)

Fig.40. Ground isotherms for July 15.

are shown in Figure 30.1 The ground isotherms for the asphalt covered surface are shown in Figures 31 - 40. It is seen that the temperatures under a paved surface are significantly warmer than that under a grassy surface and these effects significantly reduce the basement wall and floor heat losses.

4.5 INSULATION PLACEMENT

Since there are a large number of ways that insulation may be placed on the basement wall, it would not be feasible to study all the placements. Wang [33] and ASHRAE recommend that exterior insulation placement is more effective than interior insulation placement. Therefore full length and half length insulation placements were considered, the half length being insulation on the top half of the basement wall. The insulation material was taken as 5.08cm thick and its properties were similar to those of polystyrene. The thermal properties of polystyrene were taken from Szydlowski's report [32] and are listed below :-

Thermal Conductivity - $0.0274 \text{ W/m } ^\circ\text{C}$

Specific Heat - $1.21 \text{ kJ/kg } ^\circ\text{C}$

Density - 56 kg/m^3

HEATING 5 was then run for both cases and the basement wall and floor heat loss for the full length and half length insulation placement are shown in Figures 41 and 42. The full length insulation placement reduces the wall heat loss

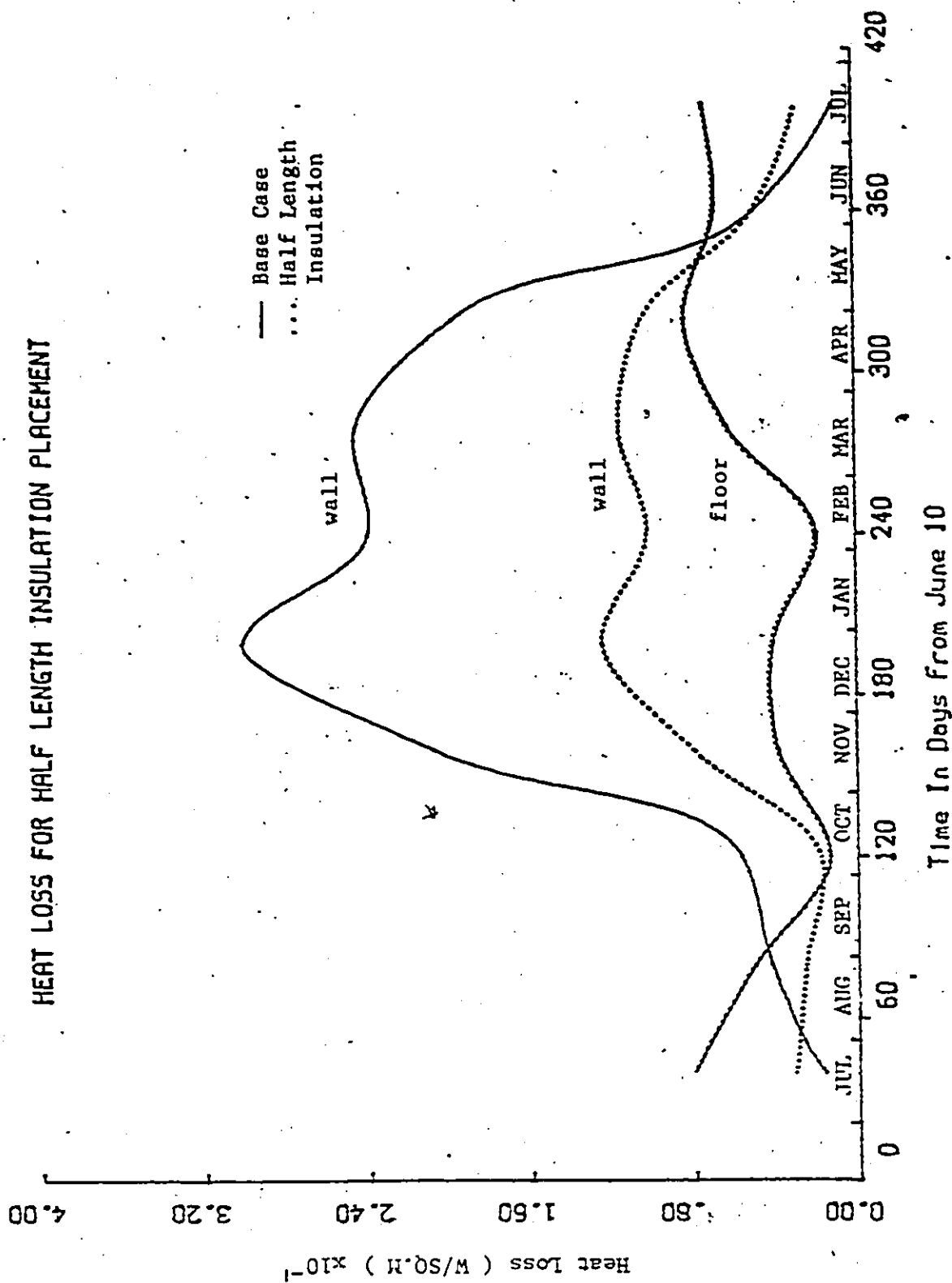


Fig.41. Annual heat loss with half length insulation on the basement wall

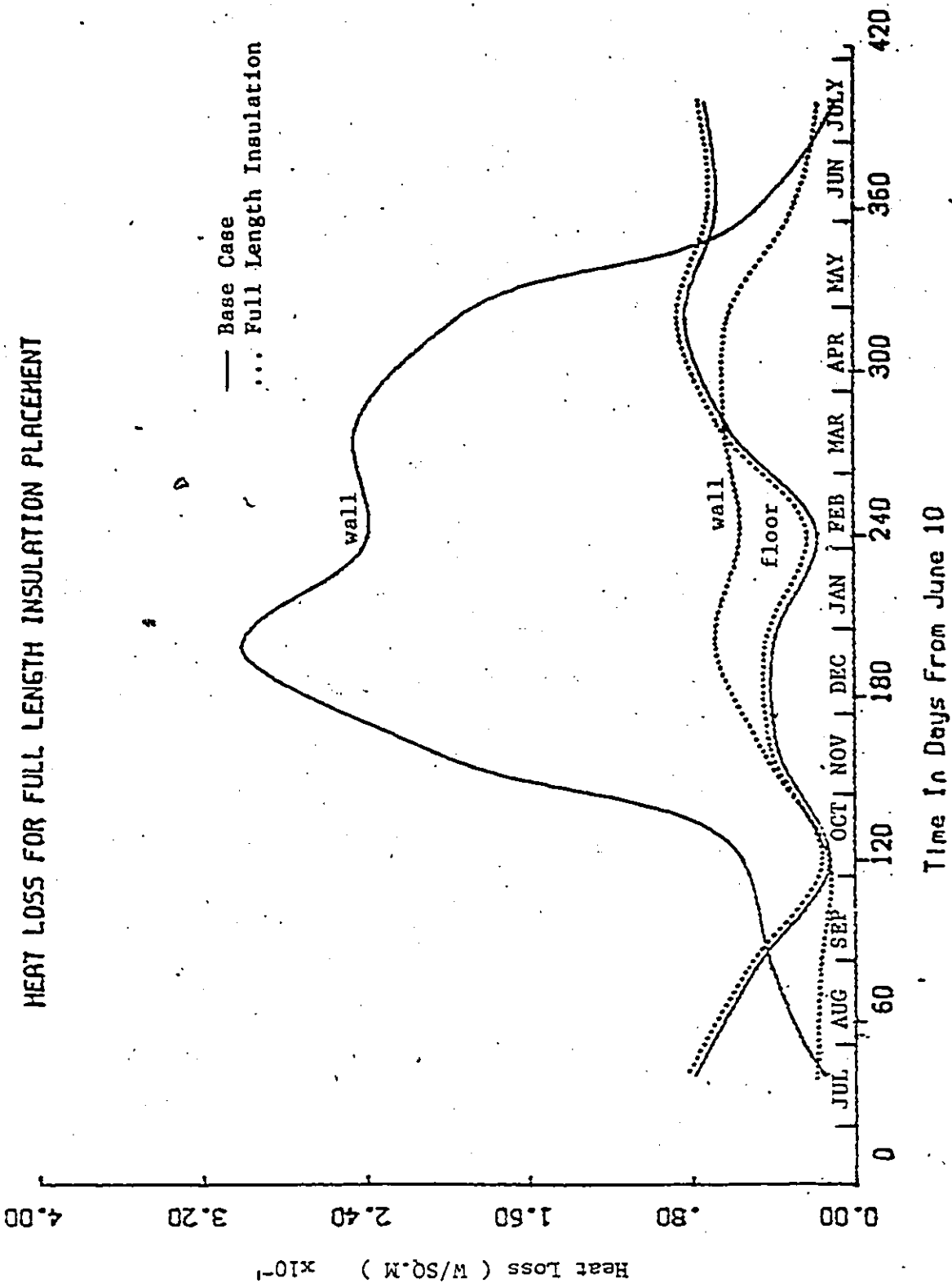


Fig.42. Annual heat loss with full length insulation on the basement wall

FULL LENGTH INSULATION ON THE EXTERIOR WALL

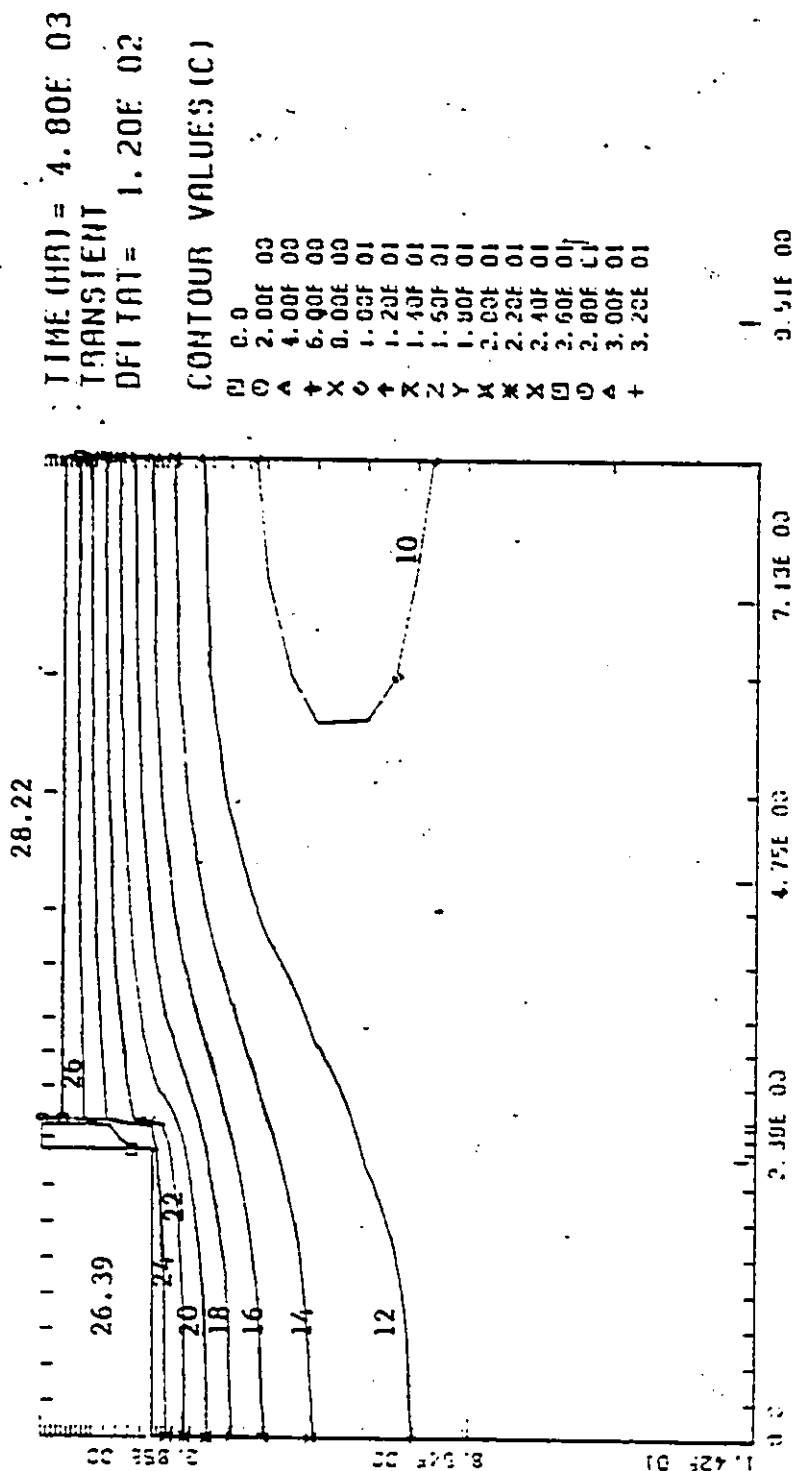


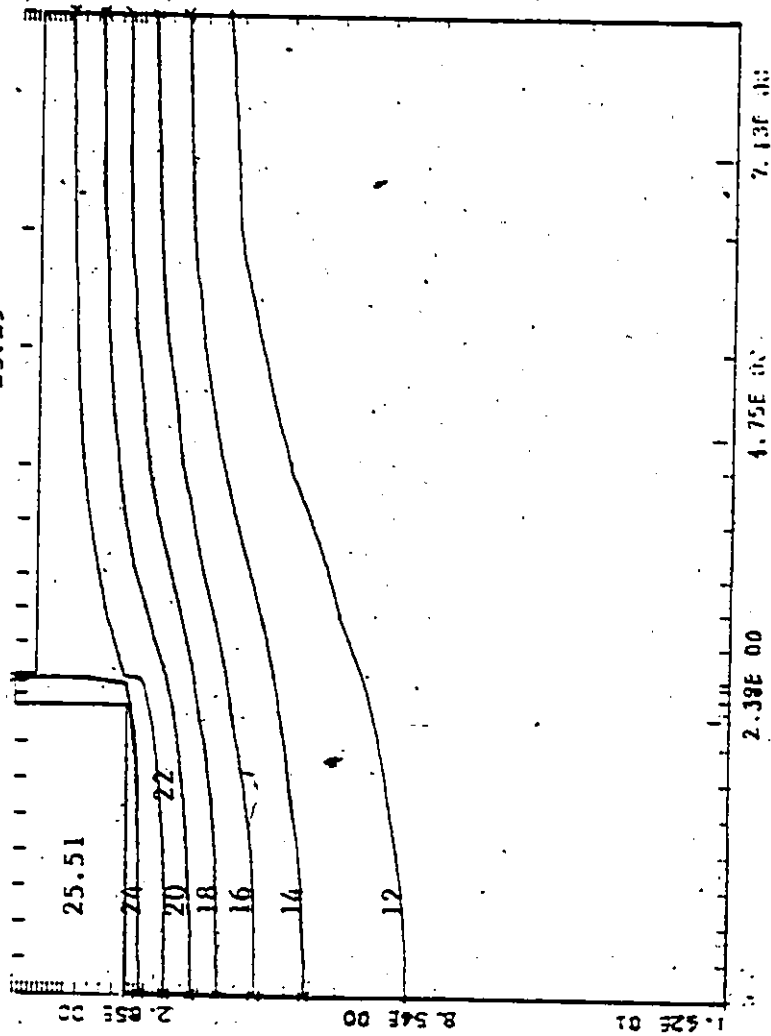
Fig.43. Ground isotherms for July 20.

FULL LENGTH INSULATION ON THE EXTERIOR WALL

TIME (HR) = 5.76E 03
 TRANSIENT
 DELTAT = 1.20E 02

CONTOUR VALUES (C)

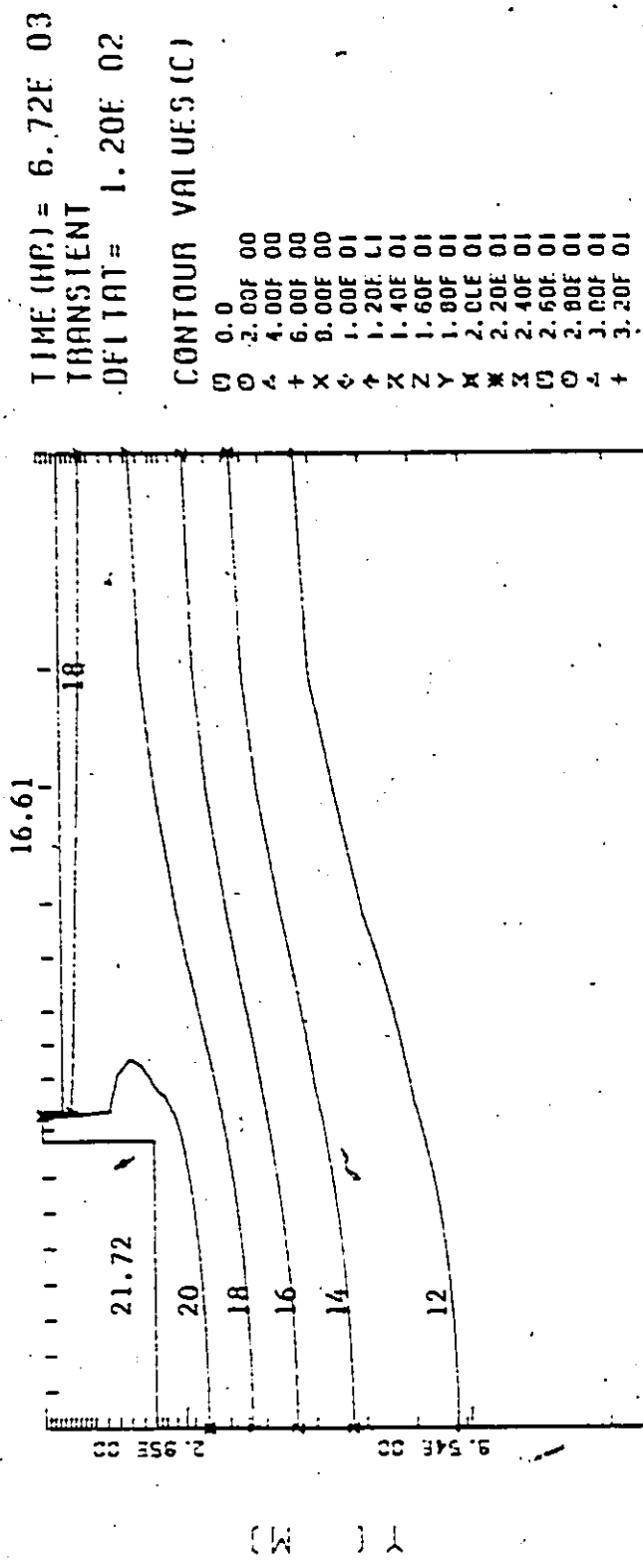
0 0.0
 1 2.00E 00
 2 4.00E 00
 3 6.00E 00
 4 8.00E 00
 5 1.00E 01
 6 1.20E 01
 7 1.40E 01
 8 1.60E 01
 9 1.80E 01
 10 2.00E 01
 11 2.20E 01
 12 2.40E 01
 13 2.60E 01
 14 2.80E 01
 15 3.00E 01
 16 3.20E 01



X (M)

Fig. 44. Ground isotherms for Aug. 29

FULL LENGTH INSULATION ON THE EXTERIOR WALL



X (M)

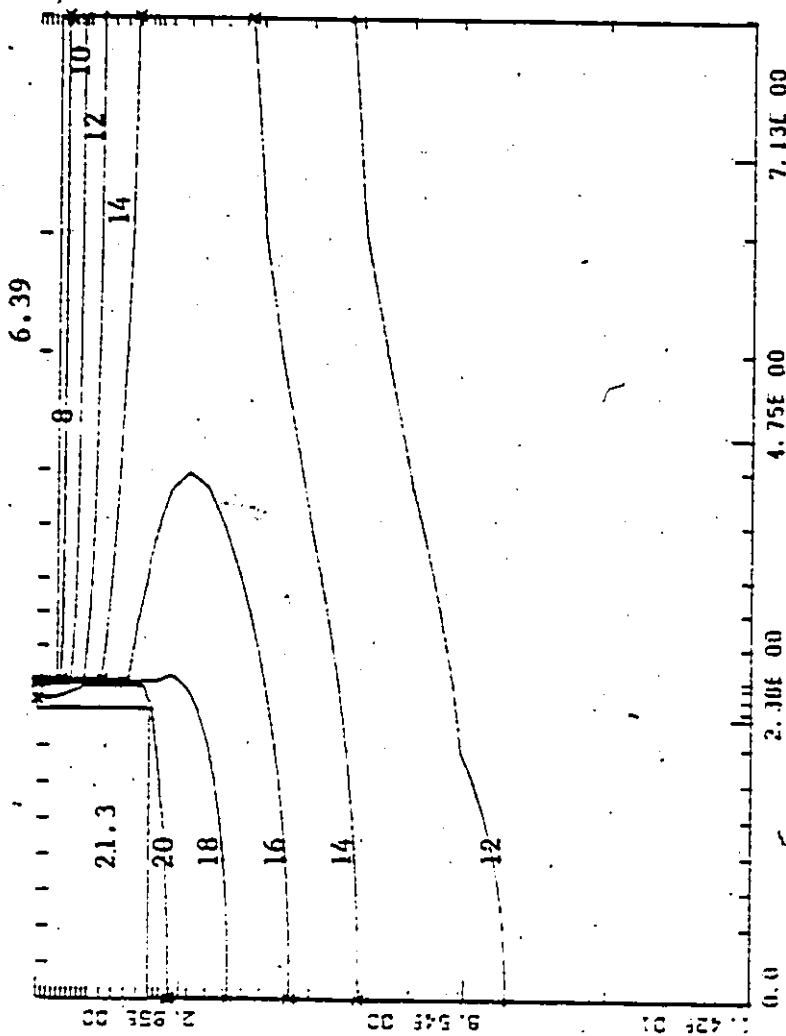
Fig.45. Ground isotherms for Oct.8

FULL LENGTH INSULATION ON THE EXTERIOR WALL

TIME (HR) = 7.68E 03
 TRANSIENT
 DELTAT = 1.20E 02

CONTOUR VALUES (C)

0.0
 2.00E 00
 4.00E 00
 6.00E 00
 8.00E 00
 1.00E 01
 1.20E 01
 1.40E 01
 1.60E 01
 1.80E 01
 2.00E 01
 2.20E 01
 2.40E 01
 2.60E 01
 2.80E 01
 3.00E 01
 3.20E 01



X (M)

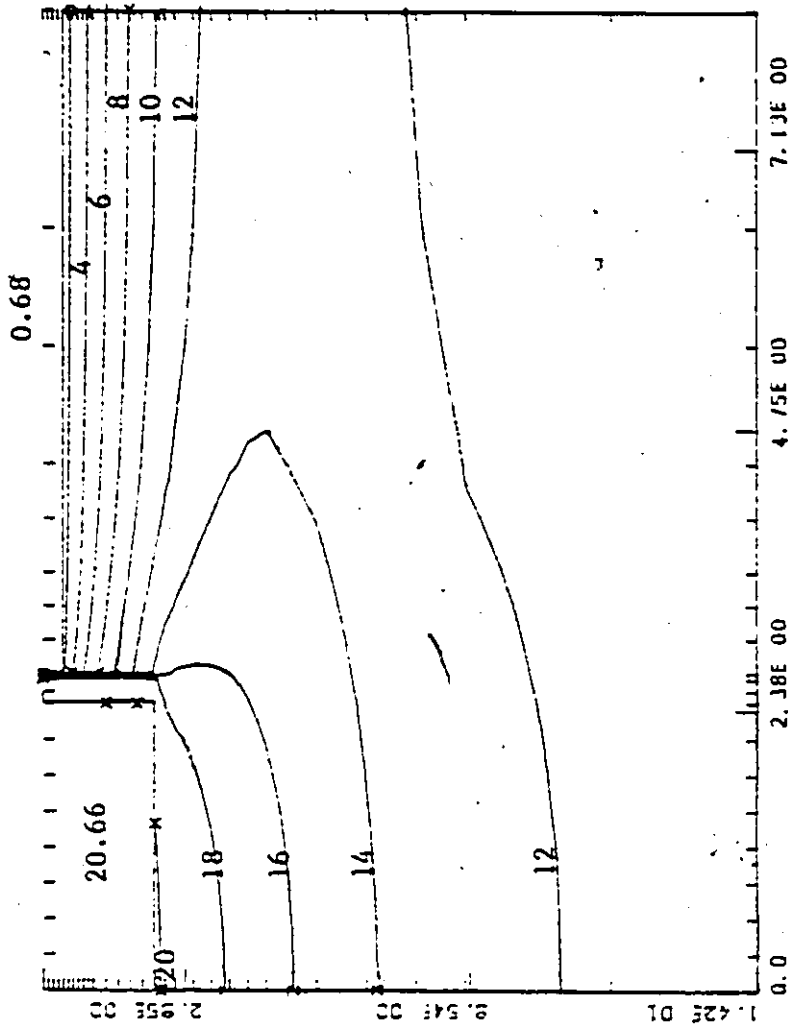
Fig.46. Ground Isotherms for Nov.17

FULL LENGTH INSULATION ON THE EXTERIOR WALL

TIME (HR) = 0.64E 03
 TRANSIENT
 DELTA T = 1.20E 02

CONTOUR VALUES (C)

0 0.0
 1 2.00E 00
 2 4.00E 00
 3 6.00E 00
 4 8.00E 00
 5 1.00E 01
 6 1.20E 01
 7 1.40E 01
 8 1.60E 01
 9 1.80E 01
 A 2.00E 01
 B 2.20E 01
 C 2.40E 01
 D 2.60E 01
 E 2.80E 01
 F 3.00E 01
 G 3.20E 01

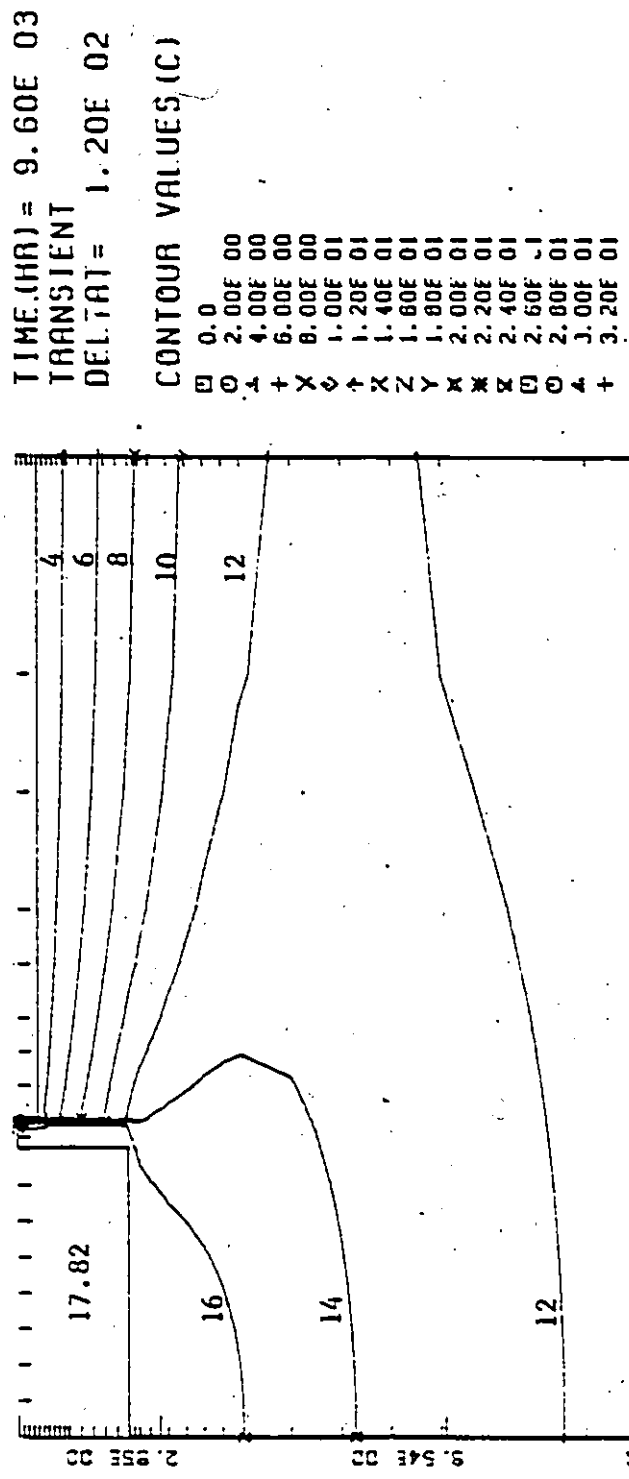


X (M)

Fig.47. Ground Isotherms for Dec.27

FULL LENGTH INSULATION ON THE EXTERIOR WALL

2.52



X (M)

Fig. 48. Ground isotherms for Feb. 5

FULL LENGTH INSULATION ON THE EXTERIOR WALL

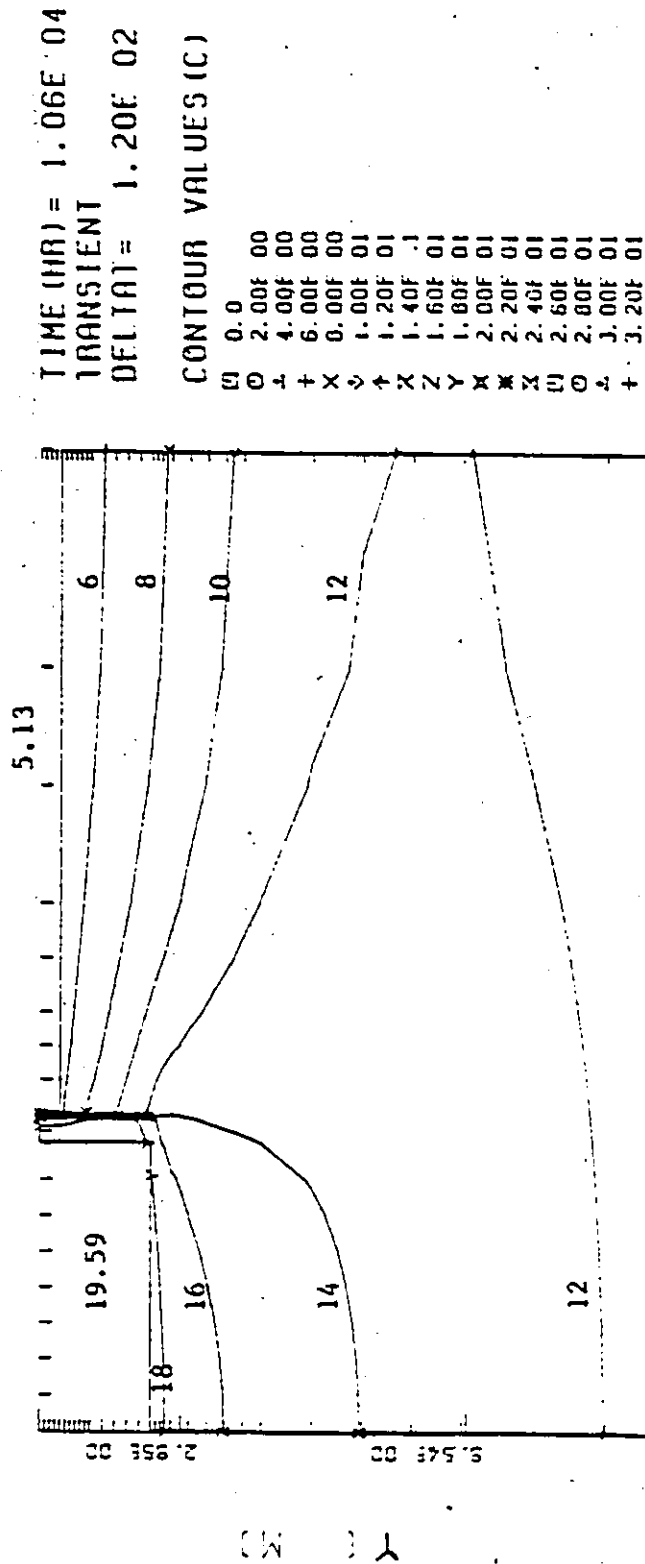


Fig.49. Ground isotherms for March 17.

FULL LENGTH INSULATION ON THE EXTERIOR WALL

TIME (HR) = 1.15E 04
 TRANSIENT
 DELTAT = 1.20E 02
 CONTOUR VALUES (C)

0	0.0
1	2.00E 00
2	4.00E 00
3	6.00E 00
4	8.00E 00
5	1.00E 01
6	1.20E 01
7	1.40E 01
8	1.60E 01
9	1.80E 01
10	2.00E 01
11	2.20E 01
12	2.40E 01
13	2.60E 01
14	2.80E 01
15	3.00E 01
16	3.20E 01

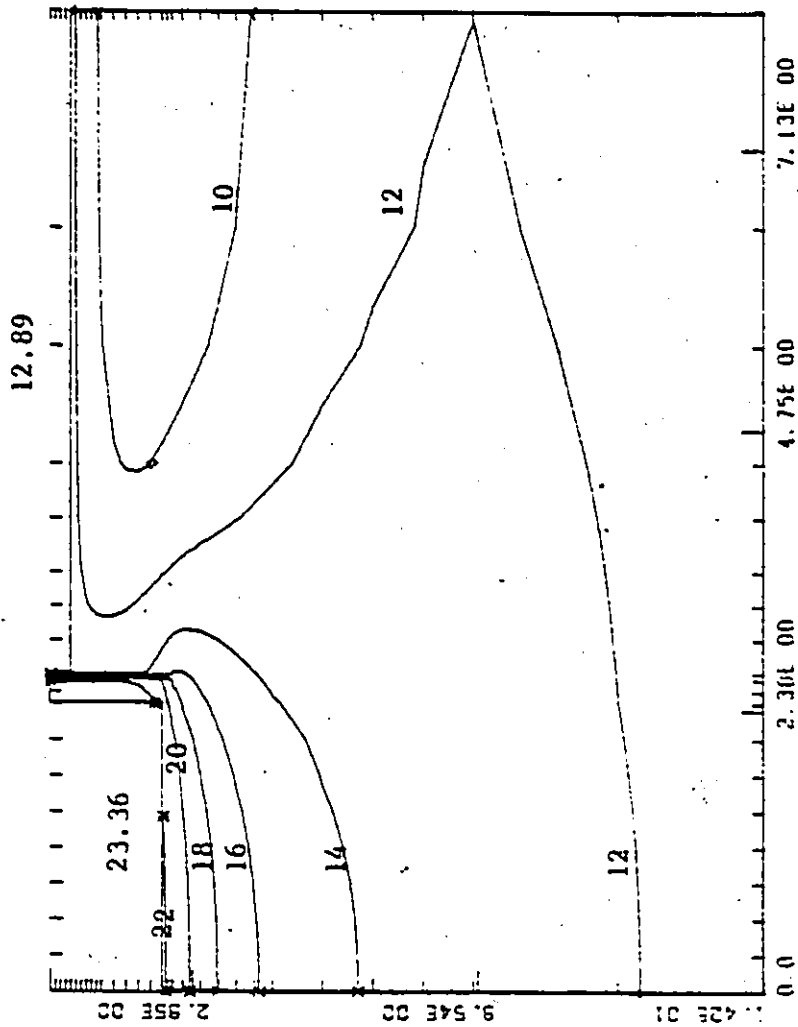


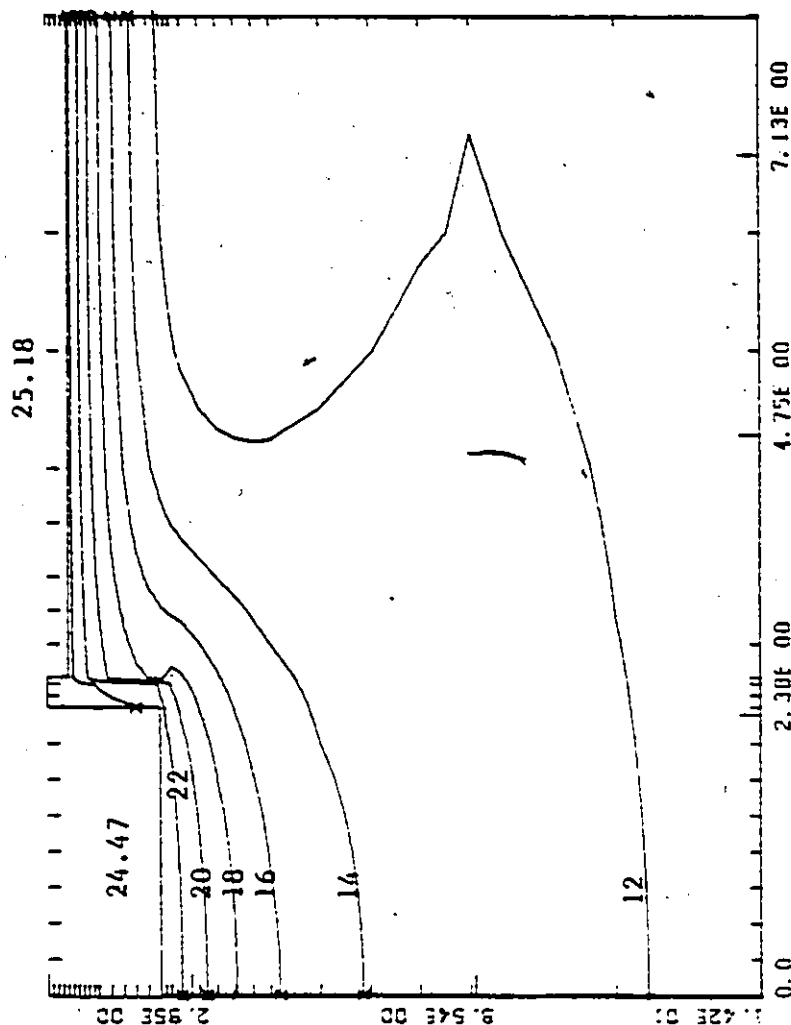
Fig.50. Ground isotherma for April 26.

FULL LENGTH INSULATION ON THE EXTERIOR WALL

TIME (HR) = 1.25E 04
 TRANSIENT
 DELTAT = 1.20E 02

CONTOUR VALUES (C)

0	0.0
1	2.00E 00
2	4.00E 00
3	6.00E 00
4	8.00E 00
5	1.00E 01
6	1.20E 01
7	1.40E 01
8	1.60E 01
9	1.80E 01
A	2.00E 01
B	2.20E 01
C	2.40E 01
D	2.60E 01
E	2.80E 01
F	3.00E 01
G	3.20E 01



X (M)

Fig.51. Ground isotherms for June 5.

by about 80% during the month of February while the floor heat loss is increased by about .37%. The half length insulation placement for the same month reduces wall heat loss by about 60% while the floor heat loss is increased by about 15%. On an average, the wall heat loss during the heating season reduces by about 75.4% and 56.2% for full length and half length insulation placement respectively. The average floor heat loss for full length and half length insulation placement during the same period is increased by about 5.4% and 0.2% respectively.

The insulation tends to reduce the effect of the basement temperatures on the temperature of the surrounding soil. This effect can be seen by referring to Figures 43 - 51 which show the isotherms around a basement with fully insulated walls. It is seen that ground temperatures under the basement floor are lower than those under an uninsulated basement. Another point to note is that the isotherms around the basement wall are no longer radial, even during the months of February, and this shows that ASHRAE's assumption of radial isotherms are not valid for an insulated basement.

4.6 BASEMENT TEMPERATURE

During this analysis, the basement air was maintained at a fixed temperature of 22 C throughout the year. All the other conditions were assumed to be the same as that for the Base Case. HEATING 5 was then used to calculate the basement heat loss.

In the Base Case the basement air was maintained at a floating temperature (i.e. it varied with time). Figure 51.1 shows the basement wall and floor heat for a fixed basement temperature of 22 C and for the Base Case. It is seen that by maintaining the basement at 22 C, the basement wall and floor heat loss during the heating season increases by about 10.67% and 27.3% respectively as compared to the Base Case. From Figure 51.1, it is seen that the shape of the basement wall and floor heat loss curves can be attributed to the floating basement temperature.

HEAT LOSS FOR FIXED BASEMENT TEMPERATURE

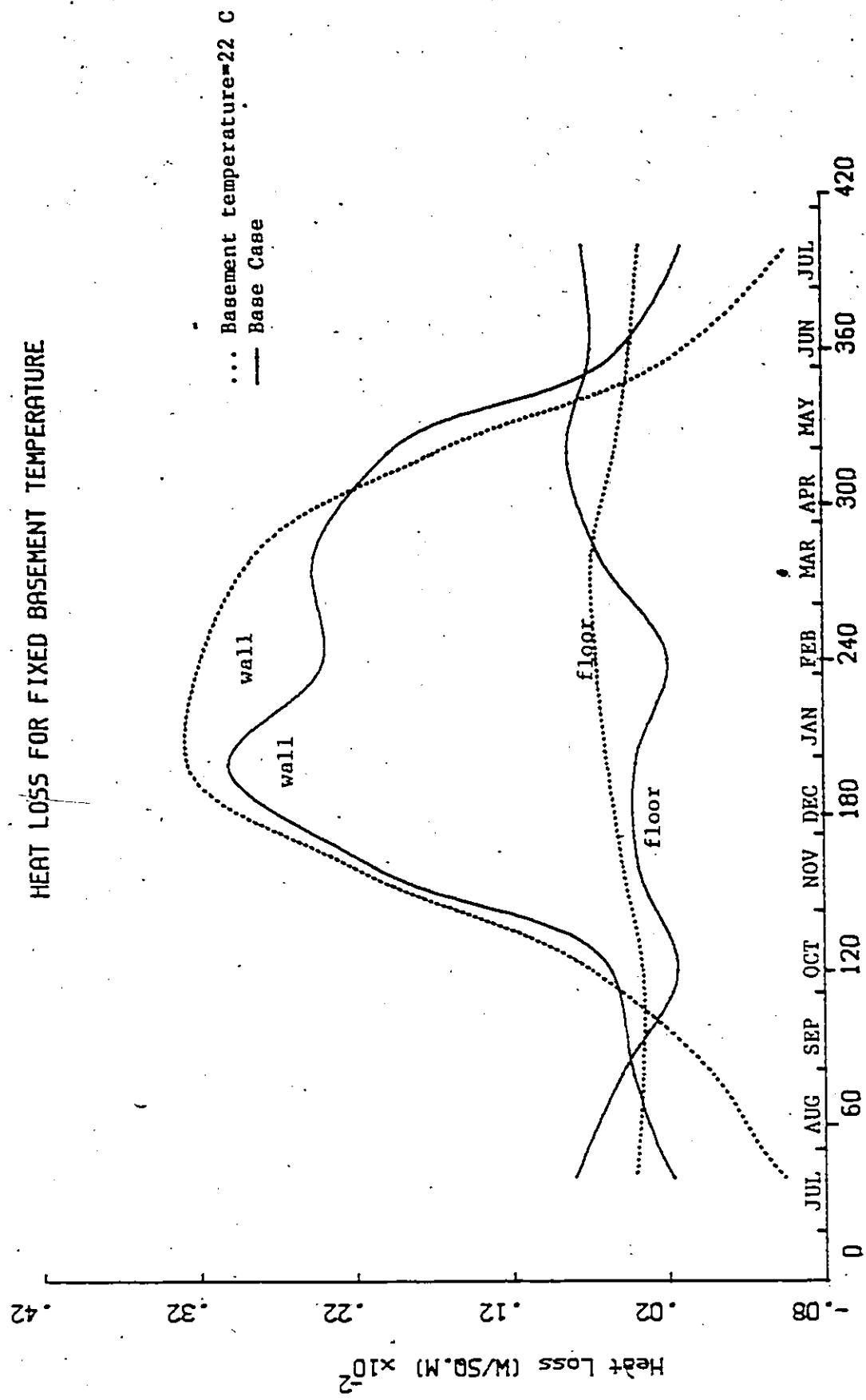


Fig.51.1.1. Annual heat loss for a basement maintained at 22 C.

Chapter V

ANALYSIS OF THE DBR/NRC BASEMENT IN OTTAWA

A basement maintained by the DBR/NRC at Ottawa was selected in an effort to predict the effect of the level of the ground water table on the basement heat loss. The ground water flow was abnormally high for that region. A drainage ditch was dug around the test site to lower the water table uniformly and to reduce the water flow at the footings. The ground water table after construction of the drainage ditch, was about 0.5m below the basement floor surface. The basement was constructed in an area of Leda clay. The basement wall and floor heat losses were measured and reported in a report published by Mitalas [37]. There were three test basements maintained by the DBR/NRC, and Basement A was chosen for this analysis.

The basement was insulated on the inside over the full height of the wall. The basement walls and floor were made of concrete and the insulation material was glass fibre. The thermal and physical properties of the materials used in the basement construction are listed in Table 5. Controlled electrical heaters were used in the basement to maintain the interior temperature constant at 21 C.

The floor heat loss could not be accurately predicted by Mitalas due to the very high ground water table. It was decided to use the HEATING 5 computer program to discover a better way to account for the effect of a high ground water table on the basement heat loss.

5.1 MODEL ASSUMPTIONS-

Several simplifying assumptions were made to develop a manageable and reasonably accurate model. Most of the assumptions made were the same as that used in the previous analysis (Chapter III). The only difference being :-

1. The soil thermal properties remain constant throughout the year.
2. The ambient air temperatures for the Ottawa area are represented by the Fourier equation :-

$$T_a = 6.0912 + 15.3684 * \cos(Z) - 1.3074 * \cos(2Z) \\ + 0.4841 * \cos(3Z) + 1.8927 * \sin(Z) - 0.5999 * \sin(2Z) \\ + 0.0125 * \sin(3Z)$$

where $Z = 2\pi(t/24 + 183)/365$ and t is in hours from January 15.

The basement was maintained at a constant temperature of 21 C throughout the analysis, as was done by Mitalas during his experiment.

3. The snow cover varies monthly and its values were taken from the report published by Scanada Consultants [47] as listed in Table 4. The thermal

SNOW COVER IN CENTIMETERS						
DAYS	NOVEMBER	DECEMBER	JANUARY	FEBRUARY	MARCH	APRIL
1	-	8	43	62	55	-
2	-	15	32	67	58	-
3	-	14	33	67	57	-
4	-	16	33	67	54	-
5	-	13	33	69	48	3
6	-	12	33	69	40	2
7	-	12	33	69	38	3
8	-	12	34	71	34	1
9	-	14	34	72	34	T
10	-	14	34	72	34	1
11	-	14	34	72	32	-
12	-	16	34	72	32	-
13	-	18	34	72	32	-
14	-	18	42	72	30	-
15	-	18	42	72	32	-
16	-	20	42	69	32	-
17	-	28	42	69	32	-
18	-	29	50	68	32	-
19	-	29	50	68	29	-
20	-	29	50	67	27	-
21	-	33	51	65	22	-
22	-	32	71	63	16	-
23	-	32	71	62	15	-
24	5	32	70	56	9	-
25	5	34	70	52	7	-
26	5	48	77	52	6	-
27	3	46	72	57	6	-
28	10	46	66	57	6	-
29	11	46	60	-	4	-
30	8	46	62	-	4	-
31	-	47	60	-	0	-

Table 4. Snow Cover In Centimeters For Ottawa (1978-79).

ELEMENT	THERMAL CONDUCTIVITY (W/m C)	DENSITY (kg/m ³)	SPECIFIC HEAT (kJ/kg C)
Wall	1.73	2243	0.84
Floor	1.73	2243	0.84
Insulation	0.0433	32	0.84
Soil (measured)	0.88	1490	1.765
Soil (80% wet)	1.56	1400	1.756
Soil (100% wet)	2.135	1650	2.062

Table 5. Building and Soil Thermal Properties.

capacity of snow is neglected in this analysis. Its thermal conductivity is taken to be 0.173 W/m C (a mean value between dense and loose snow was considered and is taken from a paper by Labs [4]). The monthly average snow cover is considered and it is converted into an effective convection coefficient. Snow cover data for 1978-79 was used because the data for 1980-81 was not available at the time of this analysis.

The basement floor, wall, and soil thermal properties were taken from ASHRAE [3] and the report published by Nitalas [37] and are shown in Table 5. A variable grid size was chosen to better predict the basement heat losses. The grid spacing near the basement wall was about 12cms. while the grid spacing near the floor was about 20cms. A total of 361 nodes were used with time steps of 146 hours (6.08333 days).

5.2 MODEL ANALYSIS

The model employs a two-dimensional cross-section, bounded by a vertical adiabatic boundary sufficiently removed to minimize its impact on the basement heat loss. The upper horizontal boundary is set by a seasonally varying convective coefficient and the lower boundary consists of an isothermal sink. Figure 52 shows the basement configuration.

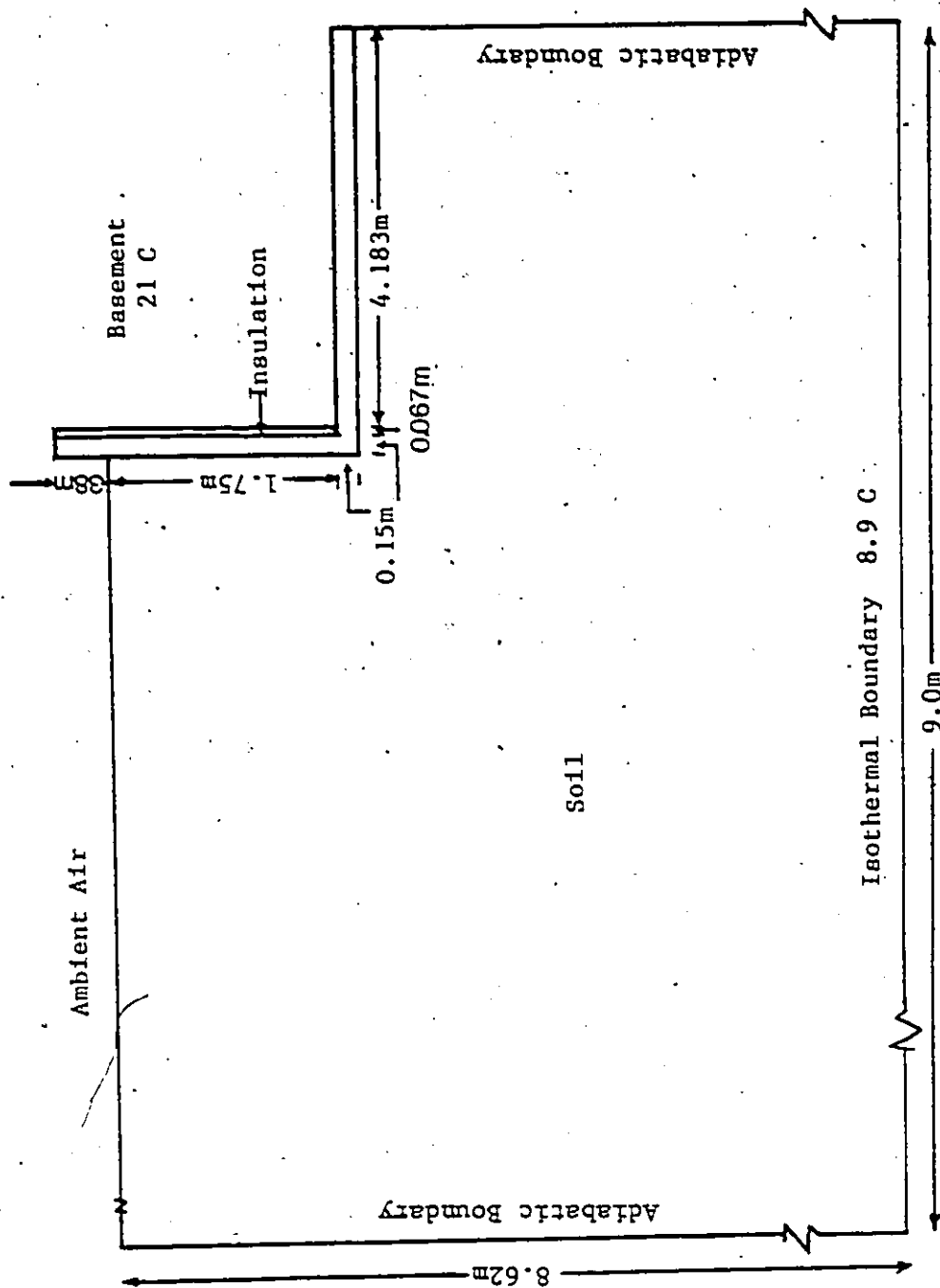


Fig.52. Basement model showing the boundary conditions

HEATING 5 was used to calculate the basement wall and floor heat loss. A third order Fourier fit of the ambient air temperature was used as an input to the model. The basement was maintained at a temperature of 21 C during this analysis. Three different models were considered for analysis. The models were :-

1. MODEL 1 :

The lower isothermal boundary was set at 8.62m below grade and the deep ground temperature was 8.9 C. The effect of the ground water was neglected and the soil properties were assumed to be constant throughout the model configuration. The soil thermal properties are :-

thermal conductivity = 0.88 W/m K

density = 1490 kg/m^3 at 42%
moisture.

specific heat = 1765 J/kg K

These values were the same as those measured by Mitalas. The calculated basement wall and floor heat losses are shown in Figures 53 and 54.

2. MODEL 2 :

The lower thermal boundary was set at 0.5m below the basement floor. The temperatures at 0.5m below the center of the basement were measured by Mitalas [48]. These temperatures were assumed to be uniform throughout the lower boundary, but varying with time.

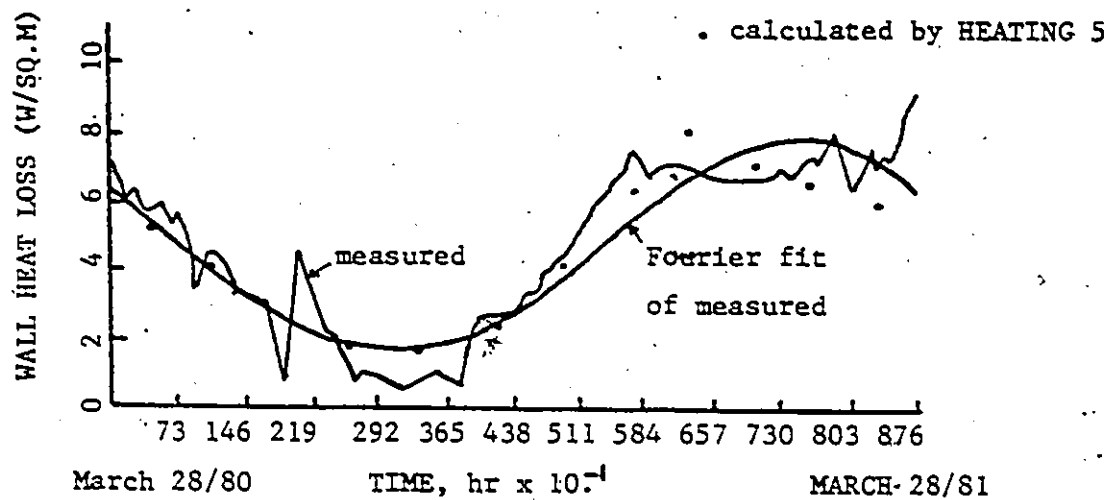


Fig.53. Wall heat loss for Model 1

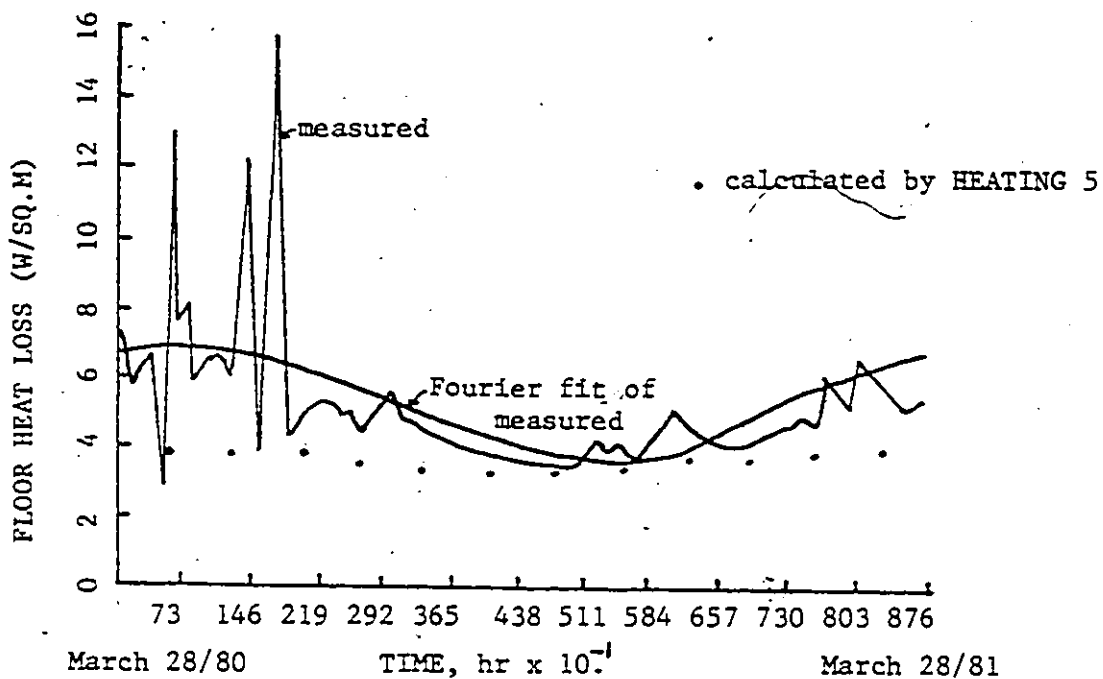


Fig.54. Floor heat loss for Model 1

A third order Fourier fit of the lower isothermal boundary was used as an input to the model. The Fourier equation used in this model was :-

$$T_s = 18.61 + 0.3175 \cdot \cos(Z) - 0.1003 \cdot \cos(2Z) \\ + 0.461 \cdot \cos(3Z) + 0.9095 \cdot \sin(Z) + 0.1329 \cdot \sin(2Z) \\ - 0.1063 \cdot \sin(3Z)$$

where $Z = 2\pi (t/24 + 183)/365$ and t is time in hours from January 15.

It was assumed that there was sufficient ground water flow to keep the temperature of the thermal boundary uniform.

Two types of soil (clay with different moisture contents) were used during this analysis. Since the ground water table is 0.5m below the basement floor, the soil between the basement floor and ground water table was assumed to be 80% wet and its thermal properties were extracted from 'Thermal Geotechnics' [27] and are listed below :-

thermal conductivity = 1.56 W/m K
density = 1400 kg/m³
specific heat = 1756 J/kg K

The thermal properties of the soil between the ground surface and the basement floor were assumed to be the same as that measured by Mitalas and are :-

thermal conductivity = 0.88 W/m K
density = 1490 kg/m³
specific heat = 1765 J/kg K

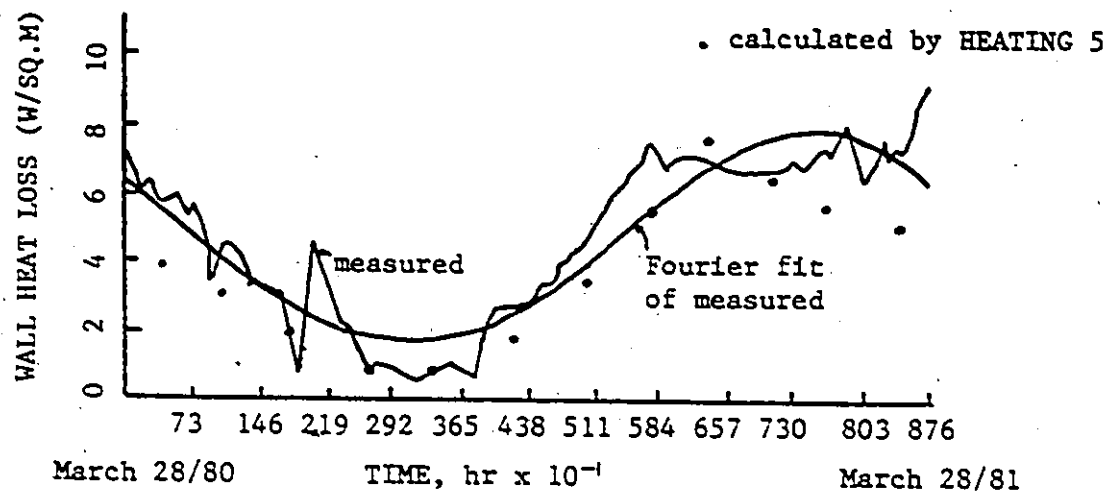


Fig.55. Wall heat loss for Model 2.

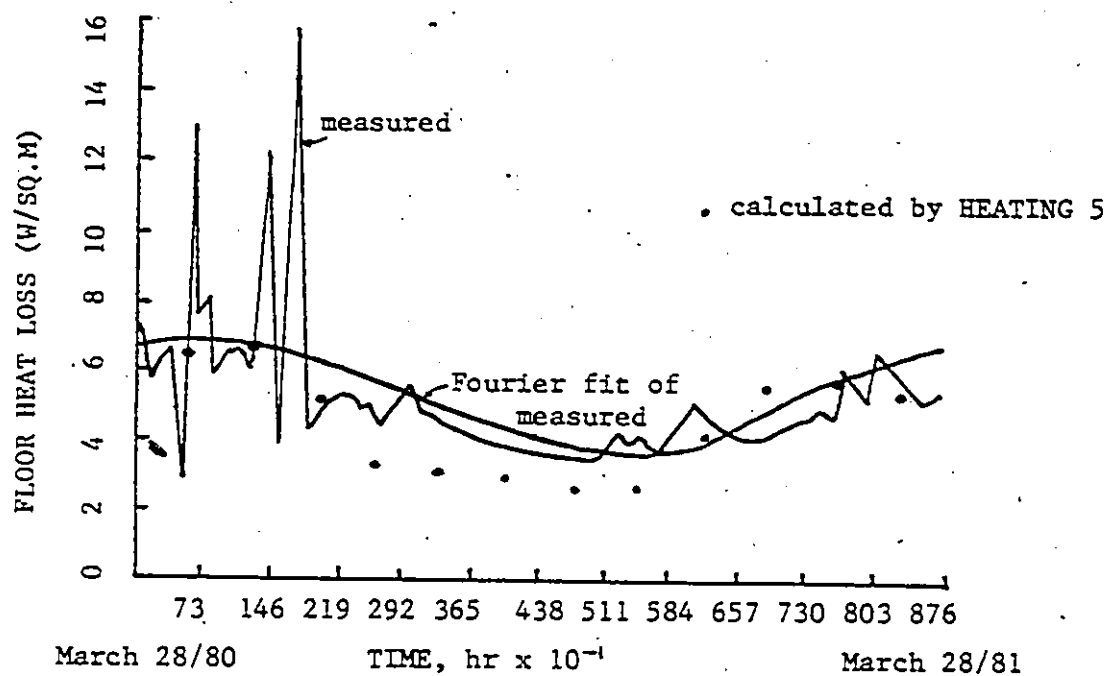


Fig.56. Floor heat loss for Model 2.

The calculated basement wall and floor heat loss for this model are shown in Figures 55 and 56 respectively.

3. MODEL 3 :

The lower isothermal boundary was set at 8.62m below grade and the deep ground temperature was 8.9 C (as in Model 1). Since the ground water table is 0.5m below the basement floor, all the soil below the ground water table was assumed to be wet soil. It was assumed that the soil (clay) 0.5m below the basement floor was 100% saturated and its thermal properties were extracted from 'Thermal Geotechnics' [27] and are listed below :-

thermal conductivity = 2.135 w/m K

density = 1650 kg/m³

specific heat = 2062 J/kg K

The soil between the basement floor and the ground water table was assumed to be 80% saturated and its thermal properties are listed below :-

thermal conductivity= 1.56 w/m K

density = 1400 kg/m³

specific heat = 1756 J/kg K

The thermal properties of the soil between the ground surface and the basement floor were assumed to be the same as that measured by Mitalas and are :-

thermal conductivity= 0.88 w/m K

density = 1490 kg/m³

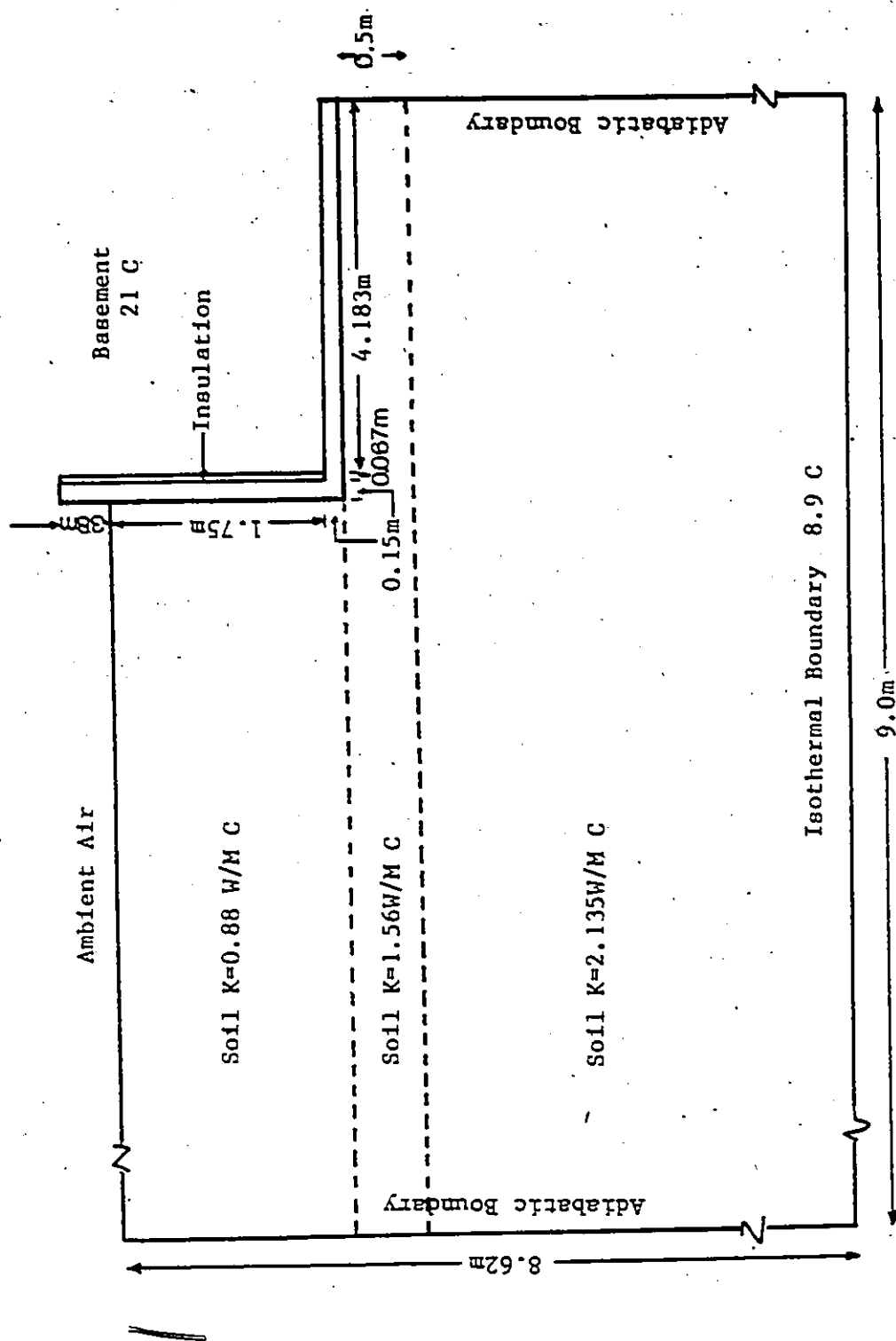


Fig.57. Basement Model 3.

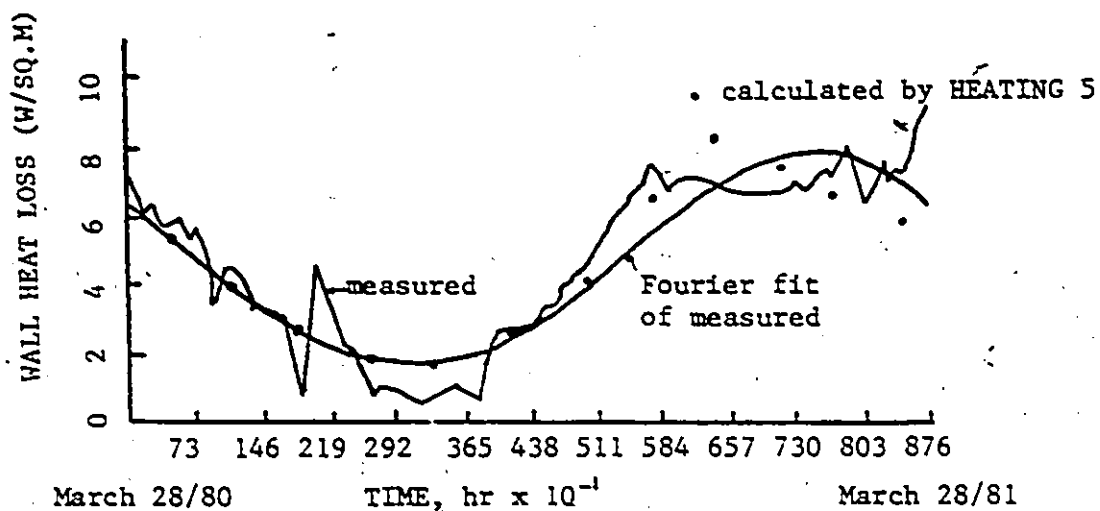


Fig.58. Wall heat loss for Model 3.

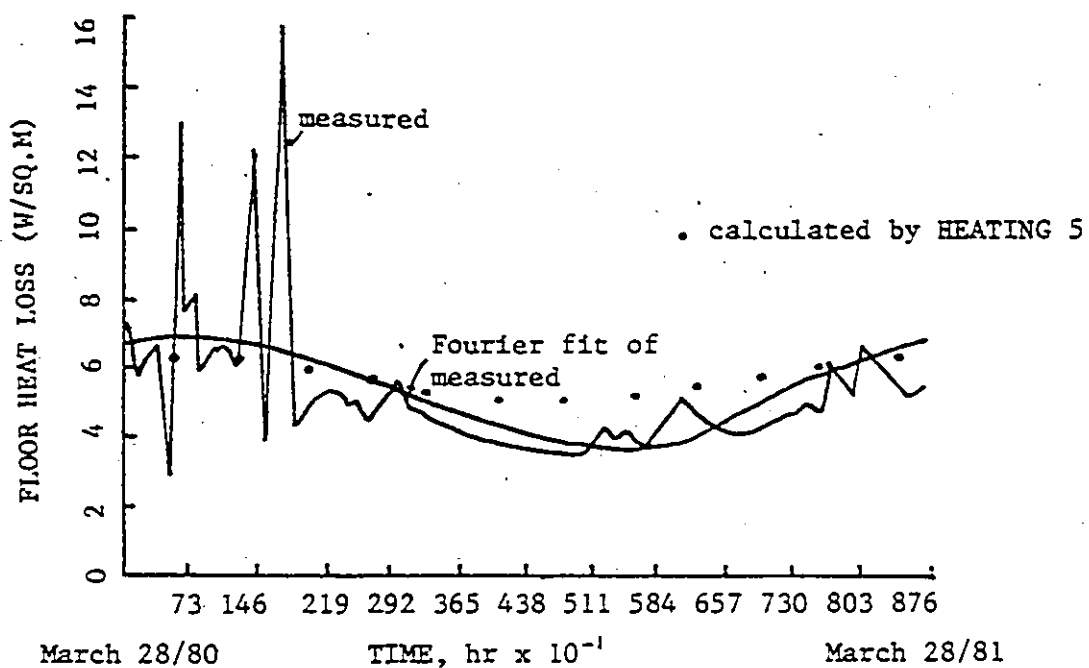


Fig.59. Floor heat loss for Model 3.

specific heat = 1765 J/kg K

The model configuration is shown in Figure 57. Figures 58 and 59 show the basement wall and floor heat loss using this model.

5.3 RESULTS

As is evidenced from Figures 53, 55 and 58, Models 1 and 3 predict the wall heat losses reasonably well, despite the fact that Model 1 neglects the effect of the ground water. There is a variation during the months of December, January, February and March. This could be due to three reasons. The first being, the thermal conductivity of the soil is different than the value assumed for the winter months. During this analysis the soil thermal properties were assumed to be constant throughout the year. The second reason being, the thermal conductivity of the snow was different from that assumed for this analysis. And thirdly, this analysis was done for 1980-81 and snow cover records for this period were not available. Therefore 1978-79 records were used. Any of these three reasons could account for the variations in the wall heat loss. Model 2 constantly underpredicts the wall heat loss. This is most probably due to the fact that the ground water flow was quite negligible. Another reason could be that there was an error in recording the soil temperatures.

Although there is hardly any difference between the wall heat loss for Models 1 and 3, it is seen from Figures 54 and 59 that Model 3 predicts a better floor heat loss than does Model 1. But Model 2 gives a relatively poor prediction as compared to the other two models. It is most probable that the ground water flow was significantly lower than anticipated and that could account for the failure of Model 2.

It could be speculated from this analysis that by assuming different thermal properties for the soil near the ground water table, reasonably accurate wall and floor heat losses could be calculated. The only limitation being that the flow of the ground water should not be large. More work should be done to see if this model would hold for other basements with a high ground water table.

Chapter VI

CONCLUSIONS AND RECOMMENDATIONS

6.1 CONCLUSIONS

The HEATING 5 computer program is sufficiently general to simulate variable geometries, boundary conditions, soil and building properties. This program has been validated and indicates that the energy performance can be accurately predicted (within 8% of that calculated by McBride during the heating season) using a Fourier fit approximation of the actual boundary condition, and approximating the soil property variations by periodic step changes.

It is found that the soil thermal conductivity can exert a significant influence on the heat loss from basements. The upper value of the soil thermal conductivity range for the Columbus, Ohio area (2.42 W/M C) overpredicts the basement wall and floor heat loss by about 6.2% and 62.2% during the heating season. The lower value of this range (0.69 W/M C) underpredicts the wall and floor heat loss by 24.3% and 54% during the heating season. The mid-range values of the thermal conductivities underpredict the heating season wall and floor heat loss by about 5.4% and 17.9% for the basement in Columbus, Ohio. It is essential that values close to the actual soil thermal conductivities be used for heat loss calculations and not mid-range values.

It is also found that similar structures (not closer than 3 meters from the basement wall) do not significantly effect the wall heat losses. The floor heat losses can be reduced by about 42% during the heating season. The reduction in the wall heat loss would be more profound if the basement extends deeper into the ground.

The level of the ground water has a considerable effect on the basement floor heat loss. During this analysis it was assumed that the lower ground thermal boundary is at the same level as the ground water table. This assumption is valid only for areas with an abnormally high ground water flow. The depth of this boundary is varied and it is found that it plays an important role in the floor heat loss while its effect on the wall heat loss is almost negligible. When the boundary is 1 meter below the basement floor, the heating season floor heat loss may increase by about 150% while the wall heat loss may increase by about 6% only.

The ground surface conditions also play an important role in basement heat losses. When there is snow cover on the ground, an insulation blanket is created which reduces the heat loss significantly. 5.7 inches (14.478 cms.) of snow can reduce the wall and floor heat loss by as much as 33% and 8% for the Ohio basement. An asphalt surface eliminates the heat loss from the ground surface due to evaporation and transpiration. This can reduce the south wall and floor heat loss by about 19% and 9.4% during the heating season.

During the summer months the wall heat loss is almost negligible. This is because in addition to the above grade portion of the wall, the below grade walls gain heat from the surrounding soil down to a depth of about 1 meter below grade.

The addition of insulation on the exterior walls of the basement significantly reduces the wall heat loss during the heating season. Full length insulation reduces it by about 75.4% while half length insulation (on the top half of the wall) reduces it by about 56.2% for the Ohio basement. The floor heat loss during the same period increases by about 5.4% and 0.2% for full length and half length insulation placement. A complicating factor is that, although the heating season heat losses are reduced by added insulation, the beneficial cooling season heat losses are also reduced.

6.2 RECOMMENDATIONS

For future investigations the following recommendations are suggested :-

1. The development of a more detailed model for calculating basement heat losses is required. It should be an extension of the model developed in this study. The present model, like others presented in the literature, assumes many factors that influence the thermal behaviour of the soil to be negligible, which may not be true under all conditions. The

latent heat of fusion of soil moisture under freezing and thawing conditions should be considered. HEATING 5 has provisions for incorporating phase changes in the model. Changes in moisture content and the heat transfer by liquid migration during shorter time intervals should be incorporated in the model. These effects have been approximated by including seasonally varying soil thermal properties in the present model. The heat transfer process taking place at the soil surface requires more detailed characterization. The effect of solar radiation and heat loss due to evapo-transpiration on the ground surface should be included. More information on these effects can be obtained from texts on Climatology.

2. Most of the data available from instrumented basements is incomplete and this makes validation of any model incomplete. Therefore, the acquisition of detailed experimental data, over an extended time period, on a variety of basement configurations is required. Ground temperatures below and around the basement should be measured. For the former, instrumentation should be done before the basement is constructed. The ground water level, flow and temperature should be measured. This can be done by drilling a well near the test-site and recording all

the required data. Soil thermal properties should be measured at various depths of the soil to include moisture effects. These measurements should be performed for at least a year to take into account the seasonal effects.

3. Similar studies should be carried out for different climates where energy demand patterns may vary considerably from those used in this analysis.
4. Although an extensive parametric study has been performed, more simulations should be done so that an empirical relationship could be developed between the basement heat loss and the different types of parameters (soil thermal conductivity, ground water level, type of surface cover, insulation placement etc.). This would greatly assist in the development of empirical relationships to more accurately predict heat losses than from existing methods. Using these relationships a less sophisticated ~~hand-held~~ calculator software package could be developed for engineers or designers who do not have access to large computers.
5. A three-dimensional study should be done to find out the corner effects on the basement heat loss.

REFERENCES

1. "Keeping The Heat In : How to Re-Insulate Your Home to Save Energy and Money (And Be More Comfortable Too)", Energy, Mines and Resources Canada, Office of Energy Conservation, Canada, August 1976.
2. Bligh, Thomas P., "Energy Conservation By Building Underground". Underground Space. Vol. 1, pp. 19-33. (1976).
3. ASHRAE Handbook of Fundamentals. (1981).
4. Labs, Kenneth., "Regional Analysis Of Ground And Above-Ground Climate Conclusion". Underground Space. Vol. 7, pp. 37-69. (1982)
5. Callender, Hugh L., "Preliminary Results Of Observations Of Soil Temperatures With Electrical Resistance Thermometers Made At The McDonald Physics Building, McGill University, Montreal". Transactions, Royal Society of Canada, 2nd Series, Vol. 1, Sec. 3, pp. 63-85. (1895)
6. Callender, Hugh L., McLeod, C.H., "Observations Of Soil Temperatures With Electrical Resistance Thermometers". Transactions, Royal Society of Canada, 2nd Series, Vol. 2, Sec. 3, pp. 109-126. (1896).
7. Crabb, George A., Smith, James L., "Soil-Temperature Comparisons Under Varying Covers". Highway Research Board Bulletin, No. 71, pp. 32-49. (1953).
8. Crawford, C.R., "Soil Temperature, A Review Of Published Records". Highway Research Board Special Report 2, pp. 19-41. (1952).
9. Gold, L.W., "Influence Of Surface Conditions On Ground Temperature". Canadian Journal of Earth Science. Vol. 4. (1967).
10. Goll, L.W., Boyd, D.W., "Annual Heat And Mass Transfer At An Ottawa Site". Canadian Journal of Earth Science, Vol. 2, No. 1.

11. Johnson, N.K., Davis, E.L., "Some Measurements Of Temperatures Near The Surfaces In Various Kinds Of Soils". Quarterly Journal of the Royal Meteorological Society, pp. 45-59. (1927).
12. Kusuda, T., "Earth Temperature Beneath Five Different Surfaces". National Bureau of Standards, Report No. 10373. (Feb. 1971).
13. Gilpin, R.R., Wong, B.K., "Heat-Valve Effects In The Ground Thermal Regime". Journal of Heat Transfer, pp. 537-542. (Nov. 1976)
14. Kusuda, T., Achenbach, P.R., "Earth Temperature And Thermal Diffusivity At Selected Stations In The United States". ASHRAE Transactions. (1965).
15. Chang, J., "Global Distribution Of The Annual Range In Soil Temperature". Transactions, American Geophysical Union, pp. 718-723. (1957).
16. Chang, J., "Ground Temperature", Vol. 1. Milton, Massachusetts: Blue Hill Meteorological Observatory. (1958).
17. Smith, W.O., "The Thermal Conductivity Of Dry Soil". Soil Science 53, pp. 435-459. (1942).
18. Kersten, M.S., "Thermal Properties Of Soils". Highway Research Board Special Report 2, pp. 161-166. (1952).
19. De Vries, D.A., "Some Remarks On Heat Transfer By Vapour Movement In Soils". Transactions of the 4th International Congress of Soil Science 2, pp. 38-51. (1950).
20. De Vries, D.A., "A Nonstationary Method For Determining Thermal Conductivity Of Soil In Situ". Soil Science 73, No. 2, pp. 83- 89. (Feb. 1952).
21. Kimbell, B.A., Jackson, R.D., Reginato, R.J., Nakayama, P.S., Iiso, S.B., "Comparison Of Field-Measured And Calculated Soil-Heat Fluxes". Soil Science Society of America Journal 40, No. 1, pp. 18-25. (1976).
22. Rollins, R.L., Spangler, M.G., Kirkham, D., "Movement Of Soil Moisture Under A Thermal Gradient". Proceedings of the Highway Research Board, No. 33, pp. 492-508. (1954).
23. Kersten, Miles S., "The Thermal Conductivity Of Soils". Proceedings of the twenty-eight Annual meeting. Highway Research Board. (1948).

24. Baladi, J.Y., Schoenhals, R.J., Ayers, D.L., "Transient Heat And Mass Transfer In Soils". AIAA-ASME Thermophysics and Heat Transfer Conference, Palo Alto, CA. (1978).
25. Carslaw, H.S., Jaeger, J.C., "Conduction Of Heat In Solids". Oxford: Clarendon Press. (1959).
26. Ingersoll, L.R., Zobel, O.J., Ingersoll, A.C., "Heat Conduction With Engineering, Geological And Other Applications". Revised Edition, Madison, Wisconsin: University of Wisconsin Press. (1954).
27. Jumikas, A.R., "Thermal Geotechnics". New Brunswick, New Jersey: Rutgers University Press. (1977).
28. Houghten, F.C., Taimuty, S.I., Gutberlet, C., Brown, C.J., "Heat Loss Through Basement Walls And Floors". ASHRAE Transactions, Vol. 48, No. 1213. (1942).
29. Kusuda, T., Achenbach, P.R., "Numerical Analysis Of The Thermal Environment Of Occupied Underground Spaces With Finite Cover Using A Digital Computer". ASHRAE Transactions, Vol. 69, pp. 439-452. (1963).
30. Boileau, G.G., Latta, J.K., "Calculation Of Basement Heat Loss". Division of Building Research Technical Paper No. 292, NRC 10477, Ottawa, Canada. (1968).
31. McBride, M.F., Blancett, R.S., Sepsy, C.F., Jones, C.D., "Measurement Of Subgrade Temperatures For Prediction Of Heat Loss In Basements". ASHRAE Transactions, Vol. 85, part 1. (1979).
32. Szydlowski, R.F., Kuehn, T.H., "Analysis Of Transient Heat Loss In Earth-Sheltered Structures". Underground Space, Vol. 5, pp. 237- 246. (1981).
33. Wang, F.S., "Mathematical Modeling And Computer Simulation Of Insulation Systems In Below Grade Applications". Proceedings of ASHRAE/DOE -ORNL Conference. Thermal Performance of the Exterior Envelopes of Buildings. Dec. 3-5, 1979.
34. Meixel, G.D., Shipp, P.H., Bligh, T.P., "The Impact Of Insulation Placement On The Seasonal Heat Loss Through Basement And EarthShelter Walls". Proceedings of the ASHRAE/DOE -ORNL Conference. Thermal Performance of the Exterior Envelopes of Buildings. Dec. 3- 5. (1979).
35. Shipp, P.H., Pfender, E., Bligh, T.P., "Thermal Characteristics Of A Large Earth-Sheltered Building

- (Parts 1 and 2)". Underground Space, Vol. 6, pp. 53-64. (1981).
36. Swinton, M.C., Platts, R.E., "Engineering Method For Estimating Annual Basement Heat Loss And Insulation Performance". ASHRAE Transactions, Vol. 87, Part 2. (1981).
 37. Mitalas, G.P., "Basement Heat Loss Studies At DBR/NRC". DBR Paper No. 1045. Division of Building Research. NRC Canada. NRCC 20416. (1982).
 38. Raff, S.J., "Ground Temperature Control". Underground Space. Vol. 3, No. 1, pp. 35-44. (1978).
 39. "HEATING 5- An IBM 360 Heat Conduction Program". Computer Science Division, Union Carbide Corporation, Nuclear Division.
 40. "Residential Fuel Utilization Efficiencies", The Ohio State University Engineering Experimentation Station, Final Report on Project 460X, Columbus, Ohio. (1977).
 41. Hillary, J.D., "Thermal Response And Energy Requirements Of A Two-Storey Residence", MSc. Thesis, The Ohio State University, Columbus, Ohio. (1975).
 42. Salvadore, J.M., "A Thermal Response And Environmental Control Equipment Simulation Of A Control Residence", MSc. Thesis, The Ohio State University, Columbus, Ohio. (1974).
 43. Smith, G.S., Yamanchi, T., "Thermal Conductivities Of Soils For Design Of Heat Pump Installations". ASH&VE Transactions, Vol. 56, pp. 355-370. (1950).
 44. "Climatological Data - Ohio", U.S. Department of Commerce, National Climatic Center, Federal Building, Asheville, N.C., Vol 82-83.
 45. Threlkeld, J.L., "Thermal Environmental Engineering". Prentice Hall, New York. (1962).
 46. Sellers, R.D., "Physical Climatology", pp. 106, The University of Chicago Press. (1965)
 47. " 'Mimic Box' Monitoring of Heat Losses of Basements In a Range of Climates", a report by Scanada Consultants Limited for the Division of Building Research, National Research Council of Canada, Nov. 1979.
 48. Mitalas, G.P., personal communication. (Dec. 1983).

Appendix A
NUMERICAL TECHNIQUE

This section deals with the numerical techniques used by the HEATING 5 computer program to solve heat transfer problems. It contains extracts of the relevant portions of the numerical technique provided by the reference manual prepared by the Union Carbide Corporation [39].

2. NUMERICAL TECHNIQUE *

2.1. Statement of the Problem

The HEATING5 Program solves the steady-state or transient heat conduction problem in either one, two, or three dimensions for either Cartesian or cylindrical coordinates or one dimension (radial) for spherical coordinates. For illustrative purposes, the equations and the discussion which follow are written for a three-dimensional problem in Cartesian coordinates.

First, the physical problem is approximated by a system of nodes each associated with a small volume. In order to define the nodes, a system of orthogonal planes is superimposed on the problem. The planes may be unequally spaced, but they must extend to the outer boundaries of the problem. A typical, internal node, which is defined by the intersection of any three planes is depicted in Fig. 2.1. Heat may flow from a node to each adjacent node along paths which are parallel to each axis. Thus for a three-dimensional problem, heat may flow from an internal node to each of its six neighboring nodes. The system of equations describing the temperature distribution is derived by performing a heat balance about each node.

The finite difference heat balance equation for node o in Fig. 2.1 is

$$C_o \frac{T_o^{n+1} - T_o^n}{\Delta t} = P_o^n + \sum_{m=1}^6 K_m (T_m^n - T_o^n) \quad (2.1)$$

where T_m^n is the temperature of the mth node adjacent to node o at time t_n , K_m is the conductance between nodes o and m, C_o is the heat capacitance of the material associated with node o, and P_o^n is the heat generation rate in the latter material at time t_n . Since planes go through the nodes and the material is homogeneous between any two successive planes along any axis, a node may be composed of as many as eight different materials, and the heat flow path between adjacent nodes may be composed of as many as four different materials positioned in parallel. For a three-dimensional problem, one C, one P, and six K's will be associated with each internal node at a particular time, t_n . These parameters are calculated as follows for node o:

$$C_o = \sum_{i=1}^8 C_{pi} V_i \quad (2.2)$$

$$P_o^n = \sum_{i=1}^8 Q_i^n V_i \quad (2.3)$$

$$K_m = \frac{1}{L_m} \sum_{\gamma=1}^4 k_{m\gamma} A_{m\gamma} \quad (2.4)$$

* This section is reproduced from "HEATING 5 - An IBM 360 Heat Conduction Program" with permission from the National Energy Software Center (U.S. Department of Energy)

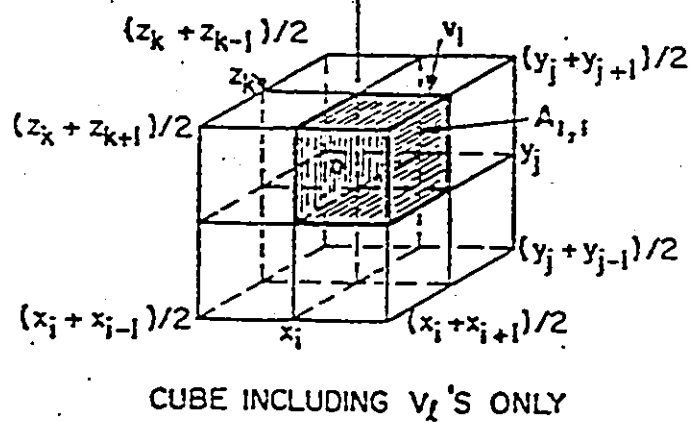
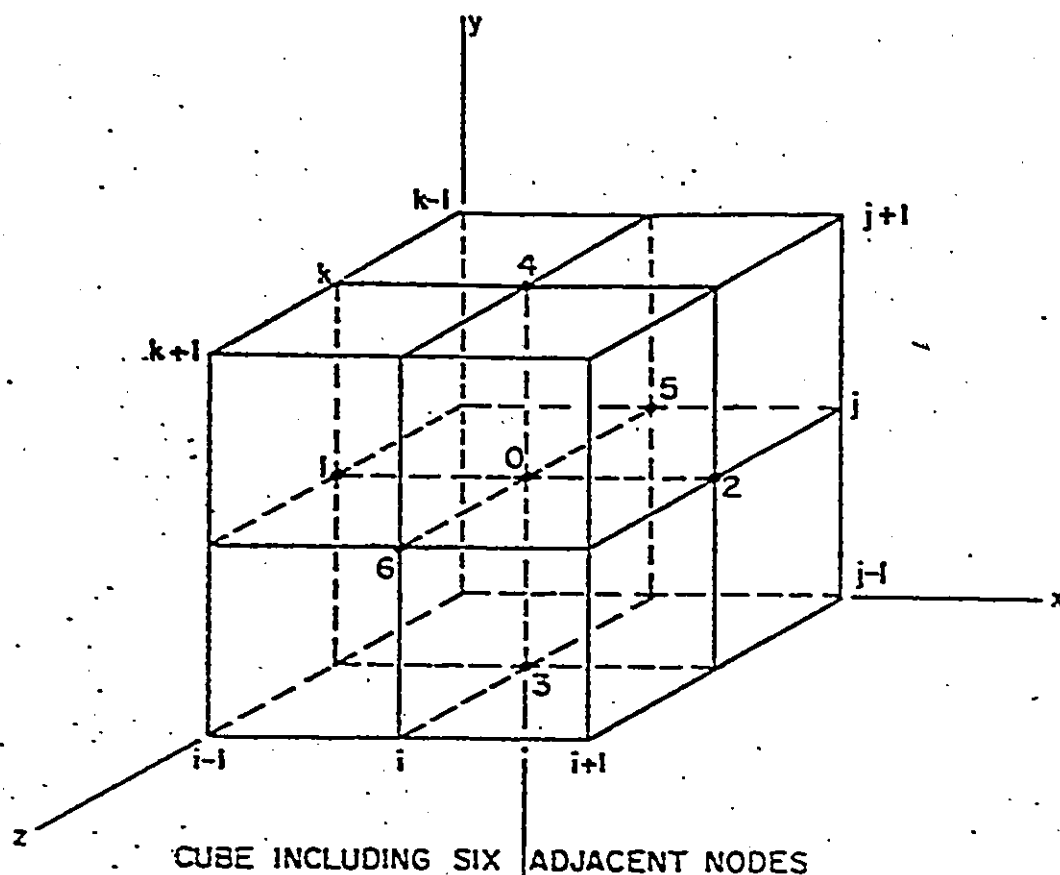


Fig. 2.1. HEATING5 Nodal Description for Three-Dimensional Problem

where

C_{pi} = specific heat for region i ,

ρ_i = density for region i ,

V_i = volume of region i ,

Q_i^* = heat generation rate per unit volume in region i at time t_n ,

L_m = distance between node o and adjacent node m ,

$k_{m\gamma}$ = thermal conductivity for region γ between nodes o and m ,

$A_{m\gamma}$ = cross-sectional area, normal to heat flow path, of region γ between nodes o and m .

With reference to Fig. 2.1, the V_i 's and $A_{m\gamma}$'s are further defined, by using examples, as follows:

$$V_i = \frac{(x_{i+1} - x_i)}{2} \frac{(y_{j+1} - y_j)}{2} \frac{(z_{k+1} - z_k)}{2} \quad (2.5)$$

$$A_{i,j} = \frac{(y_{j+1} - y_j)}{2} \frac{(z_{k+1} - z_k)}{2} \quad (2.6)$$

Since nodes lying on a surface or nodes from one- or two-dimensional problems will not necessarily have six neighbors, the general heat balance equation for node i having M_i neighbors can be written as

$$C_i \frac{T_i^{n+1} - T_i^n}{\Delta t} = P_i^n + \sum_{m=1}^{M_i} k_{\alpha_m} (T_{\alpha_m}^n - T_i^n) \quad (2.7)$$

where α_m is the m th neighbor of the i th node. By choosing the increments between lattice lines small enough, the solution to the system of equations yields a practical approximation to the appropriate differential equation.

2.2. Steady-State Heat Conduction

For a steady-state heat conduction problem, the heat balance equation reduces to

$$P_i + \sum_{m=1}^{M_i} k_{\alpha_m} (T_{\alpha_m} - T_i) = 0 \quad (2.8)$$

since the left-hand side of Eq. (2.7) is zero.

If there are I nodal points, then since Eq. (2.8) will be applied at each node, there will be a system of I equations with I unknowns. The iterative technique which is used by HEATING5 to solve the system of equations is outlined below. First, solve Eq. (2.8) for T_i .

$$T_i = \frac{P_i + \sum_{m=1}^{M_i} K_{\alpha_m} T_{\alpha_m}}{\sum_{m=1}^{M_i} K_{\alpha_m}} \quad (2.9)$$

Since the values of T_{α_m} are unknown, the temperature at node i cannot be calculated directly from Eq. (2.9). However, an iterative procedure based on Eq. (2.9) can be used to estimate the steady-state temperature distribution. If an estimate to the temperature distribution exists, then Eq. (2.9) can be applied at each node, and hopefully, a better estimate to the temperature distribution will be obtained. Then, this new estimate can be used in Eq. (2.9) to produce an even better estimate. This iterative process can be written as

$$T_i^{(n+1)} = \frac{P_i + \sum_{m=1}^{M_i} K_{\alpha_m} T_{\alpha_m}^{(n)}}{\sum_{m=1}^{M_i} K_{\alpha_m}} \quad (2.10)$$

where the superscript (n) implies the n th iterate. Instead of using the results of Eq. (2.10) as the $(n+1)$ st iterate, assume that it only yields an estimate and denote it as $\hat{T}_i^{(n+1)}$. Then define the $(n+1)$ st iterate to be

$$T_i^{(n+1)} = T_i^{(n)} + \beta [\hat{T}_i^{(n+1)} - T_i^{(n)}] \quad (2.11)$$

where the relaxation factor, β , is limited to $0 < \beta < 2$. Notice that when $\beta > 1$, the new iterate is changed more than Eq. (2.10) specifies, and thus, the iterate is overrelaxed. Likewise, when $\beta < 1$, the iterate is underrelaxed. If $\hat{T}_i^{(n+1)}$ is replaced by Eq. (2.10), then Eq. (2.11) can be written as

$$T_i^{(n+1)} = (1-\beta)T_i^{(n)} + \beta \left[\frac{P_i + \sum_{m=1}^{M_i} K_{\alpha_m} T_{\alpha_m}^{(n)}}{\sum_{m=1}^{M_i} K_{\alpha_m}} \right] \quad (2.12)$$

If the nodes are numbered along the x -axis from left to right, then along the y -axis from bottom to top and finally along the z -axis from the smallest plane to the largest, then the rate of convergence for the iterative procedure can be increased by using the most recent value of the temperature in Eq. (2.12). This algorithm can be written as

$$T_i^{(n+1)} = (1-\beta)T_i^{(n)} + \beta \left[\frac{P_i + \sum_{m=1}^L K_{\alpha_m} T_{\alpha_m}^{(n+1)} + \sum_{m=L+1}^{M_i} K_{\alpha_m} T_{\alpha_m}^{(n)}}{\sum_{m=1}^{M_i} K_{\alpha_m}} \right] \quad (2.13)$$

where L_i is defined so that $\alpha_{L_i} < i < \alpha_{L_i+1}$. Varga (Ref. 5) refers to this method as the point successive over-relaxation iterative method. To increase the rate of convergence, an exponential approximation for Eq. (2.13) is made based on the temperature change from one iteration to the next. The algorithm based on this approximation is used instead of Eq. (2.13) to calculate the new temperatures for nodes having relative temperature changes exceeding 10^{-3} . However, the algorithm is designed to bound the temperature change so that the new temperature cannot be more than two times the old temperature. This prohibits the technique from diverging due to a bad estimate of the initial temperature distribution. The exponential approximation reduces to Eq. (2.13) for small temperature changes. Successive iterations are carried out by HEATINGS until

$$\left| \frac{T_i^{(n)} - T_i^{(n+1)}}{T_i^{(n+1)}} \right| \leq \epsilon \quad \text{max} \quad (2.14)$$

where ϵ is the specified convergence criterion.

Another extrapolation procedure which is commonly used to increase the rate of convergence in an iterative solution to a system of equations is the "Aitken δ^2 extrapolation procedure." Briefly, if $T^{(n-1)}$, $T^{(n)}$, and $T^{(n+1)}$ are the temperatures at a certain point at the $n-1$ st, n th and $n+1$ st iterations, respectively, and if

$$|T^{(n)} - T^{(n-1)}| > |T^{(n+1)} - T^{(n)}| \quad (2.15)$$

and

$$[T^{(n+1)} - T^{(n)}][T^{(n)} - T^{(n-1)}] > 0. \quad (2.16)$$

then, a better estimate of the temperature is

$$T_{new} = T^{(n+1)} + \frac{[T^{(n+1)} - T^{(n)}]^2}{[T^{(n)} - T^{(n-1)}] - [T^{(n+1)} - T^{(n)}]} \quad (2.17)$$

Actually, HEATINGS uses a modification of Aitken's δ^2 method by calculating an extrapolation factor, B, and approximating Eq. (2.17) at each node with

$$T_i^{(n+1)} = \tilde{T}_i^{(n+1)} + B [\tilde{T}_i^{(n+1)} - T_i^{(n)}] \quad (2.18)$$

where $\tilde{T}_i^{(n+1)}$ represents the $n+1$ st iterate at node i before extrapolation.

A HEATINGS extrapolation cycle is defined as follows. The code completes 20 iterations and checks to see if the maximum of the absolute values of the relative temperature changes over an iteration has decreased monotonically over the last ten iterations. If not, the cycle starts over. If so, the code will extrapolate only if the relative change in extrapolation factors over two consecutive iterations is less than 5% and the maximum of the absolute values of the relative temperature changes decreases monotonically over the same two iterations. The extrapolation factor, B, which is the same for each node, is based on two maximum relative temperature changes; between the n -1st and the n th iterations and between the n th and the $n+1$ st iterations.

The value of β in Eq. (2.13) which will produce the optimum convergence rate for all points is difficult to obtain analytically for simple geometries and is practically impossible to obtain for complex geometries. If an input value is not supplied for β , then HEATINGS uses the default value of 1.9. If the rate of convergence appears to be slow, then HEATINGS reduces β by 0.1. The code determines whether or not the rate of convergence is slow in the following manner. It was noted above that during an extrapolation cycle, the relative temperature change over an iteration is monitored over ten consecutive iterations. If the relative temperature changes do not decrease monotonically over these ten iterations, then the current relative temperature change is compared with the one arising ten iterations earlier. If the current relative temperature change is greater than two-thirds of the old one, then the SOR technique is converging slowly. This process may be repeated until $\beta = 1.0$. However, the code will not increase β .

2.3. Transient Heat Conduction

HEATINGS is designed to solve a transient problem by any one of several numerical schemes. The first is the Classical Explicit Procedure (CEP) which involves the first forward difference with respect to time and is thus stable only when the time step is smaller than the stability criterion. Levy's modification to the CEP is the second scheme, and it requires the temperature distribution at two times to calculate the temperatures at the new time level. The technique is stable for a time step of any size. The third procedure, which is written quite generally, actually contains several implicit techniques which are stable for a time step of any size. One can use the Crank-Nicolson heat balance equations, the Classical Implicit Procedure (CIP) or backwards Euler heat balance equations or a linear combination of the two. The resulting system of equations is solved by point successive overrelaxation iteration. Techniques have been included in the code to approximate the optimum acceleration parameter for problems involving constant thermal parameters as well as those whose effective thermal conductances and capacitances vary with time or temperature. The implicit procedure in HEATINGS has not been designed to solve problems involving materials which are allowed to undergo a change of phase.

The implicit procedure using the Crank-Nicolson heat balance equation is the recommended technique for solving transient problems. Levy's modification to the CEP can be a useful tool for obtaining the solution to problems. However, one must experiment with the time step size before accepting the resulting solution.

The stability criterion for the CEP is a function of a temperature-dependent heat generation rate or heat flux. This fact is not accounted for in HEATINGS. Also, Levy's modification to the CEP is based on a constant heat generation rate or heat flux with respect to temperature. If one attempts to use one of the explicit transient algorithms along with a temperature-dependent source or heat flux, then the code will write out a warning message indicating that the time step allowed by HEATINGS may not yield a stable solution.

Equation (2.7) is the basic heat balance equation for transient problems. However, the right-hand side is modified for all but the CEP.

2.3.1 Classical Explicit Procedure

For a transient heat conduction problem, the heat balance equation, Eq. (2.7), can be solved for T_i^{n+1} to give :

$$T_i^{n+1} = T_i^n + \frac{\Delta t}{C_i} \left[P_i^n + \sum_{m=1}^{M_i} K_{\alpha_m} (T_{\alpha_m}^n - T_i^n) \right] \quad (2.19)$$

Since Eq. (2.19) expresses the temperature of the i th node at the $n+1$ st time level in terms of temperatures at the n th time level, it is an explicit technique, and the algorithm is known as the Classical Explicit Procedure (CEP) or the Forward Difference Equation. HEATINGS uses Eq. (2.19) to solve transient heat conduction problems. The numerical solution obtained by using this technique is stable, provided the time step satisfies the following inequality (Ref. 6).

$$\Delta t \leq \left(\frac{C_i}{M_i \sum_{m=1} K_{\alpha_m}} \right) \text{ minimum for all nodes} \quad (2.20)$$

2.3.2 Levy's Modification to the Classical Explicit Procedure

The limitation on the size of the time step as indicated in Eq. (2.20) means, in many practical problems, a very high ratio of computer time to actual time. In some cases computation costs become so high that the use of the algorithm defined by Eq. (2.19) becomes impractical. Levy [Ref. 7] proposed a modified explicit method which is stable for any time step desired. This method has been incorporated as an option in HEATINGS. The basic equation used is

$$T_i^{n+1} = T_i^n + \frac{1}{1+Z_i} \left\{ \frac{\Delta t}{C_i} \left[\sum_{m=1}^{M_i} K_{\alpha_m} (T_{\alpha_m}^n - T_i^n) + P_i^n \right] + Z_i [T_i^n - T_i^{n-1}] \right\} \quad (2.21)$$

where

Z_i = a factor for node i which will insure a stable solution for any time step Δt .

If from Eq. (2.20), $(\Delta t_{max})_i$ is the maximum time step allowed at node i for a stable solution in the regular explicit method, then the factor Z_i in Eq. (2.21) is defined as

$$Z_i = \begin{cases} 0, & \text{if } \frac{\Delta t}{(\Delta t_{max})_i} \leq 1 \\ 0.5 \left[\frac{\Delta t}{(\Delta t_{max})_i} - 1 \right], & \text{if } \frac{\Delta t}{(\Delta t_{max})_i} > 1 \end{cases} \quad (2.22)$$

Levy (Ref. 7) says that the accuracy is good if Z_i is zero for somewhat over half of the nodes. Of course, one must experiment with the size of the time step in order to obtain an acceptable solution.

2.3.3 Implicit Procedure

a. Heat Balance Equation

If the right-hand side of Eq. (2.7) is evaluated at t_{n+1} instead of t_n , then the scheme is known as the Classical Implicit Procedure (CIP) or the backwards Euler procedure. If the right-hand side of Eq. (2.7) is evaluated at $t_{n+1/2}$, then the algorithm is known as the Crank-Nicolson (CN) procedure. A general algorithm which includes both the CN technique and the CIP is

$$C_i^{n+\theta} \frac{T_i^{n+1} - T_i^n}{\Delta t} = P_i^{n+\theta} + \theta \left[\sum_{m=1}^{M_i} K_{\alpha_m}^{n+\theta} (T_{\alpha_m}^{n+1} - T_i^{n+1}) \right] + (1-\theta) \left[\sum_{m=1}^{M_i} K_{\alpha_m}^{n+\theta} (T_{\alpha_m}^n - T_i^n) \right] \quad (2.23)$$

where $0 \leq \theta \leq 1$ and where the superscript $n+\theta$ implies that the parameter is evaluated at time $t_{n+\theta}$. If $\theta = 0.5$, then Eq. (2.23) becomes the CN technique and if $\theta = 1.0$, the algorithm is the CIP. When θ is less than 0.5, the technique is no longer stable for any time step. Notice that Eq. (2.23) reverts to Eq. (2.7) when $\theta = 0$. This algorithm has been incorporated into HEATING5 for $0.5 \leq \theta \leq 1.0$.

b. Numerical Technique

If there are I nodes in the problem and if the heat balance equation, Eq. (2.23), is written for each node, then there will be I equations and I unknowns, and the resulting system of equations can be solved iteratively. The procedure that is used in HEATING5 is outlined below. If Eq. (2.23) is rewritten so that the temperatures at t_{n+1} are on the left-hand side, then the equation becomes

$$-\theta \left(\sum_{m=1}^{M_i} K_{\alpha_m}^{n+\theta} T_{\alpha_m}^{n+1} \right) + \left[\frac{C_i^{n+\theta}}{\Delta t} + \theta \left(\sum_{m=1}^{M_i} K_{\alpha_m}^{n+\theta} \right) \right] T_i^{n+1} = H_i \quad (2.24)$$

where

$$H_i = \frac{C_i^{n+\theta}}{\Delta t} T_i^n + P_i^{n+\theta} + (1-\theta) \left[\sum_{m=1}^{M_i} K_{\alpha_m}^{n+\theta} (T_{\alpha_m}^n - T_i^n) \right] \quad (2.25)$$

If we let

$$D_i = \frac{C_i^{n+\theta}}{\Delta t} + \theta \left(\sum_{m=1}^{M_i} K_{\alpha_m}^{n+\theta} \right) \quad (2.26)$$

and if we delete the superscript, $n+1$, on the temperature, T , then Eq. (2.24) can be rewritten as

$$-\theta \left(\sum_{m=1}^{M_i} K_{\alpha_m}^{n+\theta} T_{\alpha_m} \right) + D_i T_i = H_i \quad (2.27)$$

where it is now understood that T_i represents the temperature of node i at the new time level. If Eq. (2.27) is solved for T_i , then

$$T_i = \frac{\theta \left(\sum_{m=1}^{M_i} K_{\alpha_m}^{n+\theta} T_{\alpha_m} \right) + H_i}{D_i} \quad (2.28)$$

Since the values of T_{α_m} are unknown, one cannot directly solve for the temperature at node i . However, if an estimate of the temperature distribution at the new time level exists, then Eq. (2.28) can be solved at each node, and hopefully, one will have a better estimate for the temperature distribution. The procedure can be repeated using this better estimate. This process can be continued until the estimates have converged to the approximation of the temperature distribution at the new time level. This algorithm can be written as

$$T_i^{(n+1)} = \frac{\theta \left(\sum_{m=1}^{M_i} K_{\alpha_m}^{n+\theta} T_{\alpha_m}^{(n)} \right) + H_i}{D_i} \quad (2.29)$$

where the superscript (n) on T_i refers to the n th iterate of the temperature at node i at the new time level.

Instead of using Eq. (2.29) in the iterative process, the technique can be refined further. First, consider Eq. (2.29) as only an approximation to the $(n+1)$ st iterate or

$$\hat{T}_i^{(n+1)} = \frac{\theta \left(\sum_{m=1}^{M_i} K_{\alpha_m}^{n+\theta} T_{\alpha_m}^{(n)} \right) + H_i}{D_i} \quad (2.30)$$

and then define the $(n+1)$ st iterate as

$$T_i^{(n+1)} = T_i^{(n)} + \omega [\hat{T}_i^{(n+1)} - T_i^{(n)}] \quad (2.31)$$

or

$$T_i^{(n+1)} = (1-\omega) T_i^{(n)} + \omega \hat{T}_i^{(n+1)} \quad (2.32)$$

where $0 < \omega < 2$. Thus, the change in temperature based on the value at the last iteration is more ($\omega > 1$) or less ($\omega < 1$) than the calculated value. Usually, the iterative procedure converges faster when $\omega \neq 1$, and thus, ω is commonly referred to as the acceleration parameter. Combining Eqs. (2.30) and (2.32), one obtains

$$T_i^{(n+1)} = (1-\omega) T_i^{(n)} + \omega \left[\frac{\theta \left(\sum_{m=1}^{M_i} K_{\alpha_m}^{n+\theta} T_{\alpha_m}^{(n)} \right) + H_i}{D_i} \right] \quad (2.33)$$

If we always use the most recent iterates on the right-hand side of Eq. (2.33), then the algorithm reduces to

$$T_i^{(n+1)} = (1-\omega) T_i^{(n)} + \omega \left\{ \frac{\theta \left[\left(\sum_{m=1}^{L_i} K_{\alpha_m}^{n+\theta} T_{\alpha_m}^{(n+1)} \right) + \left(\sum_{m=L_i+1}^{M_i} K_{\alpha_m}^{n+\theta} T_{\alpha_m}^{(n)} \right) \right] + H_i}{D_i} \right\} \quad (2.34)$$

where $\alpha_{L_i} < i < \alpha_{L_i+1}$. It was pointed out in the previous section that this method is referred to as the point successive overrelaxation iterative method. HEATING5 applies Eq. (2.34) to each node until the convergence criteria have been met.

The convergence criteria are derived as follows. When the n th iteration has been completed, substitute the n th iterates into Eq. (2.27) and denote the heat residual as

$$R_i^{(n)} = H_i + \theta \left(\sum_{m=1}^{M_i} K_{\alpha_m}^{n+\theta} T_{\alpha_m}^{(n)} \right) - D_i T_i^{(n)} \quad (2.35)$$

Now normalize the heat residual by dividing by the right-hand side of Eq. (2.24) or

$$\frac{R_i^{(n)}}{H_i} = \frac{H_i + \theta \left(\sum_{m=1}^{M_i} K_{\alpha_m}^{n+\theta} T_{\alpha_m}^{(n)} \right) - D_i T_i^{(n)}}{H_i} \quad (2.36)$$

HEATING5 uses two convergence criteria based on this normalized heat residual. They are

$$\left(\frac{R_i^{(n)}}{H_i} \right)_{\max} \leq \epsilon_1 \quad (2.37)$$

and

$$\frac{\left(\frac{R_i^{(m)}}{H_i}\right)_{\max}}{\left(\frac{R_i^{(1)}}{H_i}\right)_{\max}} \leq \epsilon \quad (2.38)$$

The iterative procedure is started in the following manner. For the first time step, the starting estimate is equal to the initial temperature distribution. Thereafter, the starting estimate at t_{n+1} is determined by

$$\hat{T}_i^{n+1} = T_i^n + (T_i^n - T_i^{n-1})(\Delta t_{n+1} / \Delta t_n) \quad (2.39)$$

c. Temperature-Dependent Properties

For problems involving temperature-dependent thermal properties, the iterative procedure is as follows. Initially, the thermal parameters are evaluated at the initial temperatures. Then, the point successive overrelaxation iterative method as described above is applied to obtain the temperature distribution at the new time level. However, since none of the thermal parameters are updated during this procedure, the converged temperatures are only an estimate to the temperature distribution. Thus, the thermal properties are reevaluated and the entire procedure is repeated until the technique converges to the temperature distribution at the new time level. This process contains two levels of iteration. The inner loop is the basic iterative process in the point successive overrelaxation iterative method while the outer loop iterates on the thermal parameters. Let \hat{T}_i^m denote the temperature of node i after the m th iteration on the outer loop at time t_n . Upon the completion of the m th outer loop, the temperature at which the thermal parameters are evaluated is calculated as

$$\hat{T}_i^{n0} = (1 - \theta)T_i^n + \theta \hat{T}_i^{n-m} \quad (2.40)$$

The temperature distribution has converged at time t_n when the L_1 norm of the relativized temperature difference over successive iterations is less than the prescribed value or

$$\|\Delta T^{n,m}\|_1 \leq \epsilon_1 \quad (2.41)$$

where

$$\|\Delta T^{n,m}\|_1 = \frac{1}{n} \sum_{i=1}^I \left| \frac{T_i^{n,m} - T_i^{n,m-1}}{T_i^{n,m}} \right| \quad (2.42)$$

d. Estimation of the Optimum Acceleration Parameter

The rate of convergence of the point successive overrelaxation iterative method is strongly dependent on the value of the acceleration parameter ω . The optimum value of the parameter, denoted as ω_o , is usually not known prior to the solution to a problem, and it is a function of time for problems whose effective thermal conductances and capacitances vary with time or temperature. Several techniques have been developed to estimate ω_o for transient problems with constant thermal properties. The method developed by Carré (Ref. 8) has been incorporated into HEATING5. Briefly, this method consists of estimating ω_o based on the behavior of a norm of the residual vector during the iterative procedure. The estimates are computed as a function of the iteration number until the process converges to a best estimate to the optimum value. Thereafter, the code uses this converged value as the acceleration parameter.

It was observed that this process was not satisfactory for problems involving temperature- and time-dependent conductances and capacitances, so an empirical process was developed and added to HEATING5 to estimate ω_o . For the initial time step ω is equal to unity. The code will attempt to update ω every N_ω time steps relative to the last time ω was changed. The criteria which are applied to determine whether or not the current value of ω is a good estimate to ω_o are based on the number of iterations required for the inner iterative loop to converge on the first pass through the outer iterative loop at some time step. When the code determines that an attempt to update ω should be made after completion of a particular time step, then the number of iterations for this time step is compared to the number for the time step immediately following the last modification to ω . If the change in the number of iterations is equal to or exceeds the criterion I_ω (an input value), then ω is increased according to

$$\omega^{n+1} = \omega^n + 0.1 (2.0 - \omega^n) \quad (2.43)$$

where the superscript n refers to the value of ω at time t_n . On each subsequent time step a new estimate is made for ω_o using an algorithm similar to Eq. (2.43). However, ω may be either increased or decreased according to Table 2.1. When the change in the number of iterations for two consecutive time steps is less than the criterion J_ω (an input value), the code assumes that it has a good estimate for ω_o and it uses this value for the subsequent time steps until it is time to attempt another ω update. At this time, the entire procedure is repeated.

Table 2.1. Logic to Determine Whether ω Should be Increased or Decreased

Last update resulted in ω being	Change in number of iterations compared to previous time step	
	Increase	Decrease
Increased	Decrease	Increase
Decreased	Increase	Decrease

Appendix B

CARD INPUT FOR HEATING 5

This appendix contains a detailed description of the card input. Except for Card 1, the M cards, and the deck composed of the IT cards, the input data are arranged on each card in 9 column fields. All integers must be right-adjusted, i.e. the last digit of each integer must appear in a column which is a multiple of 9. Except for the IT cards, column 73 through 80 of each card are reserved for identification. The description of the card input is taken from the reference manual provided by the Union Carbide Corporation [39] and is modified to suit our needs.

B.1 CARD 1 - TITLE OF PROBLEM

This card contains a descriptive title for the problem. It can extend to the first 72 columns. This card cannot be omitted but it may be left blank.

B.2 CARD 2 - INPUT PARAMETERS

All the eight entries in this card are integers. The entries are:-

B.2.1 MAXIMUM CPU TIME

When a job is submitted to the computer, the maximum CPU time that the job is expected to run is indicated on the Class card. If the CPU time exceeds this time, then the job will be pulled by the system without printing out the current temperature distribution. In order to prevent this, the maximum CPU time (in seconds) is specified as the first entry in Card 2. As a safety factor the code subtracts five seconds from this specified time after each iteration or time step, a check is made to see if the CPU time exceeds the specific time. If so, it completes all of the output options which are specified and attempts to read the data for the next problem, if any. This time should be less than CPU time specified on the CLASS card.

B.2.2 TYPE GEOMETRY

The HEATING 5 program offers nine possible geometries which are listed below. The number associated with the possible geometry is inputted as the second entry in Card 2.

Cylindrical	Rectangular	Spherical
1 R- θ -Z	6 X-Y-Z	10 R
2 R- θ	7 X-Y	
3 R-Z	8 X-Z	
4 R	9 X	
5 Z		

B.2.3 TOTAL NUMBER OF REGIONS

The total number of regions of the entire configuration entered as the third entry. A maximum of 100 regions is allowed.

B.2.4 TOTAL NUMBER OF MATERIALS

The total number of materials are specified as the fourth entry of this card. A maximum of 100 regions is allowed.

B.2.5 NUMBER OF MATERIALS WITH CHANGE OF PHASE CAPABILITIES

The total number of materials with a change of phase capabilities is the fifth entry of this card. There can be a maximum of five such materials. If phase change is not to be considered in the problem, this entry is to be left blank.

B.2.6 TOTAL NUMBER OF HEAT GENERATION FUNCTIONS

The total number of different heat generation functions (maximum of 20) is the sixth entry of this card. This is left blank if there are no heat generation functions.

B.2.7 TOTAL NUMBER OF INITIAL TEMPERATURE FUNCTIONS

This entry is the total number of different initial temperature functions (a maximum of 25). If there are no initial temperature functions, this entry is left blank and the program will assume the initial temperature distribution to be zero degrees.

B.2.8 TOTAL NUMBER OF BOUNDARIES-

The eighth entry of Card 2 contains the total number of boundary conditions (a maximum of 50). If there are no boundary conditions, this entry must be left blank.

B.3 CARD 3-

Each entry of this card is an integer.

B.3.1 GROSS LATTICE SIZE-

The first three entries of this Card contains the total number of gross lattice lines in (1) X or R direction, (2) Y or θ direction, and (3) Z direction. There can be a maximum of 50 gross lattice lines along each axis. If any dimension is omitted, a zero or a blank is inserted in the appropriate entry.

B.3.2 TOTAL NUMBER OF ANALYTICAL FUNCTIONS-

The fourth entry contains the total number of different analytical functions. There can be a maximum of 25 of these functions. If there are no analytical functions, this entry is left blank.

B.3.3 TOTAL NUMBER OF TABULAR FUNCTIONS-

The total number of tabular functions is the fifth entry of this card. There can be a maximum of 25 functions. If there are no tabular functions, this entry is left blank.

B.3.4 TEMPERATURE UNITS-

The sixth entry contains the temperature units. A zero or a blank signifies it is in F and a 1 signifies C.

B.3.5 THREE-DIMENSIONAL-OUTPUT-MAP-FLAG-

This entry is only used for three-dimensional problems. The temperature output map is printed for each XY or R θ plane. If this entry is non zero, then the temperature output map will be printed for each XZ or RZ plane.

B.3.6 UPDATING TEMPERATURE-DEPENDENT PROPERTIES

The eighth entry on this card specifies the number of iterations which are allowed before the temperature dependant thermal properties are reevaluated for steady-state problems. Once the convergence criterion has been satisfied, the code continues to iterate, but the temperature-dependant thermal properties are now reevaluated after every iteration until the convergence criterion is satisfied a second time. It is recommended that this parameter be in the order of 10 or 20. If it is blank or zero, then the default value is unity for non linear problems.

B.4 CARD-4-


Each entry on this card is an integer.

B.4.1 TRANSIENT-OUTPUT-

For transient problems, the output may be specified in either of two ways:

1. The temperature distribution may be printed out at equally spaced times. The first entry on Card 4 must contain the number of initial time steps between outputs and the second entry must be blank. For example, if a value of 5 is entered, the temperature distribution will be printed at times whose spacing is equal to five times the initial time step.
2. The temperature distribution may be printed out at unequal time increments. To choose this option, the first entry on Card 4 must be left blank and the second entry must contain the number of times the temperature distribution will be printed out. The actual output times will be entered on the 0 cards.

The temperature distribution is automatically printed prior to the first time step for transient calculations and prior to the first iteration for steady-state problems. For steady-state only calculations, the first and second entries may be left blank.



B.4.2 GRAPHICAL-OUTPUT

The third entry on Card 4 indicates whether a graphical output is required or not. By entering a non zero integer in this field, a data set will be created which contains the temperature distributions along with certain parameters which identify the problem. The value of the integer identifies the unit number on which the data set is to be created. This data set is then used by HEATPLOT to get plots of the temperature distribution. A data set can be created on Unit 4 in our computer system. If a graphical output is required then 4 should be the third entry on Card 4. If a graphical output is not required then this entry should be left blank.

B.4.3 FREQUENCY-OF-OUTPUT-FOR-PLOTS

This entry (the fourth) specifies the number of time steps between each output of the temperature distribution on the data set defined in B.4.2 (i.e. the graphical output). If this entry is left blank or zero and if the preceeding entry (i.e B.4.2 in Card 4) is non zero, then the temperature distribution will be written on the data set each time that a normal printout as defined in B.4.1 of Card 4 occurs.

B.4.4 SPECIAL-MONITORING-OF-TEMPERATURES

If it is required to tabulate the temperatures of a few nodes without getting excessive output by having to print out the entire temperature distribution then this option is invoked. The number of iterations between print outs is entered in the fifth field of Card 4. If this entry is non zero, the node numbers whose temperatures are to be printed out are specified on the S cards. If this option is not desired, this entry is left blank.

B.4.5 INITIAL-TEMPERATURE-INPUT-UNIT

The sixth entry of this card specifies the unit number from which the explicitly specified lattice point initial temperatures are read. If the entry is a positive integer, then it specifies the unit number from which the initial temperatures are read in a formatted form. If it is negative, then the temperatures are read in an unformatted form.

B.4.6 FINAL-TEMPERATURE-OUTPUT-UNIT

If the final temperature distribution is to be saved to facilitate the restarting of the problem, it is saved on the unit number entered on the seventh entry of Card 4. This entry is left blank if the final temperature output is not to be saved.

B.4.7 PROBLEM STATUS UNIT FOR REMOTE USERS

This feature is designed to allow remote users to determine the status of the problem without having to wait for normal computer turnaround. If a positive number is entered in the eighth field of Card 4, then this designates the unit number on which error messages and selected information concerning the status of the problem is written.

B.5 CARD 5-

Each entry on this card is a floating-point number except for entries 1, 2 and 6, which are integers.

B.5.1 TYPE OF PROBLEM

The first entry on this card specifies the type of problem. It may be steady-state only, transient only, or combinations of both. The number to be entered is in accordance with the following list:-

1	Steady State (S-S) only	-	1 transient (trans.) only
2	S-S, trans.	-	2 trans., S-S
3	S-S, trans., S-S	-	3 trans., S-S, trans.
4	S-S, trans., S-S, trans.	-	4 trans., S-S, trans.
-		-	-
-		-	-
n	S-S, trans., S-S, trans., S-S, trans. etc.	-	n trans., S-S, trans., S-S, trans. etc

If, for example, a 3 is entered, the program will first perform a steady-state calculation at time zero; next the transient calculation; then a steady-state calculation at the final transient time using the final transient temperatures as the initial guess for the steady-state temperatures.

B.5.2 MAXIMUM OF STEADY-STATE ITERATIONS ALLOWED

Normally 200 to 500 iterations are sufficient to converge to the solution. If this entry is zero or blank for steady-state problems, a default of 500 is used. If the maximum number of steady-state iterations is reached, and the convergence criterion is not satisfied, then the calculation will be terminated and an error message "END STEADY-STATE CALCULATIONS, CONVERGENCE NOT SATISFIED" will be printed. This entry is left blank for pure transient problems.

B.5.3 STEADY-STATE CONVERGENCE CRITERION

This entry contains the steady-state convergence criterion and may be left blank for a transient-only problem. If this entry is left blank for steady-state problems the convergence criterion is assumed to be $1.0E-5$.

B.5.4 STEADY-STATE OVER-RELAXATION FACTOR

The value of the steady-state over-relaxation factor is the fourth entry on this card and it should be in the range $1 < B < 2$. This entry is left blank for transient only problems, B is assumed to be 1.9.

B.5.5 TIME INCREMENT

This entry contains the initial time increment for transient problem that will be solved using one of the explicit techniques. For transient problems which are to be solved using the implicit technique, this entry must be left blank. For the Classical Explicit Procedure, the time increment must satisfy certain criteria to insure stability. For steady-state only problems, this entry is left blank.

B.5.6 LEVY'S EXPLICIT METHOD OPTION

This sixth entry (an integer) is a factor by which the stable time increment is multiplied to form the time increment for Levy's explicit method. If this entry is blank or less than 2, then this method will not be used.

B.5.7 INITIAL TIME

This entry affects both transient and steady-state problems. It indicates the initial time for problem with a negative type and the time at which the time-dependant functions are evaluated for problems whose types are greater than zero.

B.5.8 FINAL TIME FOR TRANSIENT CALCULATION

The final time for the first transient calculation is specified as the eighth entry on Card 5. For steady-state problems this entry is left blank.

B.6 CARDS R1 AND R2 - REGION DATA

Each region is described by two cards which must appear in pairs. The cards are repeated for each region. The number of pairs of cards is the third entry on Card 2. There must be at least one region for each problem.

B.6.1 CARD R1**1. REGION NUMBER:**

This entry contains the number of the region to be described.

2. MATERIAL IN REGION:

The second entry of this card indicates by an integer the number of the material which occupies the region named in the first entry of this card.

3. REGION DIMENSIONS:

The dimensions of the region boundaries are entered as floating -point numbers and are arranged in the following order:-

- a) Smaller dimension of the X or R region boundary.
- b) Larger dimension of the X or R region boundary.
- c) Smaller dimension of the Y or θ region boundary.
- d) Larger dimension of the Y or θ region boundary.

e) Smaller dimension of the Z region boundary.

f) Larger dimension of the Z region boundary.

These dimensions are entered as the third through eighth entries, respectively. If the problem is one- or two-dimensional, then the region dimensions for the corresponding unnecessary coordinate or coordinates are omitted.

B.6.2 CARD-R2-

This card must be included with the appropriate R1 Card, even if it is blank. The entries on this card are as follows:

1. INITIAL TEMPERATURE OF REGION:

The initial temperature function number of the region is specified by the first entry on this card. If this entry is left blank, the program assumes the initial temperature for the region to be zero. The entry is an integer number.

2. HEAT GENERATION OF THE REGION:

This entry contains the number of the heat generation function associated with the region. If the entry is left blank the program assumes that the region does not generate heat.

3. BOUNDARY NUMBERS:

The remaining entries of this card are the boundary numbers defining the boundary conditions

corresponding to the six boundaries of the region described by the first card of this pair (i.e. R1 Card). The numbers are integers and are entered as follows:-

Each entry contains the boundary number of the region boundary appearing in the corresponding entry of Card R1. A boundary condition cannot be specified on a boundary dividing two regions unless it is a type 3 boundary condition. For one- or two-dimensional cases, region dimensions are not specified for the unnecessary coordinate or coordinates, and the corresponding boundary numbers are left blank. The entry is also left blank for boundaries which are insulated.

B.7 MATERIAL DATA - CARDS-M-AND-PC-

A group of cards consisting of an M card and possibly a PC card is required to describe each material. The total number of groups is the fourth entry on Card 2.

B.7.1 CARD-M

1. MATERIAL NUMBER:

The first entry is an integer and contains the number of the material which is to be described.

2. MATERIAL NAME:

The second entry, which must begin in column 11 and may extend to column 18, contains the name of the material.

3. CONSTANT THERMAL PROPERTIES:

Entries 3, 4 and 5 are floating-point numbers and respectively contain the constant thermal conductivity, constant density, and constant specific heat of the material. Since the density and specific heat are not used in steady-state calculations, entries 4 and 5 may be left blank for type 1 problems.

4. TEMPERATURE-DEPENDENT THERMAL PROPERTIES:

Entries 6, 7 and 8 (integers) identify the analytical or tabular functions describing the thermal conductivity, density and specific heat respectively.

B.7.2 CARD-PC

For materials with a change of phase capability, the phase-change or transition temperature and the corresponding latent heat are entered as floating point numbers in the first and second fields respectively, of Card PC. The following conventions must be adhered to in describing materials with change of phase capabilities: these materials must be the first ones described on the M cards, and the PC card is omitted for those materials which do not undergo a change of phase.

B.8 CARD G - HEAT-GENERATION FUNCTION DATA

Each different heat generation function is numbered, beginning with number 1, consecutively up to a maximum of 20 such functions. This heat generation function may be dependant on position, time and temperature. The first entry indicates the function number and the second entry indicates the constant volumetric heat generation rate. Entries 3, 4, 5, 6 and 7 indicate the analytical or tabular function describing the X- or R-dependant function parameter, the Y- or θ -dependant function parameter, the Z dependant function parameter, the time dependant function parameter, and the temperature dependant function parameter respectively. The total number of cards is indicated by the sixth entry on Card 2. The heat generation rate for a region may be positive (heat source) or negative (heat sink). The G cards are omitted if entry 6 on Card 2 is blank or zero. All entries except the second are integers.

B.9 CARD I - INITIAL TEMPERATURE FUNCTION DATA

Each initial temperature function is numbered beginning with 1 to a maximum of 25. This card consists of 5 entries. The first contains the initial temperature function number. The second entry contains the constant factor describing the constant temperature function. The 3rd, 4th and 5th entries identify the tabular or analytical functions pertaining to the X- or R-, Y- or θ -, and Z dependant function parameters.

The total number of cards is the seventh entry on Card 2, and if this entry is left blank, the I cards are omitted and the initial temperature distribution is assumed to be zero. All entries except for the second are integers.

B.10 CARDS B1, B2, B3 AND B4 - BOUNDARY DATA

Excluding insulated or contact type boundaries, each unique boundary is numbered consecutively upto a maximum of 50. The B1 and B2 cards are omitted if the eighth entry on Card 2 is blank or zero.

B.10.1 CARD B1-

1. The first entry is an integer and contains the boundary number.
2. The second entry (an integer) indicates the type of boundary i.e.
 - 1 surface-to-boundary
 - 2 prescribed surface temperature
 - 3 surface-to-surface.

If this entry is blank or zero, then no heat transfer connections will be made and this boundary will be treated as an insulated boundary.

3. The third entry (a floating point number) contains the constant boundary temperature. This entry is left blank for a type 3 boundary.

4. Since the boundary temperature can be a function of time, the fourth entry of this card contains the time-dependant parameter (an integer) which identifies an analytical or tabular function. This entry is left blank if the boundary temperature is independant of time or if it is a type 3 boundary condition.

B.10.2 CARD B2-

Each entry on this card is a floating-point number except Entry 6 which is an integer. This card is left blank for type 2 boundary condition.

1. Entry 1 contains the heat transfer coefficient, for forced convection.
2. Entry 2 contains heat transfer coefficient for radiation.
3. Entry 3 contains the heat transfer coefficient for natural convection.
4. The fourth entry contains the exponent for natural convection (or for other non linear heat transfer process).
5. The fifth entry contains the prescribed heat flux across the boundary.
6. The time- and temperature-dependant parameter flag, an integer, is the sixth and final entry in this Card. If any of the five preceding parameters are

functions of time and temperature, then additional information must be entered on B3 and/or B4 Cards. The time- and temperature-dependant flag indicates whether or not the B3 and B4 Cards are present for this particular boundary condition. Its value is determined according to the following table.

Entry 6	Additional Cards
0	None
1	B3 only
2	B4 only
3	B3 and B4

B.10.3 CARD- B3-

All five entries of this card are integers. Each integer identifies the analytical or tabular function that defines the time-dependant function associated with the respective parameter on Card B2. If an entry is blank or zero, then the associated parameter is not time dependant.

B.10.4 CARD- B4-

This card is just like Card B3 except each integer identifies the analytical or tabular function that defines the temperature dependant function associated with the respective parameter on Card B2.

The B1 and B2 Cards must appear in pairs and a pair is entered for each boundary.

B.11 CARDS L1, N1, L2, N2, L3 AND N3 -- LATTICE DESCRIPTION

For each axis, gross lattice data are entered on two sets of cards, the first specifying the lattice dimensions and the second indicating the mesh division between gross lattice lines. All of the numbers on the first set of cards (L Cards) are floating point numbers. The second set (N Cards) specify the number of equal increments which are between the gross lattice lines whose dimensions are given on the L Cards.

B.11.1 CARD L1-

The L1 cards correspond to the X or R coordinate, and the number of entries correspond to Entry 1 of Card 3. If there are more than 8 entries, subsequent cards are used.

B.11.2 CARD N1-

The N1 cards correspond to the X or R coordinate. There will be one less entry on this Card than there are on the L1 cards. Additional cards are used for more than 8 entries.

B.11.3 CARD L2-

The L2 cards correspond to the Y or θ coordinate.

B.11.4 CARD N2-

The N2 cards correspond to the Y or 0 coordinate. There will be one less entry here than there are on the L2 cards.

B.11.5 CARD L3-

The L3 cards correspond to the Z coordinate.

B.11.6 CARD N3-

The N3 cards correspond to the Z coordinate and there is one less entry here than there are on the L3 cards.

B.12 CARDS A1 AND A2 -- ANALYTICAL FUNCTION DATA

Each analytical function is described by an A1 card and one or more A2 cards.

B.12.1 CARD A1-

Each different analytical function is numbered, and there can be a maximum of 25 functions. The first entry on Card A1 is the unique analytical function number (an integer). The second entry (also an integer) is the number of coefficients which are on the A2 cards. If this entry is zero or blank, the code assumes that a user-supplied function will be supplied for the parameter which uses this particular analytical function.

B.12.2 CARD A2-

This card contains from one to four ordered pairs. An ordered pair consists of two elements, an integer and the value of the coefficient corresponding to that integer. If the second entry on Card A1 is blank or zero, then the related A2 Card is omitted.

Example:- The analytical function in the HEATING 5 program has been modified to:-

$$F(v) = A_1 + A_2 \cos(X) + A_3 \cos(2X) - A_4 \cos(3X) + A_5 \cos(3X) \\ + A_6 \sin(X) - A_7 \sin(2X) + A_8 \sin(2X) - A_9 \sin(3X) \\ + A_{10} \sin(3X)$$

$$\text{where } X = 2\pi (v/24 + A_{11}) / 365.$$

To generate an analytical function

$$F(v) = 20.0 + 20.0 \cos[2\pi/365(v/24)] \\ + 10.0 \sin[2\pi/365(v/24)]$$

the A1 and A2 Cards will be presented in a tabular form below:-

Column	9	18	27	35	45	54	63	72	CARD
	1	3							A1
	1	20.0	2	30.0	6	10.0			A2

The total number of analytical functions is the fourth entry on Card 3. The A cards are omitted if this entry is blank or zero.

B.12.3 CARDS T1 AND T2 - TABULAR FUNCTION DATA

Each tabular function is numbered consecutively beginning from 1 to a maximum of 25 functions. The tabular function is assumed to be a set of linearly connected points. The function is described by specifying a set of ordered pairs. Each ordered pair contains an independent variable and its functional value. A linear interpolation is performed between the points by the program.

B.12.4 CARD T1-

This first entry on the T1 card is the tabular function number and is an integer.

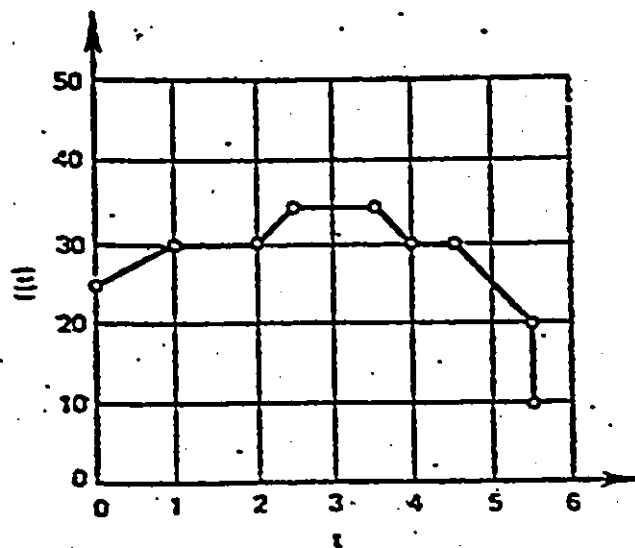
B.12.5 CARD T2-

The T2 card contains the first four ordered pairs, all floating point numbers. If there are more than four ordered pairs in the function, they are entered on subsequent T2 cards.

EXAMPLE: If the tabular function is inputted in the following manner:

Column	9	18	27	35	45	54	63	72	CARD
	1	9							T1
	0.0	25.0	1.0	30.0	2.0	30.0	2.5	35.0	T2
	3.5	35.0	4.0	30.0	4.5	30.0	5.5	20.0	T3
	5.501	10.0							T4

then the plot of the tabular function will be:-



Plot of a Sample Tabular Function

The total number of tabular functions is the fifth entry of Card 3. The T cards are omitted if this entry is left blank or zero.

B.13 CARD 3 -- OUTPUT CARDS

Each entry on this card is a floating-point number. Since the second entry on Card 4 indicates the total number of output times which are to be read, the O cards are omitted if this entry is blank or zero. The transient output times are entered in the O Cards and there can be eight entries per card. There may be a maximum of 100 output times, not counting the automatic print out which occurs prior the initial time step.

B.14 CARD-S -- NODE NUMBERS FOR SPECIAL MONITORING OF TEMPERATURE

As an optional output upto 20 nodes may be specified whose temperatures will be printed as a function of the number of iterations for steady-state calculations or the number of time steps for transient calculations. The first entry on the S card contains the total number of nodes whose temperatures are to be tabulated. The remaining fields contain the actual node numbers. If more than seven nodes are specified their numbers will appear on additional S cards. All entries on the S cards are integers. The frequency for printing out the temperatures of such nodes appear as the fifth entry on Card 4, and the S cards are omitted if this entry is zero or blank.

B.15 INITIAL TEMPERATURES AND MELTING RATIOS

These cards are generated as output by HEATING 5 if a positive number appears in Entry 7 on Card 4, and, generally, they are used only when restarting a job by inserting the generated deck. One must enter the unit number of the card reader in the sixth field of Card 4. Entry 6 on Card 4 specifies the unit on which these data are to be read. If the unit specified is other than a standard card input an appropriate DD Card should be supplied to describe the unit. If entry 7 on Card 4 is non zero, then the code generates these data at the end of a problem and writes it on the unit specified in Entry 7. The user must

insure that the appropriate DD Card has been supplied to correctly identify the unit specified on Entry 7.

Since the user may wish to explicitly specify the initial temperature or melting ration at some point or points, a description of these data is given below.

B.15.1 CARD-IT1 -- JOB DESCRIPTION-

This card image gives a descriptive title. This card may be blank but cannot be omitted. It may contain 72 alphanumeric characters.

B.15.2 CARD-IT2 -- INITIAL TIME AND LATTICE POINT NUMBERS

The first entry, a floating point number which occupies the first ten columns on the IT2 card, specifies the initial problem time. The second entry on the IT2 card is an integer and contains the total number of lattice points whose initial temperatures are explicitly specified. It occupies columns 11 through 15 of Card IT2. The third entry, also an integer, contains the total number of nodes whose initial melting ratios are explicitly specified. It occupies a five-column field i.e. columns 16 through 20.

B.15.3 CARD-IT3 -- LATTICE POINT TEMPERATURES-

The IT3 Card can contain upto five pairs of numbers. Each pair is defined as follows:-

1. The first number of the pair is a lattice point number. It is an integer and occupies a five-column field.
2. The second number is the initial temperature of the lattice point. It is a floating point number and occupies a ten-column field.

The number of pairs to be entered on the IT2 Cards is specified on Entry 2 of Card IT2.

B.16 CARD-IT4 - LATTICE-POINT INITIAL-MELTING RATIOS

The IT4 card contains initial melting ratios for each node which is currently undergoing a phase change. The format of the IT4 card is as follows:

1. the first entry is the number of a node which is currently undergoing a phase change. It is an integer and the field occupies the first five columns.
2. The second entry is the material number currently undergoing a phase change for the node which was defined in the previous field. This entry is an integer which occupies the sixth through the tenth columns.
3. The third entry, a floating point number occupying the eleventh through the twentieth columns, contains the initial melting ratio for the portion of the material associated with the node defined on the

first two entries of this card as currently changing phase.

B.17 ~~IMPLICIT-TRANSIENT-TECHNIQUE-PARAMETERS~~

If the problem involves transient calculations and if the implicit technique is used to calculate estimates to the transient temperature distribution, then the fifth entry of Card 5 must be left blank and additional data must be supplied on the IP and TP Cards.

B.17.1 CARD-IP

This entire card or any of its entries may be left blank, and the default values will be used. There are eight entries on this card. The first five are floating point numbers, and the last three are integers.

1. The first entry contains one of two convergence criteria which must be met in order for the iterative technique to terminate successfully at each step. The default is $1.0E-5$.
2. The second entry contains the second convergence criterion. The default for this parameter is $1.0E-3$, meaning the maximum normalized residual must decrease by three orders of magnitude.
3. The third entry contains the convergence criterion for problems involving temperature-dependant parameters. The default is $1.0E-5$.

4. This entry, the fourth, defines the implicit technique which will be used to solve the transient problem. The default is 0.5 (i.e Crank-Nicolson Technique).
5. The fifth entry defines the initial value of the point successive overrelaxation iteration acceleration parameter. It also defines the method that will be used to update the acceleration parameter. If this entry is positive, then the acceleration parameter will remain constant throughout the calculations and will be equal to the value of this entry. If it is blank or zero, then the acceleration parameter will be optimized empirically as a function of time. This appears to be the best option for non linear problems. If it is negative, then the acceleration parameter will be calculated using Carre's technique. The absolute entry of this entry must be less than 2.0.
6. This entry, an integer, defines the number of time steps between attempts to optimize the acceleration parameter empirically. It is used only when entry 5 is zero or blank. The default value is 1.
7. For the case when the acceleration parameter will be updated empirically (Entry 5 is blank or zero), then this entry defines the change-in-number-of-iterations criterion which must be met before the acceleration

parameter will be updated. The default is 5. For the case when the SOR acceleration parameter will be updated using Carre's technique, then this entry defines the number of iterations between updates. The default is 12.

8. The last entry is the change-in-number-of-iterations criterion which is used to determine when a good estimate to the optimum acceleration parameter has been found. This entry is used only when entry 5 on this card is blank or zero. The default is 2.

B.17.2 CARD TP-

When an implicit scheme is used to solve a transient problem, the time step may be variable. This allows the time step to increase as the solution smooths out and to decrease when some parameter varies rapidly with time. The information controlling the value of the time step is contained in one or more of the TP Cards. The size of the time step is automatically adjusted in order to get print outs of the temperature distribution at the specified time. All seven entries are floating point numbers.

1. The first entry is the initial time step.
2. After the temperature distribution has been calculated, the current time step is multiplied by a factor. The value of this factor is entered in the second field of the TP Card. The default value is 1.0.

3. The maximum value of the time step is the third entry. Once the time step reaches this value, it is no longer increased. The default is 1.0E50.
4. The fourth entry contains the maximum time that the time step information on this card applies. If the time reaches this value, then a new TP Card is read. The default is 1.0E50.
5. The fifth entry contains the maximum temperature change allowed at a node over a time step. If this entry is blank or zero, then this feature is not invoked in calculating the time step size.
6. The sixth entry contains the maximum percent of relative temperature change allowed at a node from one time level to the next one. If this entry is blank or zero, then this feature is not invoked in calculating the time step size.
7. The seventh and final entry on this card contains the minimum value of the time step. Once the time step reaches this value it is no longer decreased. The default is onetenth of the initial time step size.

B.18 BLANK CARD

If the user wishes to solve several problems with one run, a blank card is inserted between each problem deck.

Appendix C

This appendix lists the format of the JCL to run HEATING 5 at the University of Windsor. A sample problem is also presented in this appendix.

A sample basement has been simulated by the program and its dimensions are as follows:-

FLOOR:

1. The floor is 2.42 meters below grade.
2. Its thickness is 0.203 meters and its properties are listed in the program.
3. The film coefficient between the floor and basement air is 6.13 w/m C.

WALL:

1. The wall is 2.443 meters long and 0.41 meters of it is above grade.
2. The wall thickness is 0.203 meters and its properties are listed in the program.
3. The film coefficient between the wall and basement air is 8.29 w/m C.

SOIL:

1. The soil thermal properties are listed in the program. The thermal conductivity is a function of time.

2. The convective coefficient between the ground and air is taken to be a function of time.

TEMPERATURE:

The air and basement temperatures are inputted as Fourier equations and are functions of time.

The results of these calculations are printed out and are stored on Unit 4.

If it is not desired to store this output for plotting purposes the following lines have to be deleted from the JCL:

```
// EXEC PGM = IEFBR14
//D DD DSN = MENG.FILENAME.DATA,UNIT=330-1,
// VOL=SER=DISK04,
// DISP=(OLD,DELETE)
//PT04F001 DD UNIT=3330-1,VOL=SER=DISK04,
// DISP=(NEW,KEEP),DSN=MENG.FILENAME.DATA,
// SPACE=(TRK,(1,3)),
// DCB=(RECFM=VBS, LRECL=3620,BLKSIZE=3624)
```

The second entry on Card 4 (i.e 4) should be deleted.

XXXX=ACCOUNT NUMBER

YYY=INITIALS

Z =CLASS

FILENAME=the file on which the output is stored. It should occupy eight columns.

The JCL required to run HEATING 5 along with a sample problem are presented below:-

```
//HEATING5 JOB (XXXX,YYY),'NAME',CLASS=A,
//          MSGLEVEL=(1,1),REGION=750K
//          EXEC PGM=IEFBR14
//D.                                               DD
DSN=MENG.FILENAME.DATA,UNIT=3330-1,VOL=SER=DISK04,
//          DISP=(OLD,DELETE)
/*
//          EXEC PGM=HEATING5
//STEPLIB DD DSN=MENG.TUCKER.LOADLIB,
//          UNIT=3330-1,VOL=SER=DISK01,DISP=OLD
//PT01P001 DD UNIT=SYSWK,SPACE=(TRK,(1,3))
//PT02P001 DD UNIT=SYSWK,SPACE=(TRK,(1,3))
//PT03P001 DD UNIT=SYSWK,SPACE=(TRK,(1,3))
//PT04P001 DD UNIT=3330-1,VOL=SER=DISK04,
//
DISP=(NEW,KEEP),DSN=MENG.FILENAME.DATA,SPACE=(TRK,(1,3)),
//          DCB=(RECFM=VBS,LRECL=3620,BLKSIZE=3624)
//PT05P001 DD UNIT=SYSWK,SPACE=(TRK,(1,3))
//PT06P001 DD SYSOUT=A
//PT07P001 DD SYSOUT=B
//PT08P001 DD DDNAME=SYSIN
//PT10P001 DD UNIT=SYSWK,SPACE=(TRK,(1,3))
//SYSIN DD *
SAMPLE PROBLEM FOR CALCULATING BASEMENT HEAT LOSS
```

1800		7	9	3
9	8			
	7	9	2	2
	3	4		1
	2			
0.0	13400.0			
1	1	0.0	2.44	2.24
1				2.443
2	2	0.0	2.44	2.443
2				14.23
3	3	2.44	2.643	0.0
3		3	4	0.41
4	3	2.44	2.643	0.41
4		2		2.24
5	3	2.44	2.643	2.24
5				2.443
6	2	2.44	2.643	2.443
6				14.23
7	2	2.643	8.32	0.41
7				2.24
8	2	2.643	8.32	0.41
8				2.24
9	2	2.643	8.32	2.443
9				14.23
				6
1	CONFLOOR	6228.0	2243.0	840.0
2	SOIL	1.0	1922.0	1670.0
3	CON.WALL	4176.0	977.0	840.0

1 18.0

2 13.0

3 9.0

4 14.5

5 15.7

6 12.9

7 6.5

8 8.0

9 10.0

1 1 1.0 1

22063.0

2 1 1.0 1

29844.0

3 1 1.0 1

29844.0

4 1 1.0 2

1.0 1

-2

5 1 1.0 2

1.0 1

-2

6 2 11.67

7 2 11.67

8 2 11.67

	0.0	2.44	2.643	3.553	4.473	6.473
8.32						
	8	2	4	2	2	1
	0.0	0.41	1.01	2.24	2.443	2.64
4.44	8.44					
14.23						
	4	6	5	2	1	5
4	2					
	1	8				
	1	22.355	2	3.328	3	0.584
4	0.735					
	6	1.263	7	0.334	10	0.8
11	183.0					
	2	8				
	1	13.6472	2	13.2061	3	1.0718
5	0.8706					
	6	4.2709	8	0.425	9	1.1805
11	183.0					
	1	18				
	0.0	7164.0	2160.0	7164.0	2161.0	4968.0
2880.0	4968.0					
	2881.0	4356.0	6552.0	4356.0	6553.0	4968.0
7296.0	4968.0					
	7297.0	7164.0	10920.0	7164.0	10921.0	4968.0
11640.0	4968.0					

180

11641.0 4356.0 15312.0 4356.0 15313.0 4968.0

16056.0 4968.0

16057.0 7164.0 17520.0 7164.0

2 18

0.0 122652.0 2160.0 122652.0 2161.0 102204.0

2880.0 102204.0

2881.0 81756.0 6552.0 81756.0 6553.0 102204.0

7296.0 102204.0

7297.0 122652.0 10920.0 122652.0 10921.0 102204.0

11640.0 102204.0

11641.0 81756.0 15312.0 81756.0 15313.0 102204.0

16056.0 102204.0

16057.0 122652.0 19680.0 122652.0

120.0 1.0 1.0

//

Appendix D

A reference manual has been prepared to run the HEATPLOT program.

D.1 INPUT DESCRIPTION

D.1.1 CARD-1, FORMAT (A3,2X,2E10.0)

1. PLOTTER:

The first entry specifies the type of plotter to be used. It is EAI if the plots are to be made on the pen and ink plotter, CAL if the plots are to be made on the CALCOMP pen and ink plotter, or CRT if the plots are to be made on the CALCOMP CRT plotter.

2. XAX:

The length of the horizontal axis in inches is the second entry on this card. If blank the default is 10 inches.

3. YAX:

The third entry is the length of the vertical axis in inches. The default is 9.0 inches.

D.1.2 CARD-2, FORMAT(15I5)**1. NL:**

The first entry is the number of contour levels to be plotted. If negative the contour values will be calculated by the program. The number of contour values will be equal to (NL). If zero, no contours will be plotted. If positive, the contour values will be read in. NL should be equal to the number of values on the VALS Card. $0 < NL < 50$.

2. N TIME:

The number of time positions for which contours or temperature vs. distance profiles are to be plotted. If not zero, the times will be read from the TIMES card. $0 < N TIME < 20$.

3. N PLANE (1):

The number of Y-Z or θ -Z planes for which contours are to be plotted if the problem is three dimensional. The X-axis position will be read from the X PLANES card. $0 < N PLANES (1) < 10$. This value is left blank for a two-dimensional problem.

4. N PLANE (2):

The number of X-Z or R-Z planes for which contours are to be plotted if the problem is three-dimensional. The Y-axis positions are read in the Y PLANES cards. This value is left blank for a two-dimensional problem. $0 < N PLANE (2) < 10$.

5. N PLANE (3):

The number of X-Y or R- θ planes for which contours are to be plotted if the problem is three-dimensional. The Z-axis positions will be read from the Z PLANES card. $0 < \text{N PLANE (3)} < 10$.

6. NSCAL:

The sixth entry is an option to input the scale factors. If any scale factors are to be read in, NSCAL must be 1. The scale factors will be read from the SCAL1 and SCAL2 cards. If this entry is zero or blank, the program will compute the scale factors.

7. ITMVTP:

The seventh entry is an option for temperature-time profiles. If negative, temperatures for ITMVTP nodes will be plotted on one graph. If zero, no temperature-time profiles will be made. If positive, temperatures for ITMVTP nodes will be plotted one node on each graph. The node numbers will be read from the NODES card. $0 < \text{ITMVTP} < 20$.

8. LPLOT:

This entry is an option for temperature-distance profiles. If -1, profiles along a line at every time will be one plot. If zero, no temperature-distance profiles will be plotted. If 1, one profile will be on each graph. The times will be read from the TIMES card.

9. LREG:

The ninth entry specifies an option to specify region on which temperature contours will be plotted. If the region is to be read in, LREG must be 1. The region will be read from the REGION card. If zero, contours will be drawn over the entire region for each plane specified.

10. LREV(1):

This is an option to reverse the X-axis of contour plots. If zero, the X-axis will be from a minimum to maximum. If 1, it will be from a maximum to minimum.

11. LREV(2):

This is an option to reverse the Y-axis of the contour plots. If zero or blank it will be from a minimum to maximum, and if 1, it will be from a maximum to minimum.

12. LREV(3):

This is an option to reverse the Z-axis of the contour plots. If zero or blank, it will be from a minimum to maximum, and if 1, it will be from a maximum to minimum.

13. LAX(1):

This is an option to switch the Y-Z or θ -Z axis of the contour plots. If zero or blank, the axis will not be switched and if 1, it will be switched.

14. LAX(2):

The fourteenth entry is an option to switch the X-Z or R-Z axis of the contour plots.

15. LAX(3) :

This is an option to switch the X-Y or R- θ axis of contour plots.

D.2 CARD UNITS -UNITS DATA (FORMAT (3(A4,1X)))

This card contains the data for the units used.

1. UNITS (1) :

This entry contains the time units for labels and legends.

2. UNITS (2)

This entry contains the temperature units for labels and legends.

3. UNITS (3) :

This contains the distance units for labels and legend.

D.3 CARD VALS, FORMAT (7E10.0)

This card contains the values of the isotherms to be plotted. It is omitted if NL is equal to zero. There can be a maximum of 50 entries. VALUE (I), I=1,NL.

D.4 CARD TIMES, FORMAT (7E10.0)

The times for which contours and temperature versus distance profiles will be made are entered on this card. If the input time is not the same as a time on the temperature distribution data set, the time on the data set closest to the input time will be plotted. TIME (I), I=1,N TIME.

D.5 CARD XP, FORMAT (10I5)

This card contains positions on the X-axis for which Y-Z or θ -Z contours are to be plotted. It is omitted if N PLANE (1) is equal to zero. There can be a maximum of 10 entries.

D.6 CARD YP, FORMAT (10I5)

This card contains the positions on the Y-axis for which X-Z or R-Z contours are to be plotted. It is omitted if N PLANE (2) is zero. There can be a maximum of 10 entries.

D.7 CARD ZP, FORMAT (10I5)

This card contains positions on the Z-axis for which X-Y or R- θ contours are to be plotted. It is omitted if N PLANE (3) is zero. There can be a maximum of 10 entries.

D.8 CARD SCAL-1 - SCALING FACTORS, FORMAT (3E10.0)

Scaling factors are in Units/inch for axis involving temperature contours.

D.8.1 R SCAL

This is the scale factor for X- or R-axis.

D.8.2 TH SCAL

This entry contains the scale factor for the Y- or θ -axis.

D.8.3 Z SCAL

This entry contains the scale factor for the Z-axis.

D.9 CARD SCAL-2 - FORMAT (6E10.0)**D.10 TH SCAL**

This entry contains the scale factor, in units/inch, for Time in Time vs. Temperature plots.

D.10.1 TP SCAL

This entry contains the Temperature scale, in units/inch, for Time vs. Temperature plots.

D.10.2 ~~TYMIN~~

This entry contains the minimum temperature for Time vs. Temperature plots.

D.10.3 ~~DSCAL~~

This entry contains the scale factor, in units/inch, for Distance in Distance vs. Temperature plots.

D.10.4 ~~TSCAL~~

This entry contains the Temperature scale factor, in units/inch, for Distance vs. Temperature plots.

D.10.5 ~~TYDMIN~~

This contains the minimum temperature for distance vs Temperature plots.

Card SCAL1 and Card SCAL2 are coupled. If NSCAL=1, both cards must be included. Scale factors will be computed for those scale factors left blank. Minimum temperature will be zero if left blank. Omit both cards if NSCAL=0.

D.11 ~~CARD REGION - CONTOUR-REGION, FORMAT (15I5)~~

This card contains the grid line numbers bounding the region for which temperature contours are to be plotted. Omit this card if LREG=0.

D.11.1 NB (1)

This entry is the number corresponding to the fine grid line of the minimum X value in region.

D.11.2 NB (1)

This entry is the number corresponding to the fine grid line of the maximum X value in region.

D.11.3 NB (2)

This entry contains the number corresponding to the fine grid line of the minimum Y value in region.

D.11.4 NB (2)

This entry contains the number corresponding to the fine grid line maximum Y value in region.

D.11.5 NB (3)

This entry contains the number corresponding to the fine grid line of the minimum Z value in region.

D.11.6 NB (3)

This entry contains the number corresponding to the fine grid line of the maximum Z value in region.

D.12 CARD NODES - NODES FOR TEMPERATURE-TIME PROFILES

This card contained the node numbers for which temperature-time profiles are to be plotted. There can be a maximum of 20 entries. This card is omitted if IPHVTP=0.

D.13 CARD PROFILES - NUMBER OF TEMPERATURE-DISTANCE PROFILES

This card is omitted if LPLOT=0, or if the model is one-dimensional.

D.13.1 NPROFIL (1)

The first entry contains the number of temperature-distance profiles to be plotted parallel to the X-axis, or normal to Y-Z plane, for two- or three-dimensional models.

D.13.2 NPROFIL (2)

The second entry is the number of temperature-distance profiles to be plotted parallel to the Y-axis, or normal to the X-Z plane, for two- or three-dimensional models.

D.13.3 NPROFIL (3)

This contains the number of temperature-distance profiles to be plotted parallel to the Z-axis, or normal to the X-Y plane, for two- or three-dimensional models.

D.14 CARD INDX-1 - X PROFILES, FORMAT (14I5)

The number of the fine grid lines of the Y and Z axes, respectively, which define the IZ and IY planes whose intersection is the line along which the temperature-distance profiles are to be plotted parallel to the X-axis. For two-dimensional problems, the number of the fine grid line for the missing axis must be one or zero. Omit if NPRFIL(1)=0.

D.15 CARD INDX-2 - Y PROFILES, FORMAT (14I5)

This card is similar to the INDX 1 card but it contains the numbers of the fine grid lines of the X and Z axes. This card is omitted if NPRFIL(2)=0.

D.16 CARD INDX-3 - Z PROFILES, FORMAT (14I5)

This card is similar to the INDX 1 and INDX 2 cards, but contains the number of the fine grid lines of the X and Y axes respectively. This card is omitted if NPRFIL(3)=0.

D.17 JCL REQUIRED TO RUN HEATPLOT ON ZETAPLOTTER

```
//HEATPLOT JOB (XXXX,YYY),'NAME',CLASS=A,MSGLEVEL=(1,1)
```

```
// EXEC ASMFC,PARM.ASM='NOLIST,LOAD,NODECK'
```

insert assembler portion of Fortran Deck

```
//SYSIN DD *
```

```
//ASM.SYSIN DD *
```

```
// EXEC ZETAPLOT,REGION=400K,
```

```
// PARM.LKED='LET,XREF,LIST'
```


insert Fortran Deck here

//PORT.SISIN DD *

//GO.FT05F001 DD UNIT=SYSWK,SPACE=(TRK,(1,5))

//GO.FT08F001 DD *

CAL 7.0 4.0

17 15

1

HR C M

0.0 2.0 4.0 6.0 8.0 10.0

12.0

14.0 16.0 18.0 20.0 22.0 24.0

26.0

28.0 30.0 32.0

0.0 960.0 1920.0 2880.0 3840.0 4800.0

5760.0

6720.0 7680.0 8640.0 9600.0 10560.0 11520.0

12480.0

13440.0

//GO.FT10F001 DD UNIT=3330-1,VOL=SER=DISK04,

// .DISP=OLD,DSN=MENG.BHARDWAJ.DATA

//GO.SYSUDUMP DD SYSOUT=A

//

VITA AUCTORIS

- 1959 Born in Singapore on May 18.
- 1976 Completed the Indian School Certificate (I.S.C.) examination from Mount St. Mary's High School, New Delhi, India.
- 1981 Completed the Bachelor of Science degree in Mechanical Engineering from the Birla Institute of Technology, Ranchi, India.
- 1984 Currently a candidate for the degree of Master of Applied Science.